Aus der Klinik für Orthopädie und Unfallchirurgie
Klinik der Universität München

Direktion:
Prof. Dr. Wolfgang Böcker
Prof. Dr. Boris Holzapfel

Dissecting the role of NELL-ligands and their possible receptors in myogenesis

Dissertation

zum Erwerb des Doktorgrades der Medizin

an der Medizinischen Fakultät der

Ludwig-Maximilians-Universität zu München

vorgelegt von

Julian Justin Kruse

aus

Wuppertal

2023

Mit Genehmigung der Medizinischen Fakultät
der Universität München

Berichterstatter:	Prof. Dr. Wolfgang Böcker
Mitberichterstatter:	PD Dr. Thomas Niethammer Prof. Dr. Claudia Veigel
Mitbetreuung durch den promovierten Mitarbeiter:	Dr. Maximilian Saller
Dekan:	Prof. Dr. med. Thomas Gudermann
Tag der mündlichen Prüfung:	27.07.2023

Dedicated to my dogs Scotty, Rusty, and Nala,
in appreciation of their loyalty and unconditional love.

Contents

Abstract

Myogenesis, the formation of skeletal muscle, occurs in four sequential, partially overlapping phases. Muscle precursor cells (MPCs) first proliferate, then migrate, differentiate, and fuse to myotubes. This spatiotemporal process is highly complex, and thus MPCs are subject to various autocrine and paracrine differentiation and migration signals. Non-myogenic muscle cells (nMMCs), such as fibroblasts or motor neurons, have also been shown to influence MPCs through several ligand-receptor pathways.

Nel-related protein 1 (NELL1) and NELL2 are two ligands mainly investigated in their role in neuronal development, osteogenesis, and various tumors. More distinctively, NELL1 was shown to improve the constructive remodeling outcome in muscle injury models. In addition, NELL2 offers an interesting differential expression profile during early myogenesis. Furthermore, the Roundabout (ROBO) receptor family are the only currently known NELL receptors, and ROBOs were demonstrated to be involved in myoblast guidance and alignment. Therefore, I hypothesized that NELLs might be promising candidates that differentially influence myogenesis. Furthermore, I hypothesized that NELLs affect the cells involved in myogenesis by binding to receptors of the ROBO family.

In this study, I used a gene expression-based approach and *in vitro* studies to examine these potentially important ligands for myogenesis. To explore the expression profile of NELLs in myogenic (MMCs) and non-myogenic muscle cells (nMMCs) separately, I bred the myogenic reporter mouse line $Rosa26^{mT/mG};Acta1^{Cre}$. Comparison to other myogenic sequencing data revealed that NELL2 is weakly expressed by E15.5 nMMCs. During migration, myoblasts express NELL2 strongly, while interestingly, NELL2 is downregulated in early fusion. The effect of NELLs on myoblasts during various stages of myogenesis was assessed using recombinant proteins (RP) and $SCP1^{RFP;NELL2::AP}$ conditioned media on C2C12 cells in random migration, directed migration, alignment, and fusion assays. Aligning with the expression profile, a pro-migratory effect of NELL2 was recognized, while NELL1 was not observed to influence myoblast migration. No chemotaxis effect of NELLs on directing myoblast migration was observed. Also, no evidence of a NELL influence on alignment or fusion of C2C12 cells was shown.

In sum, I identified NELL2 as a new pro-migratory ligand in myogenesis. Myoblasts during the migration phase express NELL2, which seems to work in an autocrine or paracrine manner. By NELL2 binding, C2C12 cells move slightly faster, while fusion appears to be inhibited. Future experiments should concentrate on further dissecting the effect of NELL2 on myogenesis and aim to identify if the influence is enabled by ROBO2 or another myoblast receptor.

Zusammenfassung

Myogenese, die Entwicklung der Skelettmuskulatur, erfolgt in vier aufeinander folgenden, sich teilweise überlappenden, Phasen. Zuerst proliferieren Muskelvorläuferzellen (MPCs), dann migrieren, differenzieren und fusionieren diese zu Myotuben. Dieser raumzeitliche Prozess ist hochkomplex, so dass MPCs verschiedenen autokrinen und parakrinen Differenzierungs- und Migrationssignalen unterliegen. Es wurde außerdem gezeigt, dass auch nicht-myogene Zellarten (nMMCs) wie Fibroblasten oder Motoneurone, MPCs über verschiedene Liganden-Rezeptor Signalwege beeinflussen.

Nel-related protein 1 (NELL1) und NELL2 sind zwei Liganden, deren Rolle hauptsächlich in der neuronalen Entwicklung, Osteogenese und verschiedenen Tumoren untersucht wurden. Es hat sich jedoch auch gezeigt, dass NELL1 das Ergebnis des konstruktiven Umbaus in Muskelverletzungsmodellen verbessert. Darüber hinaus weist NELL2 ein interessantes differentielles Expressionsprofil in der frühen Myogenese auf. Zudem sind die Rezeptoren der Roundabout-Familie (ROBO) die einzigen derzeit bekannten NELL-Rezeptoren, und es wurde gezeigt, dass ROBOs an der Chemotaxis und Ausrichtung der Myoblasten beteiligt sind. Daher stellte ich die Hypothese auf, dass NELLs vielversprechende Signale sind, welche die Myogenese differenzial beeinflussen. Außerdem stellte ich die Hypothese auf, dass NELLs, die an der Myogenese beteiligten Zellen durch die Bindung an Rezeptoren der ROBO-Familie modulieren.

In dieser Studie habe ich eine Genexpressionsanalyse zusammen mit *in-vitro* Studien verwendet, um diese potenziell wichtigen myogenese Liganden zu untersuchen. Um das Expressionsprofil von NELLs in myogenen (MMCs) und nicht-myogenen Muskelzellen (nMMCs) getrennt zu untersuchen, habe ich die myogene Reportermauslinie $Rosa26^{mT/mG};Acta1^{Cre}$ gezüchtet. Ein Vergleich mit anderen myogenen Sequenzierungsdaten ergab, dass NELL2 von E15.5 nMMCs nur schwach exprimiert wird. In der Migrationsphase exprimieren Myoblasten NELL2 stark, währenddessen interessanterweise, die NELL2 Expression in der frühen Fusion herunterreguliert wird. Der Einfluss von NELLs auf Myoblasten in den verschiedenen Stadien der Myogenese wurde mit rekombinanten Proteinen und $SCP1^{RFP;NELL2::AP}$ konditioniertem Medium auf C2C12-Zellen in zufälligen Migrations-, gerichteten Migrations-, Ausrichtungs- und Fusionsversuchen untersucht. In Übereinstimmung mit dem Expressionsprofil wurde eine migrationsfördernde Wirkung von NELL2 festgestellt, während NELL1 die Migration nicht beeinflusste. Es wurde kein Chemotaxis-Effekt von NELLs auf die direktionale Migration beobachtet. Auch ein Einfluss von NELL auf die Ausrichtung oder Fusion von C2C12-Zellen konnte nicht nachgewiesen werden.

Zusammengefasst, habe ich NELL2 als neues Migrationssignal in der Myogenese identifiziert. Myoblasten exprimieren während der Migrationsphase NELL2, das autokrin oder parakrin zu agieren scheint. Durch eine Bindung an NELL2, migrieren

die C2C12-Zellen etwas schneller, während sich eine nicht signifikante Hemmung der Fusion präsentiert. Weitere Studien sollten sich darauf konzentrieren, die Wirkung von NELL2 auf die Myogenese genauer zu untersuchen und herauszufinden, ob der Einfluss durch ROBO2 oder einen anderen Rezeptor ermöglicht wird.

List of Figures

List of Tables

Abbreviations

ACTA1 – actin alpha 1

BGP - osteocalcin

BMP4 - bone morphogenetic protein 4

BSP - bone sialoprotein

CCD – central core disease

c-hairy1 - chicken hairy homolog 1

c-Met - tyrosine-protein kinase Met

Cdc42 - cell division cycle 42

CDH - congenital diaphragmatic hernia

Cited2 - Cbp/p300-interacting transactivator 2

CM - conditioned medium

COL10 - mRNA encoding type X collagen

CoM - center of mass

CosM - costal musculature

CrM – crural musculature

CTR - central tendon region

DEPC - diethylpyrocarbonate eagle medium

Drl - derailed

Duf – dumbfounded

EGF - epidermal growth factor

EGFL – EGF-like

F-actin – actin filament

FACS - fluorescence-activated cell sorting

FBS - fetal bovine serum

FC - founder cell

FCM - fusion competent myoblast

Fgf - fibroblast growth factor

Fgfr1 - Fgf receptor 1

FMI - forward migration index

Gata4 - GATA binding protein 4

gDNA - genomic DNA

GFP - green fluorescence protein

GnRH - gonadotropin-releasing-hormone

GTPase - guanosine triphosphatase

HGF - hepatocyte growth factor

HS - horse serum

HSPG - heparan sulfate proteoglycan

ISH - *in situ* hybridization

Kon - kon-tiki

Lbx1 - ladybird homeobox homolog 1

MAS - muscle attachment sides

MMC - myogenic muscle cell

MPCs - muscle progenitor cells

Msx1 - msh homeobox 1

mT - tdTomato

MTJ - myotendinous junction

Myf5 - myogenic factor 5

MyoD1 - myogenic differentiation 1

NBT - nitro-blue tetrazolium

NEL - neural EGF-like

NELL - neural EGFL Like

nMMC - non-myogenic muscle cell

Nr2f2 - nuclear receptor subfamily 2 group f member 2

NTMT - alkaline phosphatase buffer

ON - overnight

OPN - osteopontin

P/S - penicillin-streptomycin

Pax - paired box

PBS - phosphate-buffered saline

PFA - paraformaldehyde

Rac1 - RAS-related C3 botulinum substrate 1

RE - restriction enzyme

Rho - ras homolog family member

ROBO - roundabout guidance receptor

Rock1 - rho-associated coiled-coil containing protein kinase 1

RP - recombinant proteins

Rst - roughest

RT - room temperature

Scx - scleraxis

Shh - sonic hedgehog

SLIT - slit guidance ligand

Sns - sticks-and-stones

SSC - saline sodium citrate

st - Hamburger-Hamilton stage

ST - septum transversum

Tgf - transforming growth factors

Tnmd – tenomodulin

TPC - tendon progenitor cell

TPM - transcripts per million

Vasp - vasodilator-stimulated phosphoprotein

vWC - von Willebrand factor type C

Wnt - wingless-type

Wt1 - wilms tumor 1

Introduction

1.1 The skeletal muscle system

Skeletal muscles are a fundamental necessity for vertebrates. Their movement allow and maintain breathing, reproduction, and food and water consumption. Depending on the task and species, a different combination of muscles and their coordination is required. For example, in humans and other mammals, simple breathing is a complex spatiotemporal interaction of the diaphragm, costal and abdominal muscles, which jointly coordinate an expansion of the thoracic cavity throughout life.

However, skeletal muscles do not only enable movement. Temperature and energy homeostasis in humans also dramatically relies on muscle tissue. Besides consuming more glucose in comparison to any other organ, skeletal muscles also represent the major glycogen storage (Jensen et al., 2011). A stable glucose level is maintained through the uptake and delivery of glucose under the influence of insulin, and additional glucose can be provided in moments of higher demand, such as a fight-or-flight response. During muscle contraction, approximately 30-70% of the utilized energy is released as thermal energy, contributing to approximately 20% of body heat at room temperature and 40% of the necessary heat under cold exposure (Blondin & Haman, 2018; González-Alonso, 2012).

The consequences of various muscle pathologies underline the importance of a physiological functional muscle and its correct development. For instance, Duchenne muscular dystrophy (DMD) leads to progressive muscle weakness, predominantly in young men. Mutations in the coding sequence of the dystrophin gene lead to loss-of-function, which induces various degenerative pathways in the myofibers (Duan et al., 2021). Consequently, patients develop paresis and muscle atrophies at a very young age and are unable to walk by the age of 12-15 years (Zierz et al., 2014). As cardiac and respiratory muscles are also affected, patients later develop cardiac arrhythmias, cardiomyopathies, and respiratory insufficiencies, limiting their life expectancy to just 20 years (Zierz et al., 2014).

The nemaline myopathy is defined by pathologic sarcoplasmic nemaline bodies presumably originating from genetically heterogeneous thin filament abnormalities

commonly caused by actin alpha 1 (*ACTA1*) and Nebulin mutations (Christophers et al., 2022; Romero et al., 2013). The nemaline myopathy affects 1 in 50 000 births and presents variably, from relatively mild to severe (Christophers et al., 2022). Newborns with the severe form present with general weakness and hypotonia in the respiratory, bulbar, and facial muscles, while milder forms present with less involvement of facial muscles and the diaphragm (Sarnat, 1994). Life expectancy varies from a few months to a normal life depending on the unpredictable severity (Benwell et al., 1994).

These examples emphasize the central role of skeletal muscles in vertebrates. It is not difficult to imagine that mutations, metabolic disorders, or auto-immune diseases which cause minor inaccuracies during neuromuscular development or regeneration could significantly impact an individual's survival.

1.1.1 The embryonic origin of skeletal muscles

Understanding the origin of muscle cells and the complex pathways of the early stages of muscle development is crucial to comprehending the complexity and delicacy of myogenesis. In the first days of vertebrate development, the blastula undergoes gastrulation by forming three distinct germ layers: The ectoderm, mesoderm, and endoderm, which give rise to the different tissues of the organism. The ectoderm forms the nervous system and external parts of the body, such as the skin epidermis, mouth epithelium, and the central and peripheral nervous system. The endoderm forms the epithelium of the gastrointestinal tract, liver, pancreas, thymus, thyroid, as well as the respiratory and urinary tract. Moreover, the mesoderm forms the vascular system, dermis, blood cells, connective tissue, and the smooth, cardiac, and skeletal muscles. In the mesoderm, the fundamental tissue structure for developing muscles are the somites, which are formed by paraxial mesoderm cells in a craniocaudal manner (Hirsinger et al., 2000). These somites are composed of pluripotent mesoderm cells that are situated along the craniocaudal axis bilaterally of the neural tube and undergo differentiation, which is partially induced by signals from adjacent somitic cells (Aoyama, 1993; Christ et al., 1972). The intrinsic- and extrinsic-induced differentiation induces a separation of the somite into the myotome, dermomyotome, sclerotome, and the syndetome. During developmental progression, cells in the ventral part of the somite are influenced by notochord-derived Sonic Hedgehog (SHH), which induces paired box 1 (PAX1) and PAX9 expression in these cells of the

forming sclerotome (Dockter, 2000). The dorsal ectoderm and dorsal neural tube express members of the Wnt family (WNT1, WNT 3a, WNT4, WNT6), leading to an expression of PAX3 and PAX7 in the dorsal somitic cells that form the dermomyotome (Fan & Tessier-Lavigne, 1994; Kassar-Duchossoy et al., 2005; Nimmagadda et al., 2007). The dermomyotome is the origin of all muscle progenitor cells (MPCs) for hypaxial, epaxial and some facial muscles (Nimmagadda et al., 2007).

The MPCs in the dermomyotome are subjected to a variety of proliferation factors, such as WNT3a, Fibroblast Growth Factor 4 (FGF4), and Bone Morphogenetic Protein 4 (BMP4), which increase proliferation and inhibit premature differentiation and cell-cycle exit of MPCs, to provide a sufficient number of MPCs for later myofiber development (Amthor et al., 1999; Galli et al., 2004; Kahane et al., 2001). MPCs in the dorsolateral and mediolateral lip of the dermomyotome start to express the myogenic transcription factors Myogenic Factor 5 (MYF5) and Myogenic Differentiation 1 (MYOD1) and therewith form the myotome (Bentzinger et al., 2012). In the myotome, the transcription factors MYF5 and MYOD1 induce a transcriptional cascade by upregulating MYOG and MRF4 expression, and ultimately myogenic cytoskeletal proteins like ACTA1, DESMIN, and MYH1 (Kassar-Duchossoy et al., 2005; Naidu et al., 1995; Venuti et al., 1995; Yee & Rigby, 1993). Interestingly, some MPCs from the dermomyotome avoid this differentiation cascade by maintaining their PAX3 and PAX7 expression during their migration to their target side (Ben-Yair & Kalcheim, 2004; Gros et al., 2005). These MPCs give rise to satellite cells (muscle-specific adult stem cells) of skeletal muscles (Ben-Yair & Kalcheim, 2004; Gros et al., 2005).

1.1.2 Migration of MPCs – from somites to limbs

While MPCs that later form muscles of the ventral body wall and anterior vertebra do not have to leave their somatic origin, MPCs of other hypaxial muscles, like the muscle of the extremities and diaphragm, must migrate long distances (Rudnicki et al., 1993). At the brachial and lumbar levels of the spine, MPCs delaminate from the lateral part of the dermomyotome and migrate (Figure 1.1) toward their target side (Christ & Ordahl, 1995). These migrating MPCs must be directed by attracting and repelling signals as well as local ECM interactions for correct muscle formation (Figure 1.1) (Yin et al., 2013).

Central myogenic factors in early MPC migration are PAX3 and Ladybird homeobox 1 (LBX1) (Figure 1.1) (Schäfer & Braun, 1999). *Lbx1* is expressed in migrating MPCs, and its loss-of-function leads to abnormal limb muscles, supposedly due to faulty migration (Brohmann et al., 2000). Interestingly, some limb muscles, the diaphragm, and the tongue were not affected in *Lbx1* knockout mice (Gross et al., 2000). Gross et al. concluded that LBX1 is, therefore, necessary for the lateral migration of MPCs, yet not for their ventral migration (Gross et al., 2000). Absent limb muscles due to a loss of MPC migration to the limbs were also observed in *Pax3* knockout mice, revealing the importance of PAX3 in distal MPC migration (Bober et al., 1994; Daston et al., 1996; Tajbakhsh et al., 1997) *Msx1*, a homeobox gene like *Lbx1*, was shown to suppress *Pax3* expression and its myogenic activity by inhibiting differentiation and enabling migration (Bendall et al., 1999).

Important cytokines for myogenesis also include the hepatocyte growth factor (HGF) together with its C-MET receptor (Figure 1.1)(Schmidt et al., 1995; Tatsumi et al., 1998). Unviable *c-Met* knockout mice show no migration of MPCs into the diaphragm, limb buds, or tongue (Amano et al., 2002). However, besides HGF expression in the respective limb muscle areas and along the MPC migration route, it does not seem to function as a chemoattractant for MPCs (Mennerich et al., 1998).

Another crucial family of migration-influencing factors are fibroblast growth factors (FGFs). FGF2 and FGF4 were shown to stimulate the migration of MPCs toward the limb buds (Figure 1.1) (Webb et al., 1997). In accordance, the myoblasts of mice with an *Fgfr1* (FGF receptor 1) knockout could not migrate toward the limb buds (Itoh et al., 1996).

Taken together, while several factors are currently known that enable correct MPC migration along large distances, a better understanding of the exact and even unknown pathways is crucial to fully explain the migration behavior of MPCs during skeletal muscle development.

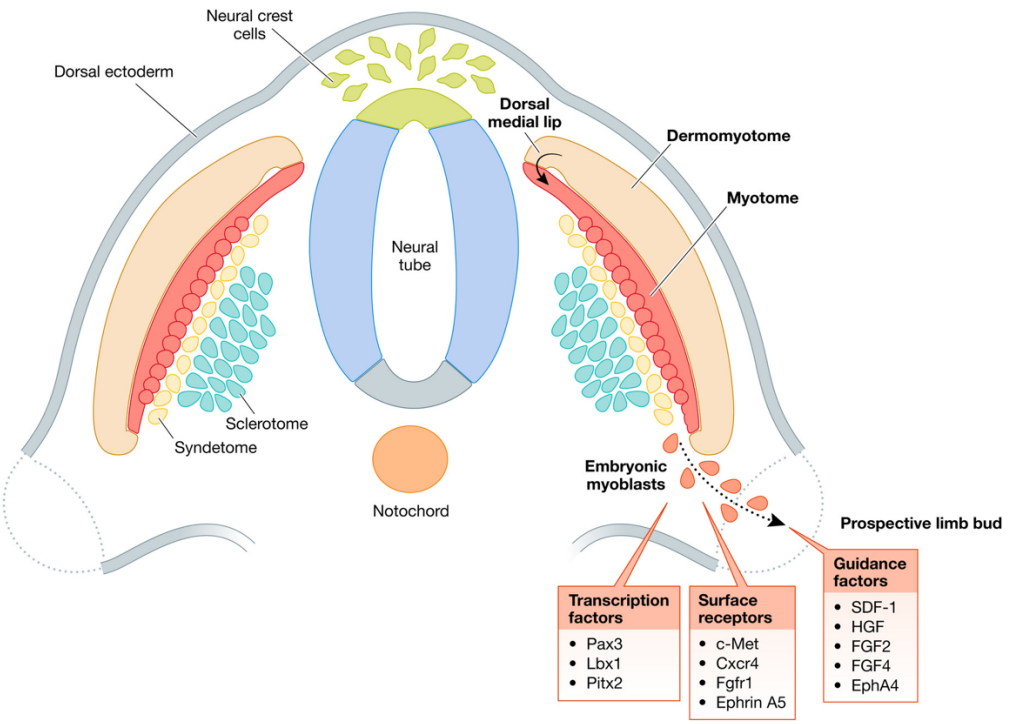

Figure 0.1: Schematic illustration of the dermomyotome and signals involved in myoblast migration.

The migration of MPCs to the prospective limb buds is controlled by transcription factors (e.g., PAX3, LBX1), surface receptors (e.g., C-MET, FGFR1), and guidance factors (e.g., HGF, FGF2, FGF4). Adopted from S. Choi et al., 2020.

1.1.3 Myoblast alignment and fusion – From single myoblasts to powerful contractile elements

In order to create large multinucleated myofibers, an average of 246 myoblasts need to fuse in mice (Cramer et al., 2020). Fusion of myoblast into myotubes can be separated into five steps: 1. Recognition of both binding partner cells; 2. Adhesion of the cells; 3. Membrane alignment; 4. Membrane pore formation and cell fusion; and 5. Cell resolution (Rochlin et al., 2010).

In Drosophila, the formation of individual muscle is based on one founder cell (FC), which in turn fuses with fusion-competent myoblasts (FCMs) (Frasch, 1999). For the recognition of FCs by FCMs and migration of FCMs towards FCs, currently, three signal molecules have been identified: Sticks-and-stones (Sns), Dumbfounded (Duf), and Roughest (Rst)(Bour et al., 2000; Ruiz-Gómez et al., 2000; Strünkelnberg et al., 2001). Duf and Rst are transmembrane proteins expressed explicitly in the founder cells and attract FCMs (Beckett & Baylies, 2007; Menon et al., 2005). Sns, on the other

hand, is expressed in FCMs and was shown to be essential for recognizing and adhering to FCs, possibly by acting as a receptor to Kirre and Rst (Kocherlakota et al., 2008).

In vitro studies with the immortalized mouse myoblast cell line C2C12 identified various signal molecules that are involved in myoblast fusion. Pro-fusion signals include the mannose receptor, mouse odorant receptor 23 (MOR23), CD164, and interleukin 4 (Chargé & Rudnicki, 2003; Griffin et al., 2009; Jansen & Pavlath, 2006; Sohn et al., 2009). These signals induce and support migration towards other myoblasts and thus facilitate fusion. The membrane protein Nephrin, a homolog of SNS in drosophila, was also identified to be involved in myoblast fusion as the knockout of *Nephrin* in mice led to incompletely fused myotubes and underdeveloped muscles (Sohn et al., 2009).

GTPases are a family of hydrolase enzymes that play a crucial role as molecular switches in almost all cellular processes (Johnson & Chen, 2012). Prior to fusion, expression of the GTPase ras homolog family member E (RHOE*)* is increased and induces myoblast elongation and alignment by RHOA, M-CADHERIN and Rho-associated coiled-coil containing protein kinase 1 (ROCK1) regulation (Fortier et al., 2008). Especially the expression of the cell adhesion molecule M-CADHERIN is enhanced and accumulates at the cell-cell contact sites (Fortier et al., 2008). Furthermore, GTPase *Cdc42* (cell division cycle 42) and *Rac1* (RAS-related C3 botulinum substrate 1) deletion in migrating myoblasts provokes a downregulation of the cytoskeleton proteins F-ACTIN, vasodilator-stimulated phosphoprotein (VASP) and Vinculin and presumably by that to a reduction in myocyte fusion *in vivo* (Vasyutina et al., 2009).

Functional crucial in the late stages of myoblast fusion are extracellular receptors of the integrin family (Schwander et al., 2003). ß1-integrin is required for plasma membrane breakdown and regulates the cytoskeleton of myofibers and, therefore, sarcomere assembly (Schwander et al., 2003).

Collectively, extracellular and intercellular signals are essential for the fusion and correct alignment of multinucleated myofibers.

1.1.4 Development of myotendinous junctions – linking muscles and bones

The transmission of the contractile muscle force to bones requires strong tendons. Tendon progenitor cells (TPCs), distinguished by their Scleraxis (*Scx*) expression, originate in the dermomyotome edges or the ectoderm and give rise to the tendon cells (Schweitzer et al., 2001). *Scx* knockout mice show deficiencies in tendon cell differentiation (Murchison et al., 2007). This influence on tendon cell maturation is underlined by the inductive effect of SCX on tendon extracellular matrix genes such as tenomodulin (*Tnmd*) and *Col1a1* (Léjard et al., 2007; Shukunami et al., 2018). Transforming growth factors ß2 and ß3 (TGFß2/3) were shown to be central inductors of SCX and are expressed by neighboring cartilage and myoblasts (Anthwal et al., 2008; Pryce et al., 2009).

For the tendons' correct location, TPCs must align at muscle attachment sides (MAS) between muscles and bones. Ligand-receptor-driven pathways provide the needed directive information. In Drosophila, Kramer et al. showed that TPCs express the slit guidance ligand (Slit), which initially repels MPCs by binding to the roundabout guidance receptor 2 (Robo2) and later attracts MPCs to the MAS (SG Kramer et al., 2001). Additionally, the Derailed (Drl) receptor is expressed in myotubes and epidermal locations along the MAS and helps correct muscle-tendon junction development (Callahan et al., 1996). Interestingly both Slit-Robo and Drl are also involved in guiding axons during development, suggesting the utilization of similar pathways for the guidance of myoblasts and axons (Bonkowsky et al., 1999; Rajagopalan et al., 2000). During myoblast migration and in myotubes at MAS, the transmembrane protein Kon-tiki (Kon) was shown to positively influence directed migration towards the MAS and support tendon cell attachment in drosophila (Schnorrer et al., 2007).

After the assembly of myofibers and TPCs in the MAS, the myotendinous junctions (MTJ) form. MTJs consist of linkage proteins between the extracellular matrix of the tendon to the myofiber cytoskeleton, such as the last A-band of the myofibers, actin filaments, sarcolemma, and external lamina (Miosge et al., 1999; Patel & Lieber, 1997; Tidball, 1991; Trotter, 1993, 2002). The extracellular matrix proteins are provided by the MPCs and TPCs and consist of proteins such as laminins, thrombospondin,

collagens, and the collagen-binding protein P68 (Subramanian et al., 2007; Tidball, 1994; Trotter, 1993).

Hence, pathways involved in MTJ development are essential for correct myogenesis, and TPCs share similar pathways with axon guidance.

1.1.5 The diaphragm –Anatomical structure, development and pathologies

Due to its thin radial myofiber layers and broad surface area, the diaphragm is a well-suited muscle for experimental studies. The diaphragm is organized into three major anatomical structures: The central tendon region (CTR) in the middle of the diaphragm is a trefoil leaf-shaped aponeurosis providing the attachment side for the surrounding myofibers (Pearce, 2009). The musculature of the diaphragm is separated into the costal musculature (CosM) and the crural muscle (CrM) (Pearce, 2009). The CosM consists of a thin layer of radial myofibers stretching from the ribs to the central tendon region. The CrM extends from the vertebrae to the central tendon region, surrounds the aorta and esophagus, and comprises a thicker structure of myofibers.

Three embryonic sources provide cells for the diaphragm: the pleuroperitoneal folds (PPFs), the septum transversum (ST), and the somites (Pearce, 2009). The ST is the initial barrier separating the thoracic and abdominal cavities (Perry et al., 2010). A gene expressed in pre-somitic and somitic dorsal mesoderm, Cbp/p300-interacting transactivator 2 (*Cited2*), is also expressed in the ST, suggesting the ST originates in the dorsal mesoderm (Dunwoodie et al., 1998). Besides a potential scaffold function, it is unclear to what part of the diaphragm the ST contributes. Until now, the ST was only shown to play an essential role in liver development (Asahina et al., 2011).

The PPFs are two bilateral triangular-shaped cell structures, first present around developmental stage E11 in mice (Figure 1.2)(Iritani, 1984; Merrell & Kardon, 2013). PPFs can be identified by their nuclear receptor subfamily 2 group f member 2 (*Nr2f2),* Wilms tumor 1 (*Wt1),* and *Gata4* expression (Clugston et al., 2008). Around E10.5 in mice, MPCs and phrenic nerve axons migrate into the PPFs (Figure 1.2)(Babiuk et al., 2003). At E12.5, the MPCs start to differentiate and fuse into myofibers (Figure 1.2)(Babiuk et al., 2003; Murphy & Kardon, 2011). Between E12.5 and E15.5, the development of the diaphragm expands laterally, ventrally, and medially, which results in an anatomically complete diaphragm by E16.5 (Figure 1.2)(Babiuk et al.,

2003; Murphy & Kardon, 2011). However, biochemical signals involved in the radial alignment of the differentiating myoblasts are currently unknown. Moreover, the fibroblasts for the CTR and connective tissue in the CosM and CrM are provided by the PPFs (Figure 1.2)(Merrell & Kardon, 2013).

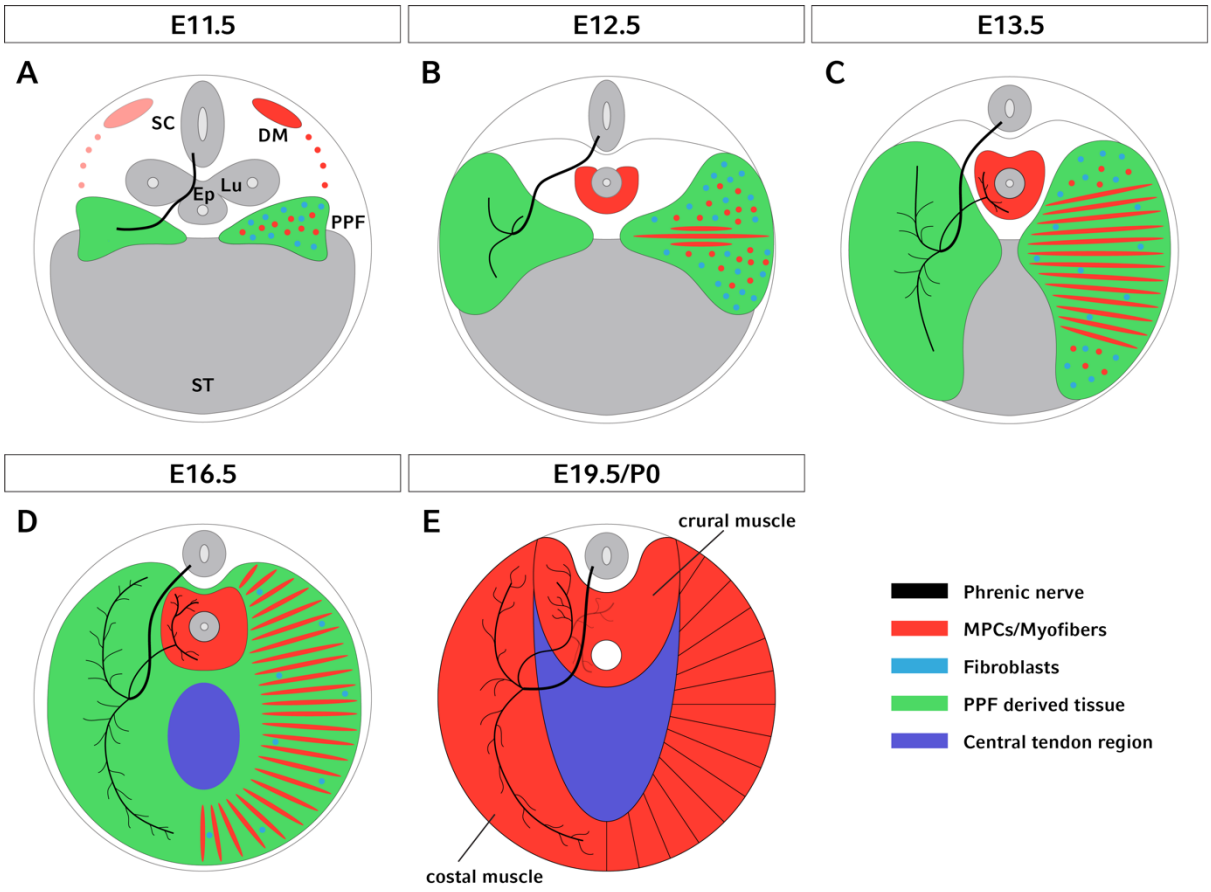

Figure 0.2: The development of the diaphragm.
At E11.5, MPCs and phrenic nerve axons migrate into the PPFs (A). Between E12.5 and E15.5 (B-D), the PPFs expand laterally, ventrally, and medially. By differentiation and fusion of myoblasts, an anatomically complete diaphragm is formed by E16.5. Until birth (E19.5/P0), the myofibers undergo hypertrophy to build a fully functional diaphragm (E). The illustration separates phrenic nerve innervation, MPC migration, and fusion for a better explanation. Note that this development is bilateral and simultaneous. Adapted from Saller et al. (Saller et al., 2017).

A pathology that underlines the importance of correct diaphragm development and the importance of myogenesis signaling is the congenital diaphragm hernia (CDH). CDHs are, with a prevalence of 1:4,000, a common congenital pathology associated with significant morbidity and mortality (Pober, 2007). The integrity of the diaphragm is interrupted by tissue discontinuity (holes) and/or regions that completely lack

skeletal muscles. As the diaphragm, besides its contractive function for breathing, separates the thoracic cavity from the abdominal cavity, the interrupted integrity can lead to herniation of abdominal organs into the chest cavity upon the newborn's first breath (Pober, 2007). These herniations can compress the lung and heart and directly affect respiration and circulation in a critical manner.

Syndromes like Fryns, Craniofrontonasal, and Beckwith-Wiedemann, or chromosomal abnormalities like trisomy 9 and 21, are associated with CDH (Holder et al., 2007). More specifically, several genes associated with CDH, including *Fog2a, Couptf2, Wt1a, Slit3,* and *Gata4*, have been identified in knockout mice (Ackerman et al., 2005; Carmona et al., 2016; Yu et al., 2013; Yuan et al., 2003). Interestingly, myogenic cells show no expression of *Gata4*. However, a strong expression of *Gata4* in fibroblasts of the PPFs was shown, and *Gata4* null fibroblasts cause CDHs in mice (Merrell et al., 2015). Hence, fibroblast signaling is essential for correct diaphragm development. Underlining this, decreased *Tcf4* and *Prx1* expression in PPFs may also cause CDHs (T. Takahashi et al., 2016). Moreover, *Slit3* knockout mice were observed to develop, among other malformations, CTR ruptures, possibly by tendon thinning (Liu et al., 2003; Yuan et al., 2003).

Therefore, the involvement of a variety of signals and notably different cell types is essential for proper diaphragm development.

1.2 NELL proteins and why they are likely to influence myogenesis

Epidermal growth factor-like (EGFL) repeats are part of many secreted proteins as well as membrane proteins and are involved in various protein binding interactions (Engel, 1989; Kuroda & Tanizawa, 1999). Some of these EGFL domain-containing proteins include the well-studied NOTCH receptor and the SLIT ligands (Rothberg et al., 1990; Wharton et al., 1985). In chickens, a protein containing five EGFL domains was identified by Matsuhashi et al. as the neural epidermal growth factor-like (NEL) protein (Matsuhashi et al., 1995). NEL contains two hydrophobic domains, four cysteine-rich structures, one histidine-rich domain, and five EGFL domains (Matsuhashi et al., 1995). *In situ* hybridization (ISH) in the early stages of chicken development showed a strong expression of *Nel* in neural tissue, like the brain, spinal cord, and dorsal root ganglia (Matsuhashi et al., 1995; Watanabe et al., 1996).

Nel-like 1 (*Nell1*) and *Nel-like 2* (*Nell2*) are two homologs of *Nel*, which were identified by Kuroda et al. in humans and mice (Figure 1.3)(Watanabe et al., 1996). The nucleotide sequence of human *Nell1* is very similar (87%) to mouse and rat *Nell1*. Human *Nell2* has an even higher similarity of 90% for mice and >90% for rat *Nell2* (GeneBlast; NCBI, USA). Mouse NELL1 and NELL2 show an approximately 87% homology and have a very similar domain structure (Figure 1.3)(GeneBlast; NCBI, USA). Both NELL proteins contain a laminin G-like domain, a coiled-coil (CC) domain, four von Willebrand factor type C (vWC)-like domains, and six EGFL domains (Figure 1.3)(Watanabe et al., 1996). Watanabe et al. found that an extra EGF-like repeat could arise in *Nel* by a frameshift, creating a higher similarity between *Nel* and human *Nell2* (Watanabe et al., 1996). Whole genome sequencing identified another *Nell1* sequence and *Nell2* as the human counterpart of *Nel* (Watanabe et al., 1996). The name NEL-like is, therefore, somewhat misleading.

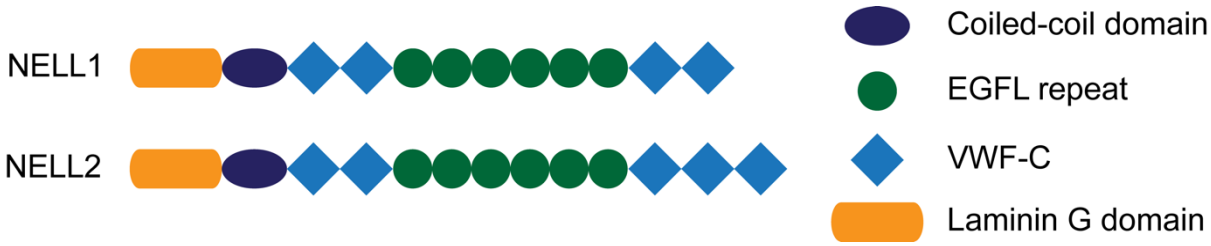

Figure 0.3: The similarity of NELL1 and NELL2.
Mouse NELL1 and NELL2 have a highly similar domain structure. NELL1 consists of one laminin G domain, a coiled-coil domain, six EGFL domains, and four VWF-C domains. NELL2 has the same domain structure with an additional VWF-C domain.

1.2.1 NELL1, an osteogenic signal that potentially influences myogenesis

The human *Nell1* gene of 907,311 bp length encodes an 810 amino acid protein with various structural domains (S. Kuroda et al., 1999). In a thrombospondin-1-like fashion and probably through the coiled-coil domain, NELL1 forms a homotrimer when secreted (S. Kuroda et al., 1999). Kuroda et al. showed that NELL1 binds to certain forms of protein kinase C (-β1, -δ, -τ) through the EGFL domains, while Takahashi et al. showed moderate affinity to immobilized heparin through its thrombospondin-like domain (K. Takahashi et al., 2015).

Nell1 expression in mice during embryogenesis starts in E11.5 mice and stays expressed until P17 (S. Kuroda et al., 1999). In rats, *Nell1* expression was explicitly shown in neural cells, suture fusion, and osteoprogenitor cells of the developing calvarial bone (S. Kuroda et al., 1999; Ting et al., 1999). In line with the expression pattern of *Nell1* in rats, *Nell1* expression in humans was shown in mesenchymal cells and osteoblasts within recently fused sutures and notably earlier in the prematurely fusing suture sites (Ting et al., 1999). Pathological tissues, including the human leukemic pre-B cell line, Burkitt's lymphoma Raji cells, embryonal neuroepithelial tumors like neuroblastoma, medulloblastoma, and neurocytoma, show *Nell1* expression (S. Kuroda et al., 1999; Luce & Burrows, 1999; Maeda et al., 2001). Furthermore, NELL1 was identified to cause malignancy-associated membranous nephropathy in *Nell1*-expressing tumors (Zhai et al., 2019).

Interestingly, NELL1 interacts with various pathways involved in osteogenesis. The osteoinductive growth factors FGF2 and TGFβ1 induce *Nell1* expression, possibly via the *Cbfa1*/*Runx2* pathway (Aghaloo et al., 2006). Moreover, while *Osf2*/*Runx2* expression leads to an upregulation of *Nell1* expression, MSX2 inhibits *Nell1*

expression via *Osf2*/*Runx2* (Shirakabe et al., 2001; Truong et al., 2007). In mesenchymal stem cells, the osteogenic bone morphogenic protein 9 (BMP9) induces NELL1 expression, potentiating the osteogenic differentiation and overcoming the BMP9-induced adipogenesis by the anti-adipogenic effect of NELL1 (He et al., 2017). Cowan et al. and Zhang et al. investigated the regulatory effect of NELL1 on differentiation markers. Osteoblastic differentiation markers like bone sialoprotein (BSP), osteocalcin (BGP), osteopontin (OPN), and the chondrocyte differentiation marker mRNA encoding type X collagen (COL10) were strongly upregulated by NELL1 (Cowan et al., 2006; Xinli Zhang et al., 2002).

Several studies have identified and investigated the role of NELL1 in osteogenic differentiation and bone formation. Ting et al. identified a high *Nell1* expression in human unilateral coronal synostosis and rat cranial intramembranous bone (Xinli Zhang et al., 2002). Transgenic *Nell1* overexpressing mice led to premature closing of sutures and calvarial overgrowth (Xinli Zhang et al., 2002). Interestingly these skeletal defects were limited to calvarial bones (Xinli Zhang et al., 2002). *In vitro* studies with differentiating osteoblasts that overexpress *Nell1* showed a strong expression of late osteoblast differentiation markers (*Bnp-7*, *osteocalcin*, *osteopontin*), while osteoblasts with a reduced *Nell1* expression showed reduced and delayed differentiation (Xinli Zhang et al., 2002). The same transgenic mouse model and overexpressing osteoblasts also showed enhanced cell apoptosis dependent on the expression level, possibly causing premature suture closing (Zhang et al., 2003). Moreover, Cowan et al. showed that NELL1 stimulates enchondral ossification and chondrocyte hypertrophy (Cowan et al., 2006). *Nell1* reduction in mice also demonstrates severe osteogenic anomalies. Desai et al. revealed that the reduction of *Nell1* transcripts in mice causes neonatal lethality, with various bone malformations, including alterations of the vertebral curvature and enlarged skulls (Desai et al., 2006). Therefore, the importance of NELL1 as an important osteogenesis and chondrogenic differentiation promoter is obvious.

Several studies that investigated the role of NELL1 in human cancers could show that NELL1 functions as a tumor suppressor gene. Hypermethylation of NELL1 promotor and loss of heterozygosity, both leading to reduced gene expression, was shown in a variety of human cancers (Eissa et al., 1998; Jin et al., 2007). These cancers include colon cancer, esophageal squamous cell carcinoma, and esophageal adenocarcinoma (Jin et

al., 2007; Mori et al., 2006). NELL1 was shown to stimulate cancer stem-like differentiation in lung cancer and could potentially be used as a therapeutic target in lung cancer treatment (Hasebe et al., 2012).

More importantly for this study, NELL1 might play a role in muscular soft tissue repair (Turner et al., 2014). Turner et al. showed that NELL1 improves the constructive remodeling outcome in muscle injury models, which leads to an increase in the contractile force of the repaired muscle model (Turner et al., 2014). Thus, NELL1 might directly affect muscle regeneration and could also play a role in the embryologic development of muscles.

These various biological functional properties of NELL1 show that it is an essential protein in embryogenesis, tumor development, and soft tissue repair. Further studies are needed to dissect the role of NELL1 in the myogenic pathways and other tissues in more detail.

1.2.2 NELL2, a neurotropic protein with a myogenic expression pattern

Even though Human NELL1 and NELL2 show just a 55% homology, they have a highly similar domain structure (Watanabe et al., 1996). NELL2 contains one coiled-coil domain, six EGFL domains, five vWC domains, and one laminin G-like domain (S. Kuroda et al., 1999; Matsuhashi et al., 1995).

Nelson et al. showed that *Nell2* is expressed in an interesting differential manner during muscle and neuronal development (Nelson et al., 2002). In neuronal development, *Nell2* expression spikes during differentiation of sensory and motor neurons, and expression can be observed in the brain, retina, spinal cord, and peripheral sensory ganglia (Nelson et al., 2002). At E4.5, high *Nell2* expression can be seen in the mantle layer of the spinal cord, especially in motor neuron regions (Nelson et al., 2002). The expression declines in the following days and is restricted to motor neuron pools (Nelson et al., 2002). In early chicken development, faint *Nell2* expression was initially discovered in somites and the neural tube in the Hamburger-Hamilton stage (st) 13-15 (Nelson et al., 2002). By st 17, the lateral dermomyotome, containing the hypaxial precursor cells, showed a localized *Nell2* upregulation (Nelson et al., 2002). Later at st 21, *Nell2* expression can be detected in the posterior region of the ventral and dorsal forelimb (Nelson et al., 2002). Around st 25, *Nell2* expression is

strongly reduced, besides a weak expression in the proximal forelimb at E6.5 and E8.5 (Nelson et al., 2002). Nelson et al., in summary, showed that *Nell2* is spatiotemporally regulated in specific regions of the nervous system and dermomyotome. The expression of *Nell2* in hypaxial muscle precursor cells, the continuous expression during migration to their target fields, and the downregulation in the terminal differentiation program suggest NELL2 is a migration cue in myogenesis. *Nell2* expression was also detected at equivalent levels in B-cells, T-cells, monocytes, and natural killer cells (Luce & Burrows, 1999).

Unsurprisingly, NELL2 has been defined multiple times as a neurotrophin, a growth factor inducing neuron differentiation, survival, and development (E. J. Choi et al., 2010; D. H. Kim et al., 2014). Jaworski et al. identified NELL2 as a repulsive guidance cue, repelling spinal commissural axons across the midline of the spinal cord (Jaworski et al., 2015). This is mediated through the second and third EGFL-domain of NELL2 binding to the FN1 domain of ROBO3 (Jaworski et al., 2015).

In the developing mouse retina, NELL2 enhances retinal ganglion cell differentiation and protects these cells from apoptosis (Nakamoto et al., 2014). While the repulsive guidance in the spinal cord is mediated through the ROBO3 receptor, *Robo3* is not expressed in retinal ganglion cells (Blackshaw et al., 2004). However, *Robo1* and *Robo2* are expressed within the retinal ganglion cell layer, but the expression profile does not match the retinogeniculate projection (Erskine et al., 2000). Nakamoto et al. also identified that the cysteine-rich domain exerted inhibition of retinal axons, while Jaworski et al. revealed that the EGFL-repeats were responsible for axon repulsion (Jaworski et al., 2015; Nakamoto et al., 2014). This suggests that NELL2 acts through its different domain binding to unknown receptors (Nakamoto et al., 2019). The similarity to thrombospondin 1 also implies that NELL2 interacts with various cell-surface molecules (Nakamoto et al., 2019).

NELL2's neurotropic properties also affect endocrine pathways. It was revealed to act on glutamatergic neurons, through which it influences Gonadotropin-Releasing-Hormone (GnRH) release (Ha et al., 2008). The anti-apoptotic effect of estrogen on neuronal cells was granted to NELL2 (E. J. Choi et al., 2010). It may also be a modulator of the effect of estrogen on the reproductive circle (Ryu et al., 2011). In male rats,

NELL2 was shown to be involved in the sexually dimorphic nucleus development (Jeong et al., 2008).

As *Nell1*, *Nell2* expression is also modified in cancer cells. In neuroepithelial tumor cells and Burkitt's Lymphoma cells, *Nell2* is upregulated (S. Kuroda et al., 1999; Maeda et al., 2001). However, the role of NELL2 in human cancers remains unclear. Besides malignant tumors, *Nell2* expression was also revealed to be elevated in hyperplastic prostate and enhanced cell proliferation while inhibiting apoptosis through the ERK pathway (Liu et al., 2021).

The expression pattern of *Nell2* during muscle development, together with the differentiation effects on other tissues, make NELL2 a likely candidate for influencing myogenic development.

1.2.3 NELL-ROBO, possible binding partners for myogenesis.

The only known binding partner of NELL ligands are ROBO receptors. As previously described, the binding of NELL2 to ROBO3 was revealed to mediate the repulsion of the spinal commissural axons in the spinal cord (Jaworski et al., 2015). The study also showed that NELL1 binds to ROBO3. However, it is not expressed in the spinal cord and does not affect axon guidance (Jaworski et al., 2015). On another note, the skeletal defects of *Nell1*-deficient mice described by Desai et al. might resemble the progressive scoliosis disorder of humans with a *ROBO3* mutation (Desai et al., n.d.; Jen et al., 2004). Therefore, in a different spatiotemporal tissue location, NELL1 could still function as a ROBO3 ligand (Yamamoto et al., 2019). Yamamoto et al. investigated the binding of NELL-ligands to the other ROBO receptors, ROBO1 and ROBO2 (Yamamoto et al., 2019). While ROBO1 does not bind NELL1 or NELL2, NELLs were identified to bind to a cryptic binding site on the ROBO2 fibronectin type III domain (Yamamoto et al., 2019). This hairpin-like binding site might become unmasked by conformational changes in the extracellular domain or by proteolytic digestion (Yamamoto et al., 2019). A reduction in neural crest cells in the vertebral column in NELL1-deficient mice and reduced cranial neural crest cells in *Robo1* and *Robo2* knockout mice show an overlapping phenotype and therefore suggest binding of NELL1 and ROBO2 and possibly ROBO1 (Li et al., 2017; Ting et al., 1999; Yamamoto et al., 2019).

There is no reported expression of *Robo3* during muscle development, while in Drosophila, *Robo1/2* are expressed in muscle attachment sites (SG Kramer et al., 2001). Therefore, if NELLs play a role in myogenesis, ROBO2 might be the cryptic receptor enabling the signaling.

1.2.4 SLIT-ROBO system, showing the potential power of the ROBO receptors.

The function of SLITs, the other ligand family that bind to ROBO, has been dissected in much greater detail when compared to NELLs. SLIT1-3 bind with their LRR2 domain to the first Ig-domain of ROBO1 and ROBO2 (Figure 1.4)(Morlot et al., 2007).

Both SLIT and NELL ligands have some similarities in their biological effect. Like NELL2, SLIT1/2 have a repulsive effect on ROBO1/2-positive axons after midline crossing (Long et al., 2004). *Slit2* expressed by motor axons was shown to regulate fasciculation and migration through ROBO1/2 (Jaworski & Tessier-Lavigne, 2012). Like NELL1, SLIT-ROBO also is involved in bone metabolism (Niimi, 2021). SLIT3, derived from osteoclasts, was identified as an anabolic bone factor, acting on *Robo1/2*-expressing osteoblasts to promote migration and proliferation (Xinli Zhang et al., 2002).

Besides the involvement in axon guidance, SLIT-ROBO is crucial for heart development (Zhao & Mommersteeg, 2018). Here, a variety of defects between various SLIT or ROBO mutations show the specific ligand-receptor combinations needed for correct heart development (Zhao & Mommersteeg, 2018). SLIT3-ROBO1 binding is involved in the membranous ventricular septum development, while SLIT2-ROBO1/2 binding is required for the formation of the aortic semilunar valve leaflet (Jaworski & Tessier-Lavigne, 2012).

More importantly, for myogenesis, SLIT1/2 act together with their receptor ROBO as a complex guidance cue in muscle precursor migration (Halperin-Barlev & Kalcheim, 2011). In the first phase of migration, *Slit1* is expressed by the sclerotome and acts repulsive, guiding *Robo1/2*-expressing MPCs away from the midline (Halperin-Barlev & Kalcheim, 2011). During the second phase of migration, SLIT1, expressed by tendon progenitor cells in the MAS, acts as an attractive cue on the cells it repelled before (SG Kramer et al., 2001). Saller et al. also identified that SLIT1/2 are expressed by motor neuron growth cones and attract myogenic progenitor cells showing another cell type

besides fibroblasts is involved in myogenesis (Saller, 2016). Thus, SLIT, together with ROBO1/2, acts as a dynamic migration signaling in myogenesis. However, the underlying mechanism of the changes in the effect of SLIT within a few hours remains unclear.

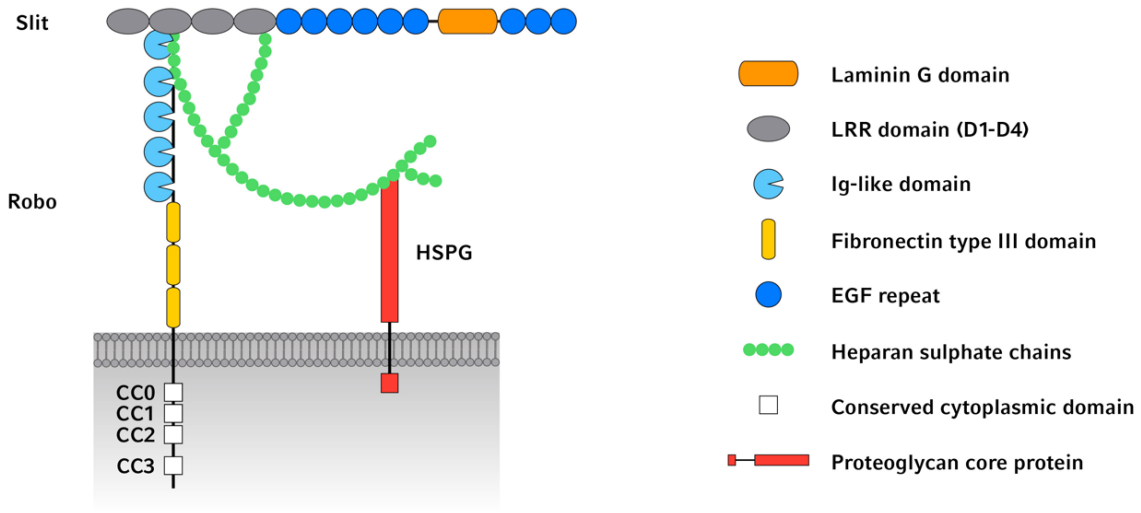

Figure 0.4: SLIT-ROBO binding.
SLIT1-3 bind with their second LRR domain to the first Ig-domain of ROBO1 and ROBO2. Heparan sulfate proteoglycans (HSPGs) stabilize the binding with heparin sulfate chains as co-receptors (Fukuhara et al., 2008). Adapted from Saller et al. (Saller, 2016).

1.3 Aim of this study

Myogenesis is a highly complex process controlled by various paracrine and autocrine signals. While some of these ligand-receptor pathways are well investigated, most are presumably still unknown. Identifying these pathways is crucial for skeletal muscle tissue engineering, and some of these ligand-receptor systems could be used in therapeutic approaches for skeletal muscle pathologies such as sarcopenia. Therefore, with this study, I aim to reveal a new ligand-receptor pathway that is highly probable to impact myogenesis - the NELL-ROBO system.

1.3.1 Revealing the effect of NELLs on myogenesis

Various NELL findings identified these ligands as potential myogenesis signals worth investigating. NELL1 increases the contractile force in muscle injury models and, therefore, might directly affect muscle regeneration (Turner et al., 2014). NELL2 acts as a guidance cue on spinal axons to enhance differentiation in retinal ganglion cells and acts as a ligand essential for neural embryogenesis (Jaworski et al., 2015; Nakamoto et al., 2014). ROBOs, the receptor family for NELLs, are involved in a variety of pathways, which are active during embryogenesis, such as motor axon guidance, bone development, and metabolic processes, but more significantly, SLIT-ROBO was shown as a dynamic MPC guidance signal (Halperin-Barlev & Kalcheim, 2011; Jaworski & Tessier-Lavigne, 2012; B. J. Kim et al., 2018; Niimi, 2021; SG Kramer et al., 2001) The expression profile shown by Nelson et al. strengthens this theory, as *Nell2* is spatiotemporally regulated in specific regions of the nervous system and the muscle lineage (Nelson et al., 2002).

Thus, I recognized NELLs to have a high likelihood of affecting myogenesis and aimed to uncover their effect on muscle development. Therefore, I investigated the consequence of NELL1 and NELL2 on differentiating myoblasts during migration, alignment, and fusion *in vitro*.

1.3.2 Identifying the origin of *Nell2* expression during myogenesis

A variety of cell types influence skeletal muscle development by paracrine signals. TCF4 and GATA4 are expressed by muscle-specific fibroblasts and provide a pre-pattern for myoblasts in muscle development, while motor neurons express SLIT2 to attract and later repel myoblasts (Merrell et al., 2015; Saller, 2016; T. Takahashi et al.,

2016). As these cells, amongst other cell types, lie within the skeletal muscle tissue, identifying the expression origin of a protein is difficult.

Nelson et al. identified the continuous expression of *Nell2* during MPC migration by *in situ* hybridization (Nelson et al., 2004). Thus, I also expected NELL2 to be expressed by nMMCs, and hence created a reporter mouse line to separate MMCs from nMMCs. Using next-generation sequencing, I aimed to reveal a myogenesis pathway between nMMCs and MMCs with NELLs and their, presumably ROBO, receptors.

2. Material and Methods

2.1 Animal husbandry

2.1.1 Ethics statement

The handling and housing of mice were conducted according to institutional and federal guidelines of the Ludwig-Maximilians-University of Munich and the government of Upper Bavaria (TVA ROB-55.2-2532.Vet_02-16-15).

2.1.2 Animal housing & mouse lines

Mice were housed in individually ventilated cages (ICV Blue Line Sealsafe, Tecniplast, Italy) with an area of 530 cm^3. Controlled temperature and a 12 h light/dark cycle were used in the animal facility. Female mice were housed at a maximum of 5 mice per cage, while male mice were housed alone. Time mating was set up with 1 male mouse and 1 to a maximum of 2 female mice overnight (ON). Female mice were checked for insemination by inspecting for vaginal plugs, and the embryo stage was considered as E0.5.

The following mouse strains were used: *Prrx1*^{Cre} (Logan et al., 2002); *Rosa26*$^{mT/mG}$ (Muzumdar et al., 2007); *Acta1*^{Cre} (Miniou et al., 1999). As a control and general-purpose strain, Swiss mice (Lynch CJ, 1969) were used.

2.1.3 Genotyping

To determine if the mice were carrying the desired mutation, a PCR was conducted. Mouse genomic DNA (gDNA) was isolated from mouse tail tips by digestion with 100 µl of Quick Extraction Buffer (Biozym, Germany) for 10 min at 65°C, followed by an enzyme inactivation at 98°C for 2 min. Samples were centrifuged shortly to spin down not yet digested tissue.

Table 2.1: Instruments & chemicals for gDNA isolation.

Instruments	
Thermomixer	Thermomixer comfort, Eppendorf, Germany
Centrifuge	Centrifuge 5415 D, Eppendorf, Germany
Chemicals	
QuickExtract Buffer	Biozym, Germany

PCR-specific primer pairs, described in table 2.3, were used with the following amplification parameters: pre-heating (95 °C for 5 min), 10 cycles of denaturation (95 °C for 30 sec), annealing (63 °C for 30 sec), elongation (72 °C for 45 sec), 35 cycles of denaturation (95 °C for 30 sec), annealing (53 °C for 30 sec), elongation (72 °C for 45 sec) and a final extension step (72 °C for 5 min). The amplified fragment size was analyzed using gel electrophoresis on a 2% agarose gel in 1x TAE buffer with 0,05 µl/ml ethidium bromide on a UV gel imager.

Rosa26$^{mT/mG}$*;Acta1*^{Cre} embryos were genotyped by the validation of GFP^{+} muscles under a fluorescence microscope.

Table 2.2: Instruments & chemicals for PCR.

Instruments	
Thermal cyclers	Peltier Thermal Cycler 200, Bio-Rad, USA
Fluorescence microscope	peqSTAR 2x, PEQLAB, Germany
Power supply	Axio Observer Z1, Zeiss, Germany
Gel System	Peqpower 300V, Peqlab, Germany
Transilluminator	Owl Separation System B2, Thermo Fisher, USA
Chemiluminescence documentation	Bio-Print 1000, Vilber Lourmat, Germany
	BioCapt, Vilber Lourmat, Germany
Chemicals	
GeneRuler™ DNA Ladder Mix	Thermo Fisher, USA
Taq DNA Polymerase	Qiagen, Germany
PCR Nucleotide Mix	Roche, Switzerland
10x PCR Buffer	Qiagen, Germany
Water PCR Grade	Roche, Switzerland
LE Agarose	Biozym, Germany
Ethidium bromide solution	Sigma-Aldrich, USA
Buffers	
1 x TAE buffer	40 mM Tris-Acetat, Sigma-Aldrich, USA
	1 mM EDTA-HCl (pH 8.0), Sigma-Aldrich, USA

Table 2.3: Primer for genotyping

Gene		Primer sequence	Temp.
$Rosa^{mT/mG}$	Common: oIMR7318	5′-CTCTGCTGCCTCCTGGCTTCT-3′	63 °C
	Wt rev: oIMR7319	5′-CGAGGCGGATCACAAGCAATA-3′	63 °C
	Mutant rev: oIMR7320	5′-TCAATGGGCGGGGGTCGTT-3′	63 °C
Cre^{+}	fwd	5′-GTGTCCAATTTACTGACCGTACAC-3′	63 °C
	rev	5′-GACGATGAAGCATGTTTAGCTGG-3′	63 °C

2.1.4 Dissection of embryonic tissues

For the isolation of embryo diaphragms and muscles, pregnant mice were sacrificed by cervical dislocation on the day of the desired embryonic developmental stage. For organ dissection, the embryos were decapitated, skinned, and the diaphragm, tongue, heart, and extremities were dissected under a stereomicroscope (M165 FC, Leica, Germany) and kept in phosphate-buffered saline (PBS, Thermo Fisher Scientific, USA) at 4 °C. For whole-mount embryos, embryos older than E16.5 were sacrificed by intraperitoneal injecting of 0.5% Pentobarbital (200 mg/kg). Afterward, they were deskinned and stored in 1x PBS at 4 °C for later use.

2.1.5 Fixation of embryos and organs for histological slides

Histological slides were prepared for overview images. The embryos or organs were rinsed twice in PBS, fixed in 4% paraformaldehyde (PFA, Merck, Germany) in PBS overnight at 4 °C. The next day, samples were washed in PBS and transferred into a 30% sucrose solution (in 2x PBS). The following day, after the samples had sunk, they were embedded in Tissue-Tek (Tissue-Tek® O.C.T.™, Sakura, Japan) and frozen at -80 °C by inserting them into liquid nitrogen. The samples were then sectioned into 12 µm thick slices on a cryotome (Cryostar NX50™, Thermo Scientific, USA) and stored on slides at -20 °C.

2.2 Determining the gene expression profile of non-myogenic muscle cells

2.2.1 Dissection of the diaphragm from embryos for FACS

For next-generation RNA sequencing, I isolated the diaphragms, digested the tissue, and separated the cells using fluorescence-activated cell sorting (FACS). The diaphragms were collected as described in 2.1. The diaphragm was then minced in a petri dish on ice with a needle scalpel in a drop of PBS. The tissue fragments were transferred into a falcon of 4 ml Dulbecco's modified eagle medium (DMEM) without phenol red (DMEM 4,5 g/l D-Glucose, without pyruvate, Thermo Fisher Scientific, USA) with 4 mg/ml Dispase and 4 mg/ml Collagenase II and incubated in a 37 °C water bath. The digestion was supported by triturating the tissue fragment medium mix using a 5 ml pipette every 5 min. After 1 hour, the cells were filtered through a 40 µm cell strainer and centrifuged at 500 g at 4 °C for 10 min. Afterward, the supernatant was discarded, and new DMEM without phenol red indicator was added and kept on ice until FACS.

2.2.2 FACS

The FACS was conducted by the Core Facility Flow Cytometry at the Biomedical Center Munich (LMU, Munich). As a control, the diaphragm cells of *Rosa26*$^{mT/mG}$ (no GFP expression) and *Acta1*^{Cre} (no fluorescence) were used. The cells were separated based on the side scatter, forward scatter, and their fluorescence (RFP and GFP). The cells were then sorted into 300 µl Lysis Buffer (RNEasy RLT-Buffer, Qiagen, Germany) with 1% ß-mercaptoethanol (Sigma-Aldrich, USA), and cells were stored at -80 °C.

2.2.3 cDNA synthesis and quantitative PCR

A qPCR on the sorted cells was performed to prove the successful separation of nMMCs from MMCs. The RNA obtained from the cells of the FACS was reverse-transcribed using the transcription first-strand synthesis kit (Roche, Switzerland) according to the manufacturer protocol. A 1:5 dilution of the cDNA in RNase-free H_2O was used. The reaction was performed using a solution of 1 µl appropriate FAM-primer (*Acta1* and *Gapdh*, PrimeTime qPCR Assay, IDT, USA; Table

2.4), 8 µl H_2O, 10 µl master mix (Roche, Switzerland), and 1 µl of the primer in a LightCycler 96 System (Roche, Switzerland).

Table 2.4: qPCR primer

Primer ID for qPCR	
Acta1	Mm.PT.58.7312945
Gapdh	Mm.PT.39a.1

2.2.4 Next-generation sequencing

To analyze the expression profile of the nMMCs, I used next-generation RNA sequencing. The next-generation sequencing of the extracted RNA was conducted by the Blum Laboratory for Genomics of the Laboratory for Functional Genome Analysis (LAFUGA, LMU, Germany). The SMART-Seq v4 Ultra Low Input RNA Kit for Sequencing full-length transcriptome analysis with ultimate sensitivity (Takara Bio, Japan) was used. The HiSeq1500 device (Illumina, USA), with a read length of 50 bp and a sequencing depth of around 6 million reads per sample, was used. The reads were then aligned to the mus musculus genome (release GRCh38.99). For further statistics and comparisons, I used transcripts per million reads (TPMs) and data from other sequencing data in our laboratory.

The sequencing data obtained was compared to other data from our muscle group. The whole muscle probe is mRNA from an entire quadriceps muscle of 3.5-month-old mice. The myostatin (MSTN) muscle probe is from mice overexpressing MSTN, which inhibits muscle growth and is a model for pathological muscle. For investigating the expression compared to tendon cells, I used sequencing data of $SCP1^{GFP/SCX}$ cells, which mimic the tendon cell lineage (Kohler et al., 2013). Lastly, instead of the MMCs, I used C2C12 cells in different stages of differentiation (after 24 h, 72 h, 96 h & 144 h).

2.3 Cell culture

2.3.1 Maintaining cultured cells

Cells were kept in cell culture flasks (Nunc™EasYFlask™, Thermo Fischer, USA) with Dulbecco's Modified Eagle Medium (4,5 g/l D-Glucose, Pyruvate, Thermo Fisher Scientific, USA) with 10% fetal bovine serum (FBS, heat-inactivated, Sigma-Aldrich, USA) and 1% P/S (Penicillin-Streptomycin, Biochrom, Germany). The standard medium was changed every 3 to 4 days. Cells were kept in incubators at 37 °C and 5% CO_2.

Table 2.5: Instruments, cells, medium, recombinant proteins for cell culture.

Instruments	
Cell culture flasks	Nunc™EasYFlask™, Thermo Fischer, USA
6 well plate	Nunc™ 6 well plate, Thermo Fischer, USA
Centrifuge	Axio Universal 16R, Hettich, Germany
Fluorescence Microscope	Axio Observer Z1, Zeiss, Germany
Microscope program	ZEN lite 2012 (blue edition), Version 1.1.2.0, Zeiss, Germany
Time-lapse microscope	Microscope Axiovert S100, Zeiss, Germany
Incubator time-lapse	Incubator XL100/135 PeCon, Germany
Cells	
C2C12	Immortalized mouse myogenic cell line, ATCC
SCP1	Single-cell-derived human mesenchymal stem cell line
SCP1RFP;NELL2::AP	SCP1-cells overexpressing NELL2:AP (by Sleeping beauty vector)
SCP1RFP	SCP1-cells overexpressing RFP (by Sleeping beauty vector)

Medium, buffers and chemicals	
DMEM	Dulbecco's Modified Eagle Medium (4,5 g/l D-Glucose, Pyruvate), Thermo Fisher Scientific, USA
FBS	Fetal bovine serum, heat-inactivated, Sigma-Aldrich, USA
Trypsin	Trypsin ((1:250)/EDTA-Solution (0,5%/0,2%) w/o Ca, w/o Mg), Merck, Germany
PBS	PBS (phosphate buffered saline), Thermo Fisher Scientific, USA
HS	Heat-inactivated horse serum (HS), Life Technologies, USA
P/S	Penicillin-Streptomycin, Biochrom, Germany
DMSO	Dimethyl Sulfoxid, AppliChem, Germany
Standard Medium	DMEM with 10% FBS and 1% P/S
Recombinant Proteins	
mNELL1-RP	Recombinant Mouse NELL1 Protein, R&D Systems, USA
mNELL2-RP	Recombinant Mouse NELL2 Protein, R&D Systems, USA

2.3.2 Cell splitting

Seeded cells were split by discarding the medium and washing the cells with 3 ml PBS. Afterward, 3 ml trypsin (Trypsin/EDTA-Solution, Merck, Germany) in PBS was used to detach the cells from the flask. After 5 min at 37 °C, cell detachment was confirmed under a microscope. 3 ml standard medium was added to deactivate the trypsin. The cell suspension was transferred into a falcon, and the number of cells per ml was counted using 10 µl of the cell suspension on a Neubauer chamber (Brand, Germany). Afterward, the cells were centrifuged for 5 min at 500 g at room temperature, and the supernatant was discarded. Fresh medium was added, and the desired number of cells was transferred into new cell culture flasks.

2.3.3 Thawing and cryopreservation of cells

For thawing, cells were put into a 37 °C water bath. The cells were resuspended in 5 ml standard medium and centrifuged at 500 g for 5 min. The supernatant was discarded, and the cells were seeded in a flask with fresh medium.

For cryopreservation, cells were trypsinized and counted, as previously explained in 2.4.2. After centrifugation and discarding of the supernatant, 1 ml freezing medium (DMEM with 20% FBS, 1% P/S and 10% DMSO) per 1 million cells was added to obtain the desired cell concentration per milliliter. The cells were then transferred to cryogenic tubes (Nunc CryoTube Vials, Thermo Fisher, USA) and frozen on dry ice. Afterward, they were stored in liquid nitrogen at -196 °C.

2.3.4 Creation of Nell2 overexpressing cells

With the objective of preparing conditioned medium containing NELL2::AP, I created a NELL2::AP-overexpressing cell line. AP is a physiological enzyme for compound dephosphorylation. It can be detected using an AP activity assay, enabling me to postulate a NELL2::AP overexpression.

I used the pSBbi-RP backbone (Kowarz et al., 2015; Addgene, USA) with the insert pRK5.CT.AP-Nell2-AP, which was a gift from Dr. Alexander Jaworski (Jaworski Lab, Brown University, USA). For plasmid construction, first, digestion was conducted for the backbone vector and the insert separately with 2 µl CutSmart buffer (New England Biolabs, USA), 1 µl of each of the restriction enzymes (Hind III & PspXI), 6 µl plasmid DNA (0.033 µg/ml; pRK5.CT.AP-Nell2-AP & pSBbi-RP) and 10 µl H_2O for 2 hours at 37 °C. Afterward, gel electrophoresis in 1% agarose gel (as described in 2.1.3) was conducted to examine for correct bp length (Nell2-AP insert – 3959 bp; backbone 6423 bp). The bands with the correct bp length were manually cut out of the gel. To separate the DNA from the gel, 200 µl NTI buffer (Macherey-Nagel, Germany) per 100 mg gel was added and incubated in a 50 °C water bath for 5 min. Then, for purification, column binding tubes (Nucleospin, Macherey-Nagel, Germany) were used according to the manufacturer's protocol. The ligature of insert and backbone was accomplished by creating a solution of 2 µl 10x T4 DNA ligase buffer (Thermo Fischer, USA), 6 µl insert DNA, 3 µl backbone DNA, and 1 µl T4 ligase (Thermo Fischer, USA) kept at 4 °C ON. Escherichia Coli (E. Coli strain: DH5α) was thawed on

ice, and 20 µl of the ligature solution was added to 100 µl bacteria. The heat shock transformation and bacterial plating were then conducted as described in 2.2.1. Plasmid isolation was performed using the PureYield Plasmid Miniprep System (Promega, USA). Transformed bacteria were selected by plating the E. Coli on an LB agar plate with 100 µg/ml ampicillin (Carl Roth, Germany) at 37 °C ON. The next day single colonies were selected and transferred to 3 ml LB medium with 100 µg/ml ampicillin for 8 h at 37 °C. Then, 200 µl of the media bacteria mix was transferred to 100 ml LB medium with 100 µg/ml ampicillin and incubated on a shaker at 37 °C ON. To prove correct ligation and transformation in surviving E. Coli, isolated plasmids were digested with the same restriction enzymes as used before, and the length of insert and backbone was again controlled in gel electrophoresis. For transfection of the transposon, I used 10^5 SCP1 cells with 0.4 µg transposon and 0.9 µg pCMV transposase (pCMV(CAT)T7-SB100, Mátés et al., 2009, Addgene, USA) in a 20 µl P1 Solution with the Amaxa P1 Primary Cell 4D Nucleofector TM X Kit S and its protocol. After nucleofection, cells were incubated on a 6-well plate with 3 ml standard medium with 2 µg/ml puromycin (Thermo Fisher, USA) per well. The next day the medium was changed. Using FACS, transfected SCP1$^{RFP;NELL2::AP}$ cells were separated by RFP fluorescence from non-transfected SCP1 cells.

Table 2.6: Backbone and insert for sleeping beauty transposon.

	Plasmid DNA	BP	Restriction Enzyme
Backbone	pSBbi-RP	6423 bp	Hind III & PspXI
Insert	pRK5.CT.AP-Nell2-AP	3959 bp	Hind III & PspXI

2.3.5 AP-Activity assay

To prove the production of NELL2::AP in the SCP1$^{RFP;NELL2::AP}$ cells, I thawed SCP1^{RFP} and SCP1$^{RFP;NELL2::AP}$ as described in 2.4.3. After two days, I split the cells and seeded 50.000 cells/cm^2 in 6-wells (Thermo Fischer, USA). The next day we fixated the cells as described in 2.4.5. Afterward, cells were washed 3 times in Buffer 1. The color reaction was prepared by incubating the wells 2 times for 10 min in 2 ml NTMT. 1 ml staining solution was applied, and the cells were incubated in a dark chamber at RT until

staining was visible. The cells were washed with 2 ml H_2O and mounted using Fluoroshield with DAPI. Pictures were taken of each well with the fluorescence microscope (Axio Observer Z1, Zeiss, Germany).

Table 2.7: AP-Activity assay chemicals and buffers

Chemicals	
Hydrochloric acid fuming 37%	Merck, Germany
Tris-HCl	Sigma-Aldrich, USA
Magnesium chloride	Carl Roth, Germany
Polyvinyl alcohol (PVA)	Sigma-Aldrich, USA
Nitro-blue tetrazolium / 5-bromo-4-chloro-3-indolyphosphate (NTB/BCIP)	Sigma-Aldrich, USA
Tween-20	Sigma-Aldrich, USA
Fluoroshied with DAPI	Sigma-Aldrich, USA
Buffers	
Buffer 1	100 mM Tris 150 mM NaCl H2O
2xNTMT	20% 1 M Tris-Hcl (pH9.5) 5% 4 M NaCl 10% 1 M MgCl2 2% Tween-20 63% H2O
Staining Solution	50% PVA (10% in dH2O) 20 µl NBT/BCIP per ml of desired volume 50% 2x NTMT

2.3.6 Preparation of conditioned medium

For the preparation of conditioned medium (CM), 500,000 SCP1^{RFP} or SCP1$^{RFP;NELL2::AP}$ cells were seeded in T175 flasks for 4 days until they were 80% confluent. On day 4, the 40 ml standard medium was changed and left for 24 h. Then, the medium was

collected, centrifuged for 5 min at 500 g to remove cell debris and frozen in 5 ml aliquots at -20 °C. As a control, the same was done with SCP1^{RFP} cells.

2.3.7 Random migration assay

To analyze the effect of NELL1/2 on the migration velocity of myoblasts, a random migration assay was conducted. On the first day of the assay, cells were thawed, and 1,333 cells/cm^2 were seeded into T75 flasks. The standard medium was changed on days 2 and 4 of the assay. On day 5, cells were split and counted as described in 2.4.2. The cells were seeded at 100 cells/cm^2 in each well of a 6-well plate. The 6-well plates were incubated for another night, giving the cells time to attach and adjust. On the 6th day, either conditioned medium or medium with recombinant proteins (RP) was added. For the assay with conditioned medium, the SCP1$^{RFP;NELL2::AP}$ CM was mixed 1:1 with standard medium. As a control, the SCP1^{RFP} CM was also mixed 1:1 with the standard medium. In the RP assays, 100 /ml of NELL1-RP and NELL2-RP were used in standard medium. As a control, pure standard medium was used. The cells were incubated under a time-lapse microscope (Axiovert S100, Zeiss, Germany; Incubator XL100/135, PeCon, Germany) for 24 hours at 37 °C and 5.0% CO_2. 5 pictures of each well were taken every 10 min. The cells from the picture series were then tracked using the MTrackJ-Plugin (Meijering et al., 2012) in Fuji ImageJ (Schindelin et al., 2012).

2.3.8 Directed migration assay

In order to identify an attractive or repulsive effect of NELL1/2 on myoblasts, a directed migration assay was performed. On the first day of the assay, cells were thawed, and 1.333 cells/cm^2 were seeded into T75 flasks. The standard medium was changed on days 3 and 5 of the assay. On day 7, cells were split and counted as described in 2.4.2. A cell-medium suspension of 700.000 cells/ml was prepared. Then, the μ-Slide Chemotaxis chambers (Ibidi, Germany) were used according to the manufacturer's protocol. After seeding, the chamber was incubated for 3 hours for cell attachment. Afterward, the chambers were filled with the following medium: For the RP experiments, a 0.5% FBS medium was used in every bottom chamber as a non-attractant control. The upper chambers were filled with either 0.5% FBS with 100 μg/ml RP or 10% FBS as a positive control. For the CM experiments, the bottom chambers were filled with 0.5% FBS. The upper chambers were filled with a 1:1

mixture of 0.5% FBS and CM or FBS 10%. The cells were then observed for 24 h using a time-lapse microscope (Axiovert S100, Zeiss, Germany; Incubator XL100/135, PeCon, Germany). For quantification, the MtrackJ ImageJ Add-on (Meijering et al., 2012) was used for tracking the cells. The Chemotaxis and Migration Tool (Ibidi, Germany) was used for further analysis. The quantitative measurements for chemotaxis are the center of mass (CoM), the average of all myoblast endpoints, and the forward migration index (FMI).

2.3.9 Fusion and Alignment assay

The fusion and alignment assays were used to investigate the potential effect of NELL1/2 during the last two steps of myogenesis. C2C12 cells were thawed as described in 2.4.3 and seeded at a density of 7.000 cells/cm^2 in 6-wells with standard medium. The standard medium was changed the next day. 4 days after seeding, recombinant NELL1 or NELL2 proteins were added at 100 ng/ml in DMEM with 2% horse serum (HS, Life Technologies, USA). The cells were incubated for 4 days. For cell fixation, fused cells were washed with 5 ml PBS, and then 2 ml of 4% PFA (Merck, Germany) in PBS was added. After 15 min, the PFA was removed, and the cells were washed 3 times with PBS. Next, immunocytochemistry against MYH1E (MF20) or Desmin was conducted as described in 2.4. Afterward, DAPI was applied for 30 sec to stain the cell nuclei. Approximately 3.8 mm^2 large pictures were taken of each well with the fluorescence microscope (Axio Observer Z1, Zeiss, Germany) and quantified using ImageJ. The threshold was manually determined to best reflect the MF20 cells for quantification. For the fusion assay, the proportion of MF20 positive pixels to the total amount of pixels was measured with the %area measurement in ImageJ. For the alignment assay, I used the OrientationJ Plug-in (Daniel Sage, EPFL, Switzerland) to identify the direction in which most cells were orientated. The alignment score was then calculated as described by Jensen et al. (J. H. Jensen et al., 2020).

2.4 Immunohistochemistry

For the fusion assay and ISH, cells/myotubes were fixated as described in 2.4.5, or ISH was conducted on slides described in 2.2.3. Cells or slides were washed 3 times with 1 ml PBS. Then, 1 ml PBS with 0.1% triton (Triton X-100, Sigma-Aldrich, USA) was added. Afterward, 1 ml PBS with 0.1% triton and 10% HS was left on the cells or slides for at least 1 hour to block unspecific binding of the antibodies. The primary antibody (Table 2.10) was added at a 1:200 ratio in 1 ml PBS with 0.1% triton and 10% HS and left at 4 °C ON. The next day, cells or slides were washed 3 times with 1 ml PBS and 0.1% triton. Then, the appropriate secondary antibody (Table 2.5.1) was added at a 1:1000 ratio in 1 ml PBS with 0.1% triton and 10% horse serum and kept covered on a linear shaker for 1 hour. Afterward, cells or slides were washed 2 times with PBS and stained with DAPI (4',6-Diamidin-2-phenylindol, Sigma Aldrich, USA) for 30 sec. After being rewashed with PBS, cells or slides were covered using mounting medium (Fluoroshield, Abcam, U.K.) and a coverslip.

Table 2.8: Antibodies

Primary Antibodies	
Desmin	Rabbit Anti-Desmin, DSHB, USA
MF20	Mouse Anti-MF20, DSHB, USA
Secondary Antibodies	
Rabbit Anti-Desmin	Donkey Anti-rabbit Alexa 546, Life Technology, USA
Mouse Anti-MF20	Donkey Anti-mouse Alexa 488, Life Technology, USA

2.5 Statistics

The statistical significance of the quantitative data was analyzed using GraphPad Prism 9.3 (USA). Batches were seen as individual experiments separated in time. For the cell culture experiments (random migration assay, directed migration assay, fusion and alignment assay), 3 independent experiments were performed. In the random migration experiments, 5 locations were pooled for one independent experiment. For statistical analysis, the mean of each independent experiment was used. A p-value of 0.05 or lower was considered significant, and all p-values are shown in the graphs. When the absolute values between different experiments were significantly different, data was normalized to the mean of the control (FBS10% or CM-SCP1^{RFP}). For analysis of normal data distribution, the D'Agostino-Pearson normality test was used. Afterward, the Kruskal-Wallis test (for not normally distributed) or the one-way ANOVA Post Hoc test (for normally distributed) was used to determine significance.

3. Results

3.1 *Nells* are low expressed in non-myogenic muscle cells, but *Nell2* is intrinsically downregulated in differentiating myoblasts

3.1.1 *Rosa26$^{mT/mG}$;Acta1^{Cre}* - a muscle-specific fluorescent mouse line

Various pathways have been described by which fibroblasts, tendon cells, and neurons influence myogenesis. For instance, connective tissue fibroblasts develop a pre-pattern for myoblast migration into limb buds (Fukuhara et al., 2008; Kardon et al., 2003; Lanser & Fallon, 1987). Thus, to better understand possible NELL-related pathways in myogenesis, the identification of molecular differences between nMMCs and MMCs is crucial to identifying the role of NELLs in myogenesis.

I used *Rosa26$^{mT/mG}$;Acta1^{Cre}* mice which express a membrane-bound form of the fluorophore dTomato *(mT)* in every cell besides the cells of the myogenic cell lineage. These Acta1-expressing cells specifically express membrane-bound form GFP *(mG)*. The fluorescence of P1 mice showed a particular pattern of GFP expressing myogenic cells while all other cells expressed dTomato (Figure 3.1).

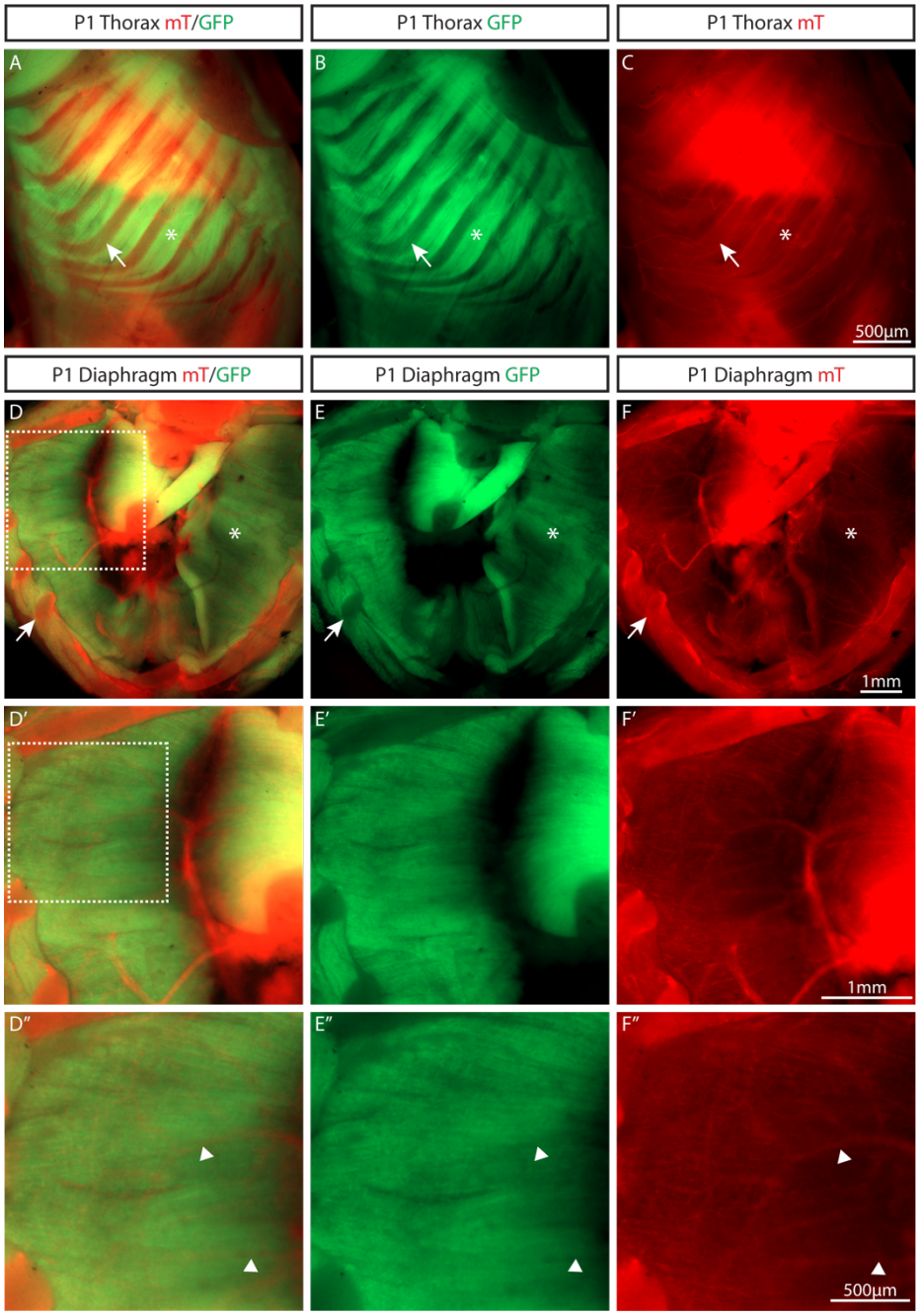

Figure 3.1: Overview of a newborn P1 *Rosa26$^{mT/mG}$;Acta1^{Cre}* thorax (A, B, C) and newborn P1 *Rosa26$^{mT/mG}$;Acta1^{Cre}* diaphragm (D, E, F)

A-C show a thorax from lateral of a P1 *Rosa26$^{mT/mG}$;Acta1^{Cre}* mice. **D-F** show a diaphragm from cranial of a P1 *Rosa26$^{mT/mG}$;Acta1^{Cre}* mice. On **A** & **D,** GFP and mT-expressing cells can be seen. On **B** & **E,** only myogenic cells (GFP-positive) are shown. On **C** & **F**, the nMMCs (mT-positive) are displayed. The white dashed boxes in **D** and **D′** show the section magnified in **D′** and **D″** respectively. As expected, the rips are mT-positive (arrow), while the intercostal muscles and diaphragm express GFP (*). In the diaphragm, mT-expressing cells (arrowhead) are seen, likely resembling vessels or axons.

3.1.2 Isolation of non-myogenic muscle cells from the diaphragm

To further analyze whether MMCs or nMMCs express *Nells* and its possible *Robo* receptors in the diaphragm, I separated nMMCs and MMCs from the diaphragm of E15.5 *Rosa26*$^{mT/mG}$;*Acta1*^{Cre} mice using FACS (Figure 3.2). The FACS successfully separated GFP-positive cells from mT-positive cells, while, unfortunately, only a small amount of GFP-positive MMCs could be isolated (Figure 3.2).

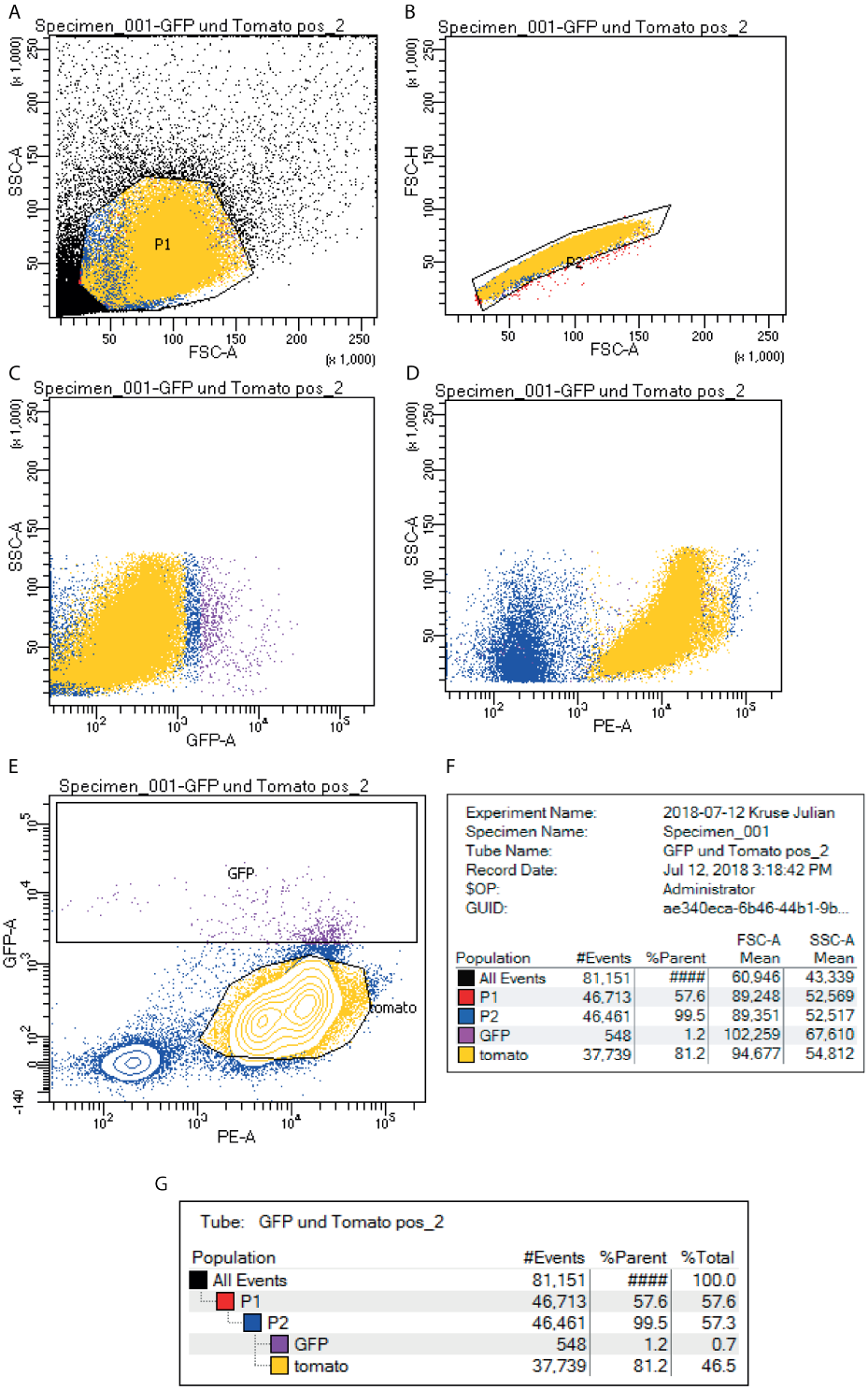

Figure 3.2: FACS of the digested E15.5 diaphragm

Cells were sorted using forward scatter (FSC), side scatter (SSC), red fluorescence (RFP, PE channel), and green fluorescence (GFP). In **E,** the separation of GFP-positive and mT-positive cells are presented. Notably, in **G,** the number of GFP-positive cells is with 548 GFP-positive events in 81,151 events very low. This FACS shows 1 of the 3 batches used. The remaining batches can be found in the supplementary data (Figures 6.1 & 6.2).

3.1.3 qPCR of non-myogenic muscle cells – proving that mT-positive cells are non-myogenic

To demonstrate that the FACS of the diaphragm cells of *Rosa26*$^{mT/mG}$;*Acta1*^{Cre} mice separated nMMC (mT-positive cells) from MMC (GFP-positive cells), I conducted a qPCR on the muscle-specific gene Desmin. The absolute Ct-values show that GFP-positive cells expressed *Des*, while mT-positive cells only expressed the positive control *Gapdh* (Figure 3.3). This selective expression of muscle-specific mRNA proves that MMCs were successfully separated from nMMCs.

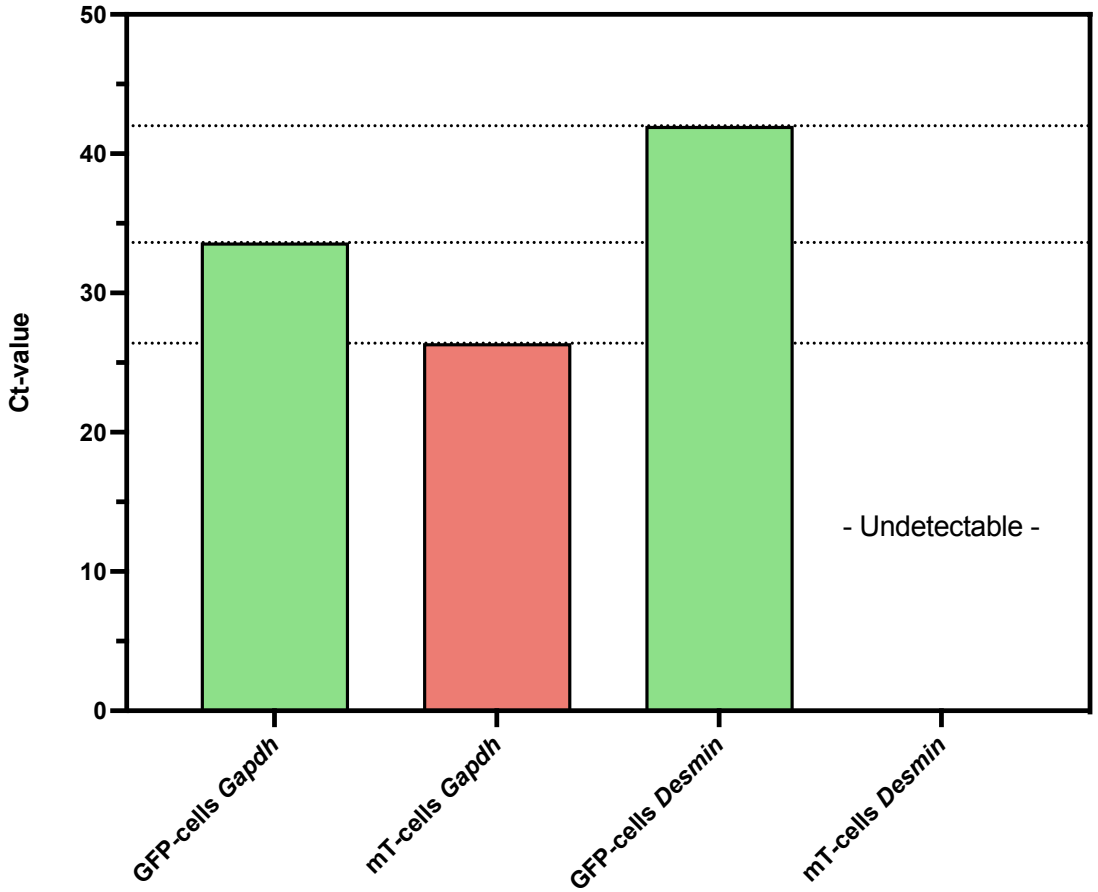

Figure 3.3: Ct-values for Desmin & Gapdh in mT- and GFP-positive cells.
The qPCR showed that *Desmin* and *Gapdh* are expressed in GFP-positive cells, while only the positive control *Gapdh* is expressed in mT-positive cells. Data represent absolute Ct values of one qPCR on the cDNA from sorted cells of 5 pooled diaphragms.

3.1.4 Non-myogenic muscle cells weakly express NELLs and ROBOs

To compare the sequencing data of nMMCs, obtained reads were normalized to transcripts per million reads (TPM). In murine diaphragm nMMCs (Figure 3.4), I found a low expression level for *Nell1* (1.111 ± 0.424 TPMs) and *Nell2* (0.831 ± 0.643 TPMs). *Robo1* (3.37 ± 0.516 TPMs) was most strongly expressed, while *Robo2* (1.061 ± 1.057 TPMs), like the *Nells*, only showed a slight expression. For *Robo3*, no expression could be detected (0.284 ± 0.236 TPMs).

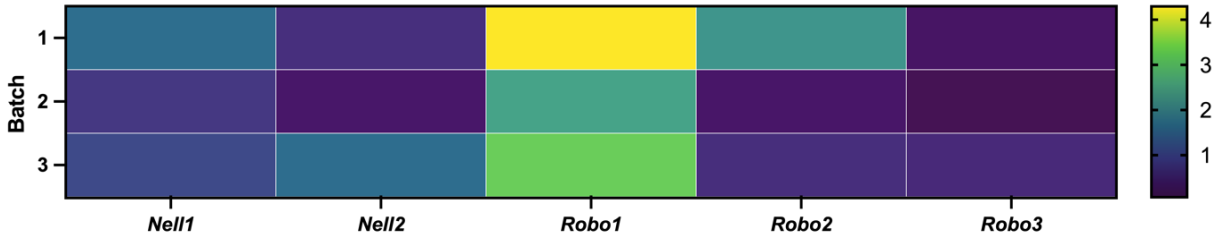

Figure 3.4: mRNA expression level of Nell and Robo in nMMCs

Heatmap of the mRNA expression level of *Nell* and *Robo* in nMMCs in TPMs. An expression of *Nell1*&*2* and *Robo1*&*2* can be observed. *Robo3* does not show any expression. The colors represent the amount of TPMs as represented on the right.

3.1.5 Nell2 expression is reduced during myoblast differentiation

For comparison to other subpopulations involved in myogenesis, I used data from previously conducted experiments by colleagues from the MUM muscle group.

For *Nell1*, an expression was only observed in diaphragmatic nMMCs (1.111 ± 0.424 TPMs) (Figure 3.5). Whole muscle (0.196 ± 0.481 TPMs), MSTN overexpressing muscle (0 ± 0 TPMs), SCP1^{SCX} cells (0.0 ± 0.0 TPMs) and C2C12 cells across the four-time points (0.333 ± 0.651 TPMs; 24 h – 0.667 ± 1.155 TPMs, 72 h – 0 ± 0 TPMs, 96 h – 0 ± 0 TPMs, 144 h – 0.667 ± 0.577 TPMs) showed a low or missing *Nell1* expression.

Nell2 expression is higher in whole muscle (1.701 ± 1.315 TPMs), MSTN overexpressing muscle (1.220 ± 1.07 TPMs), and C2C12 cells (3.5 ± 4.462 TPMs across all time points) compared to diaphragmatic nMMCs (0.831 ± 0.643 TPMs; Figure 3.5). SCP1^{SCX} cells (0.064 ± 0.055 TPMs) only showed a low-level expression. Interestingly the expression in C2C12 myoblasts was reduced (C2C12 24 h – 9.667 ± 4.619 TPMs, 72 h – 1.333 ± 2.309 TPMs, 96 h – 2.667 ± 1.528 TPMs, 144 h – 0.333 ± 0.5774 TPMs) the

longer they were in culture. Thus, as myoblasts differentiate, autocrine *Nell2* expression is reduced.

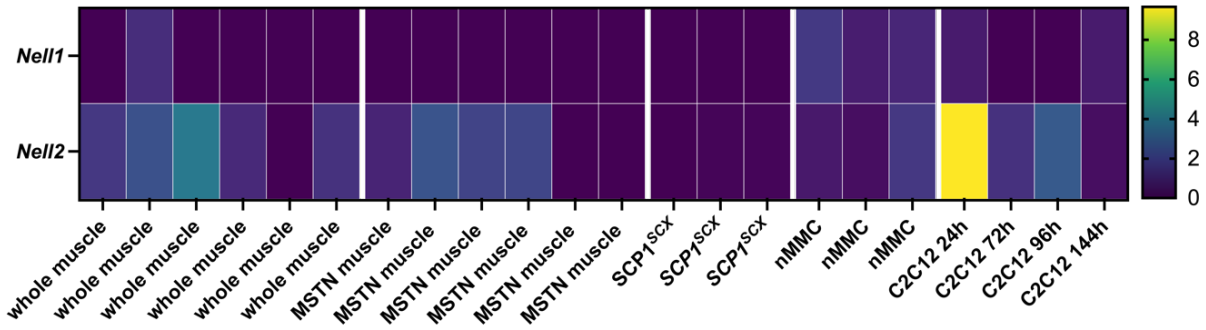

Figure 3.5: *Nell* TPM Heatmap comparison of nMMCs to other myogenic cell lines and tissues

Nell1's expression level is low in every analyzed sample besides nMMCs. *Nell2* is expressed in whole muscle and MSTN overexpressing muscle. Like for *Nell1*, nMMCs also show an expression of *Nell2*. In C2C12, *Nell2* is initially highly expressed and seems to be downregulated during myogenesis. SCP1^{SCX} cells do not show any expression of *Nell1* and *Nell2*.

3.1.6 ROBO1 is strongly expressed in myoblasts during differentiation

I investigated the ROBO-family expression as a potential NELL ligands receptor. *Robo3* (whole muscle 0 ± 0 TPMs; MSTN 0 ± 0 TPMs; SCP1^{SCX} 0.509 ± 0.409 TPMs; nMMC 0.282 ± 0.191 TPMs; C2C12 0 ± 0 TPMs across all time points) is not expressed in any of the examined tissues or cell lines (Figure 3.6). Like *Nell2*, *Robo1* (whole muscle 21.233 ± 8.837 TPMs; MSTN 25.134 ± 7.243 TPMs; SCP1^{SCX} 1.924 ± 0.468 TPMs; nMMC 3.377 ± 0.731 TPMs; C2C12 159.8 ± 52.55 TPMs across all time points, 24h: 175 ± 68.24 TPMs, 72h: 166 ± 71.69 TPMs, 96h: 150 ± 38 TPMs, 144h: 148.3 ± 56.58 TPMs) is strongly expressed by cells of the myogenic cell lineage, especially in the myoblast cell line C2C12. However, it is not regulated during myoblast differentiation. *Robo2* (whole muscle: 6.736 ± 3.063 TPMs; MSTN 9.268 ± 6.22 TPMs; SCP1^{SCX} 0.346 ± 0.437 TPMs; nMMC 1.06 ± 0.863 TPMs; C2C12 6.417 ± 4.316 TPMs across all time points, 24h: 10.67 ± 4.726 TPMs, 72h: 4.667 ± 4.509 TPMs, 96h: 3.667 ± 0.5774 TPMs, 144h: 6.667 ± 4.041 TPMs) shows a similar pattern at a lower expression level.

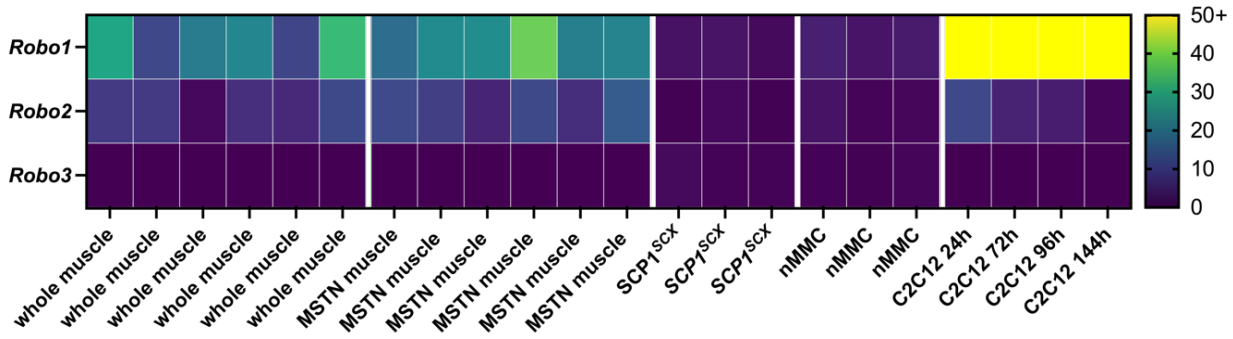

Figure 3.6: *Robo* TPM Heatmap comparison of nMMCs to other myogenic cell lines and tissues

Each field represents the TPMs of one probe. *Robo2* and, at a higher level, *Robo1* are expressed in the whole muscle, MSTN muscle, and C2C12 cells but not in tendon lineage cells or nMMCs. *Robo3* is not expressed in any of the probes.

3.2 Functional *in vitro* analysis of NELL1/2 in specific steps of myogenesis

3.2.1 Validating the overexpression of NELL2::AP in SCP1$^{RFP;NELL2::AP}$

In order to produce CM containing NELL2::AP, I created the SCP1$^{RFP;NELL2::AP}$ cell line as described in Material and Methods. I concentrated on NELL2 in this experiment, as the differential expression pattern made it the more probable ligand with an effect on myogenesis. To prove that the SCP1$^{RFP;NELL2::AP}$ successfully expressed NELL2::AP, an NBT/BCIP reaction was performed. This demonstrates the overproduction of AP and, therefore, NELL2::AP. SCP1^{RFP} cells were used as a negative control. Remarkably, both groups showed cells with extensive AP activity (Figure 3.7 - yellow line). I identified those as cells with high endogenous AP. However, a different AP-activity can be seen in the SCP1$^{RFP;NELL2::AP}$ (blue arrow). In these cells, the AP-reaction was revealed close to the nuclei, presumably in the endoplasmic reticulum of the cells. A strong AP reaction at the endoplasmic reticulum of SCP1$^{RFP;NELL2::AP}$, compared to SCP1^{RFP}, thus proves that the SCP1RFP;NELL2::AP are overexpressing NELL2::AP.

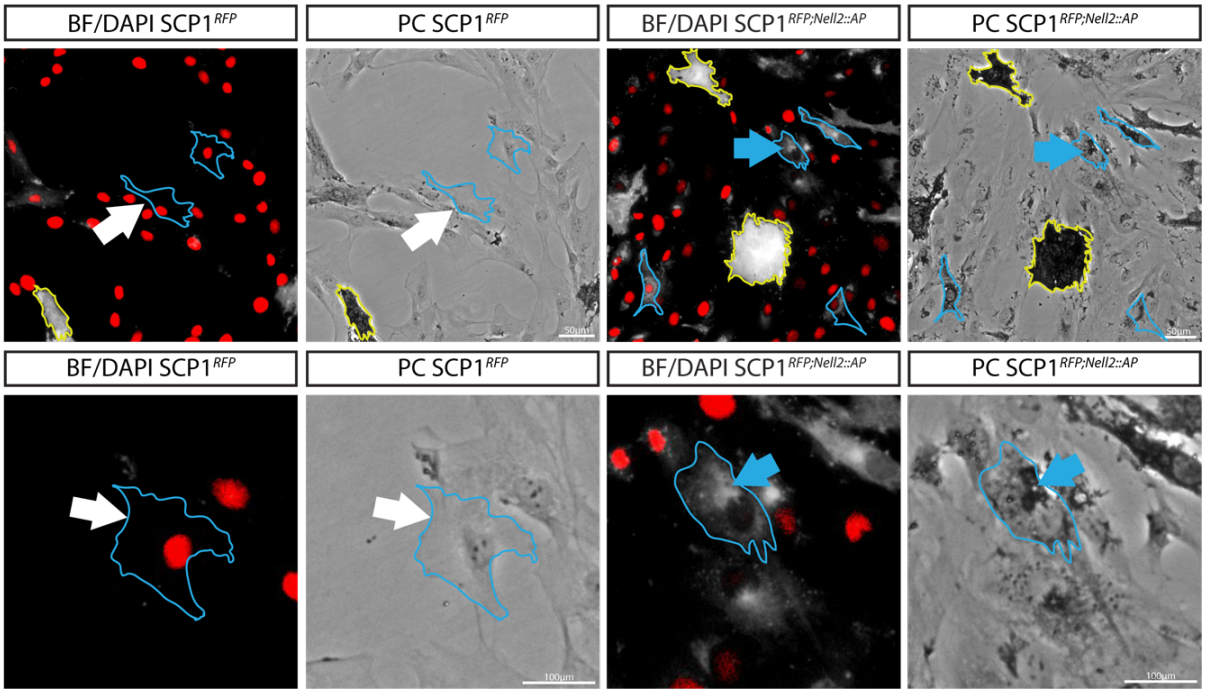

Figure 3.7: AP-activity in SCP1$^{RFP;NELL2::AP}$ cells in contrast to SCP1^{RFP} cells

The nuclei were stained with DAPI (red). Pictures were taken with brightfield (BF), fluorescence (red - DAPI), and phase-contrast (PC). The yellow lines indicate cells with high endogenous AP, while the blue lines mark the cells without AP or with localized AP activity only. In the SCP1$^{RFP;NELL2::AP}$ cells, AP-activity (blue arrows) can be seen at the endoplasmic reticulum. In contrast, the SCP1^{RFP} cells (white arrows) do not show any activity around the nucleus. Scale bar: top row – 50µm; bottom row – 100µm.

3.2.2 NELL2 acts as a pro-migratory signal on myoblasts

Myoblast migration is a fundamental part of embryonic myogenesis and is later crucial during skeletal muscle repair. The somatic muscle precursor cells undergo long-distance migration, traveling from the dermatomyotome of the somites to the limb buds, diaphragm, and tongue (Hollway & Currie, 2005). This highly complex process is orchestrated by various cell signals and ECM interactions (Yin et al., 2013)

To examine the influence of NELL ligands on myoblast migration, I divided our experiments into two parts. First, I conducted a random migration assay to examine myoblast migration under the influence of NELL recombinant proteins (RPs) and conditioned media (CM) with NELL2::AP. Additionally, I performed a directed migration assay to determine whether NELL served as a guidance cue, attracting or repelling myoblasts.

The random migration assay was conducted as described before. In the recombinant protein experiments (Figure 3.8A), a tendency for higher velocity can be seen in cells exposed to RPs of NELL1 and NELL2 (Figure 3.8A). The increase is insignificant, with p-values of 0.1207 for NELL1 (114.2 ± 9.09%) and 0.1548 for NELL2 (113 ± 8.85%) compared to 10% FBS (normalized to 100 ± 0%). For the CM experiments (Figure 3.8B), NELL2::AP (109 ± 2.88%) showed a significant increase in the velocity of myoblasts compared to myoblasts in FBS 5% (92.99 ± 4.27%, p = 0.019)(Figure 3.8B). However, the increase was not significant compared to myoblasts in CM of SCP1^{RFP} (100 ± 0%, p=0.5172)(Figure 3.8B). A velocity-enhancing effect of the proteins of interest can be considered for a subpopulation of myoblasts exposed to RP NELL1, RP NELL2, and NELL2::AP.

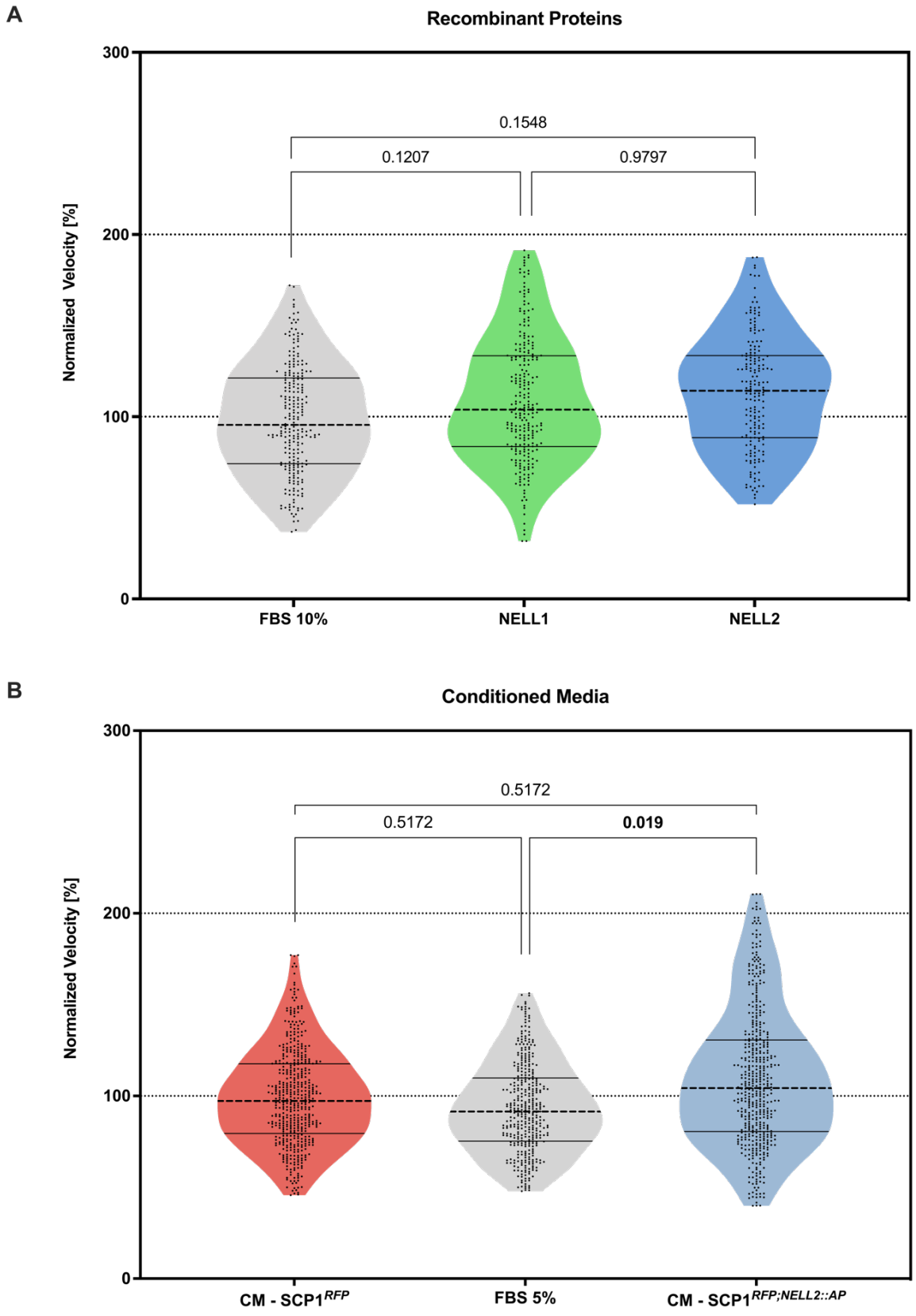

Figure 3.8: The influence of NELL1 & NELL2 on myoblast velocity

The dots in the violin plot represent the normalized velocity of every cell. The p-values shown are based on the normalized mean of every batch (n = 3). **A** Recombinant protein: No significant differences could be shown, but a slight velocity increase for both RPs NELL1 and NELL2 can be seen. **B** Conditioned Media: Comparison of C2C12 cells in CM- SCP1$^{RFP;NELL2::AP}$ to FBS 5% show a significant increase in velocity. C2C12 cells in CM- SCP1$^{RFP;NELL2::AP}$ compared to CM-SCP1^{RFP}, show no significant increase in their velocity.

3.2.3 C2C12 are not attracted or repelled by Nells

Not only the agility of myoblasts is essential for myogenesis. Myoblasts need to migrate towards their desired location, partially over long distances, for correct muscle development. These locations include the limb buds, diaphragm, tongue, and other muscular tissues. Therefore, I conducted the directed migration assays to test our hypothesis of NELL ligands acting as attractive or repulsive guidance cues on myoblasts.

The CoM and FMI represent the efficiency of forward migration along the NELL gradient (Figure 3.9). NELL ligands have no attractive or repulsive effect for both experimental setups (Figure 3.9). RP NELL1 (Figure 3.9A/B; CoM -9.753 ± 15.33 μm; FMI -0.026 ± 0.047 μm) might have a slight, but non-significant, repellent effect in comparison to FBS 10% (CoM 36.27 ± 33.04 μm; FMI 0.095 ± 0.065 μm). For NELL2, the RP assay (Figure 3.9A/B; CoM -0.0053 ± 11.87 μm; FMI 0.018 ± 0.036 μm) shows a CoM and FMI close to zero. In the CM assays (Figure 3.9C/D), the medium of SCP1^{RFP} (CoM 15.70 ± 20.68 μm; FMI 0.057 ± 0.043 μm) and FBS 5% (CoM 17.84 ± 16.32 μm; FMI 0.03288 ± 0.04264 μm) showed a tendency of attraction on myoblasts, while SCP1$^{RFP;NELL2::AP}$ (CoM 2.299 ± 8.913 μm; FMI 0.021 ± 0.028 μm) portrayed once again a very low CoM and FMI.

For the RP assays, 47% (47.3 ± 14.1%) of myoblasts were attracted by the positive control, while 24% (24.4 ± 8.4%) were repelled and 28% (28.4 ± 12%) did not migrate (Figure 3.10). The majority (46.1 ± 18%) of myoblasts under the exposure of NELL1 did not show chemotaxis, whereas 26% (25.5 ± 1.2%) were attracted and 29% (28.5 ± 17%) were repelled. 54% (53.8 ± 6.9%) of C2C12 cells under a NELL2 gradient did not migrate, and 25% (25.3 ± 10.1%) were repelled (Figure 3.10). Only 21% (20.8 ± 8.7%) of the myoblasts were attracted by RP NELL2. In the CM assays, the control (CM of SCP1^{RFP}) had an attractive effect on 38% (37.8 ± 13.6%) of the myoblasts, repelled 28%

(28.3 ± 22.9%) of the cells and 34% (33.9 ± 28.6%) of the cells did not show any chemotaxis (Figure 3.10). For the negative control (FBS 5%), a small attractive effect on 32% (31.5 ± 14.6%) of the cells can be seen, while most of the cells (51.1 ± 22.7%) did not migrate, and only 18% (17.6 ± 10.3%) were repelled (Figure 3.10). The CM with NELL2::AP had a slightly attractive effect on 37% (36.9 ± 11.5%) of the myoblasts, while 33% (32.5 ± 20.5%) did not show chemotaxis and 31% (30.7 ± 10.9%) of the C2C12 cells were repelled (Figure 3.10). This effect was smaller in comparison to the control of SCP1^{RFP} CM but greater than the negative control (FBS 5%).

Therefore, it can be concluded that NELL1/2 do not affect the chemotaxis of C2C12 myoblasts.

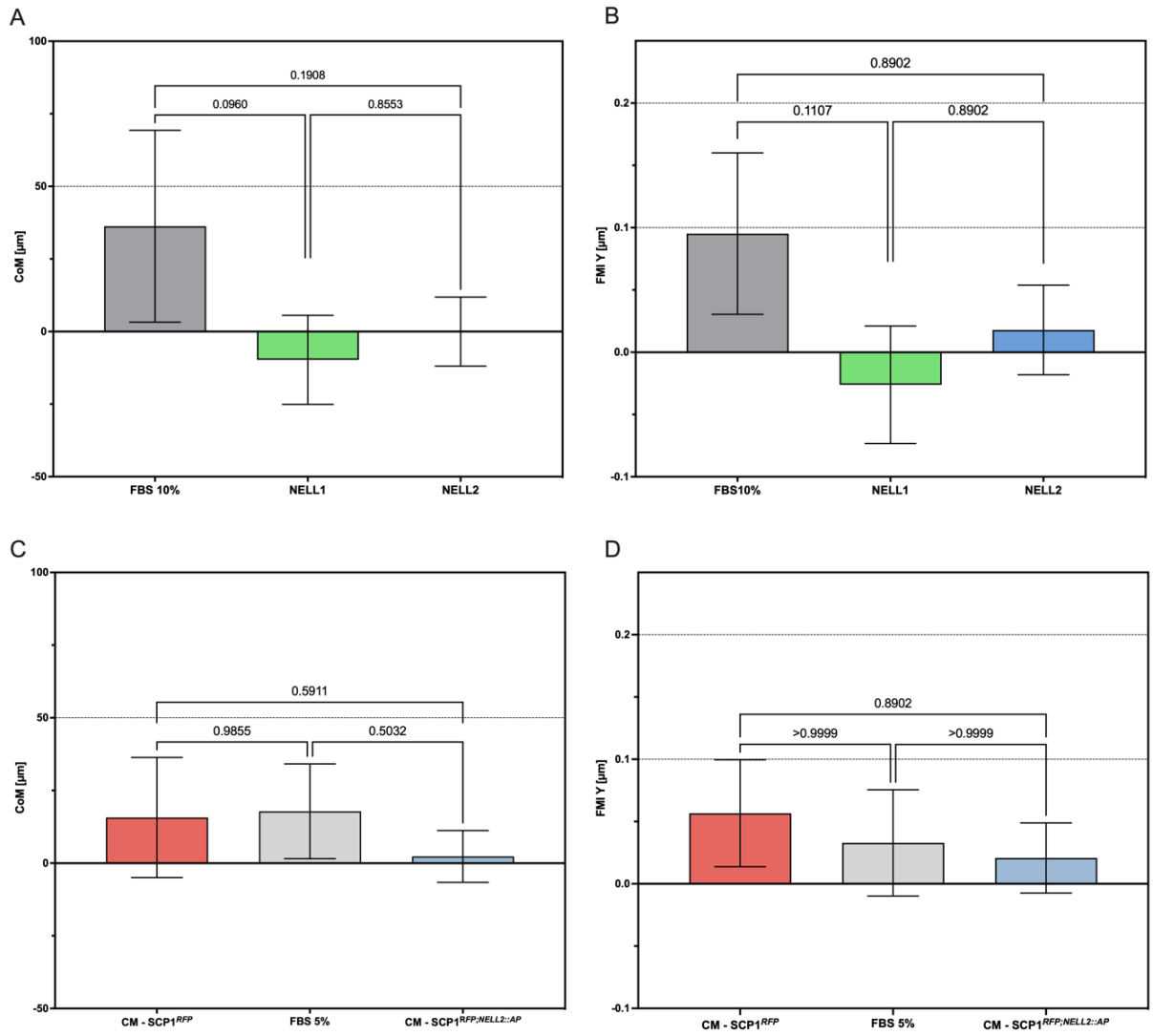

Figure 3.9: C2C12 cells are not attracted or repelled by Nell RP or NELL2::AP

The quantification of the center of mass (CoM) in **A**, along with the forward migration index (FMI) in **B** for the directed migration assays with RP indicates that NELL ligands have no impact on the direction of migration. For the directed migration assays with CM, the CoM in **C** and FMI in **D** indicate that NELL ligands have no impact on the direction of migration. The data represent the mean and SD of 3 independent experiments.

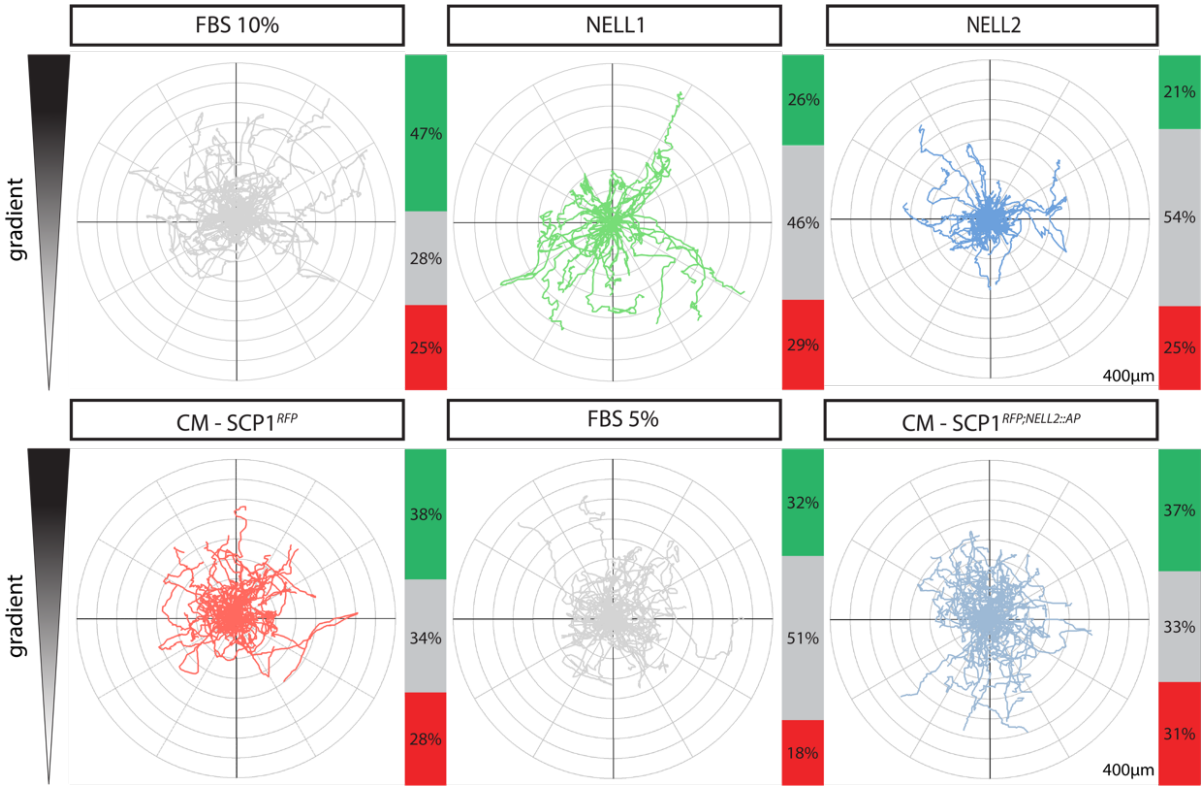

Figure 3.10: Directed migration assay on the effect of NELL ligands on myoblasts

The ratio of cells attracted (green), without chemotaxis (grey), and repelled (red) is shown on the right side of each plot. Outer ring = 400 µm. A difference in myoblast endpoints of at least 25 µm on the gradient was considered attraction or repulsion. N = 3. The ligand gradient was most concentrated on the top. For the RP assays, no attractive or repulsive effect of NELL1 and NELL2 on migration was shown. In the CM experiments, NELL2::AP had a small attractive effect on myoblasts, but this effect is reduced compared to the control CM of SCP1^{RFP}.

3.2.4 Alignment

Proper myotube alignment is essential for myogenesis to form strong and effective muscles. An apparent tissue involved in myofiber alignment are tendon cells. Muscle-tendon junctions must form to make functional movements possible (Schejter & Baylies, 2010). A ligand-receptor system of great importance for the correct formation of muscle-tendon junctions is SLIT-ROBO signaling (Ordan & Volk, 2015). As some ROBOs also bind NELL, an alignment effect of NELL through ROBO binding is conceivable. Thus, I analyzed C2C12 alignment after fusion, as previously explained.

I found that both NELL1 and NELL2 did not show any significant change in alignment (Figure 3.11). The alignment index of myoblasts under the influence of NELL1 (0.172 ± 0.034) was slightly lower when compared to 2% HS (0.225 ± 0.04)(Figure 3.11B). For

NELL2, no significant effect was seen (0.207 ± 0.014) (Figure 3.11B). Therefore, I deduced that NELL ligands have no significant impact on myoblast alignment.

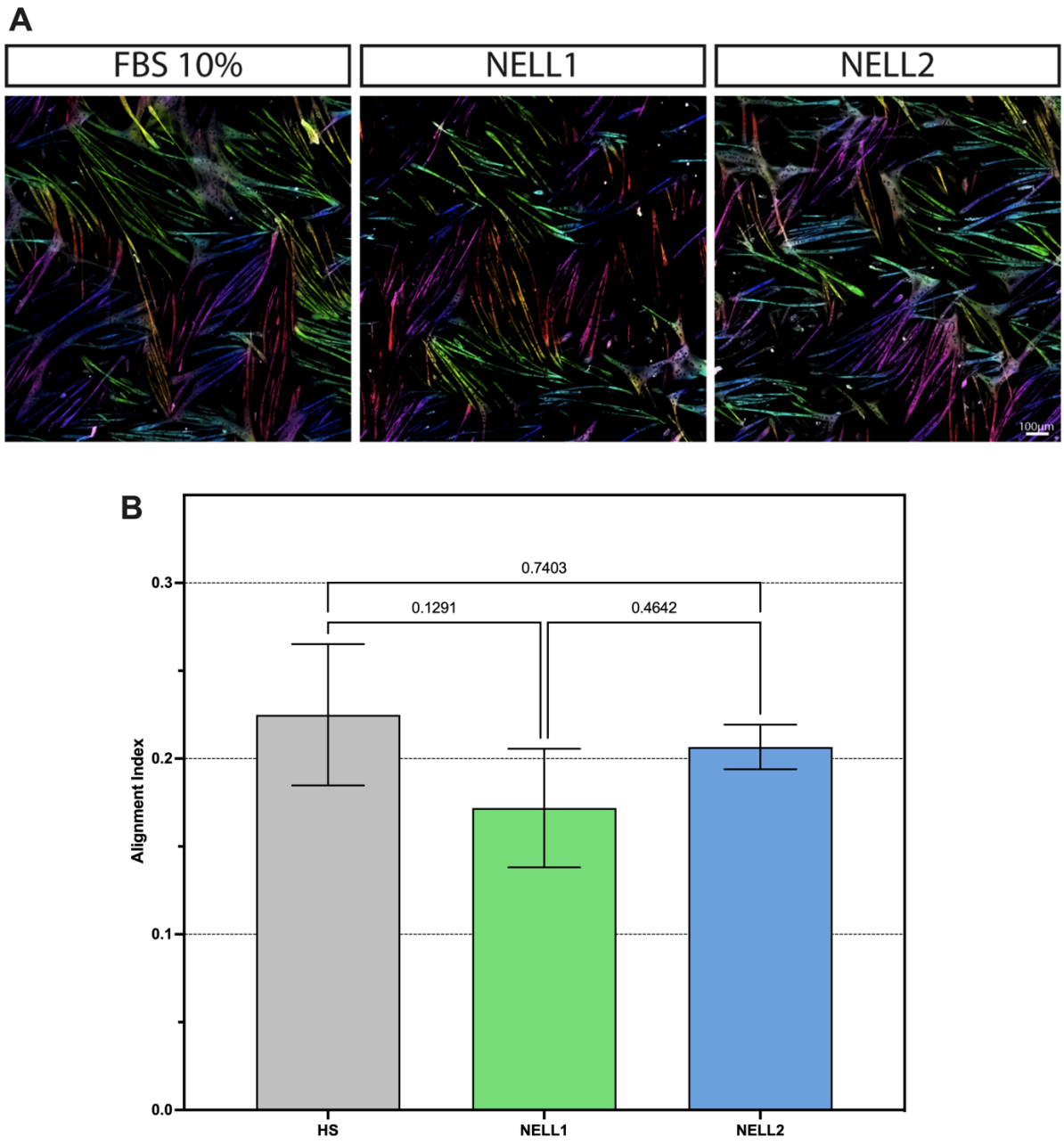

Figure 3.11: Alignment quantification of differentiated C2C12 cells under ligand influence

A. Cells are colored depending on their orientation angle. The pixel hue is proportional to the local orientation angle of myofibers, which ranges from −90° to +90° relative to horizontal. Scale bar – 100 µm **B** To analyze the orientation further, the alignment index was applied to the data. For NELL1, an inhibition of alignment can be interpreted, even though the effect is not significant compared to HS 2% (p=0.129). For NELL2, no effect can be seen (p=0.740).

3.2.5 NELL2 shows a tendency to inhibit myoblast fusion

The fusion of myoblasts to multinuclear myotubes is essential for myofiber formation and, therefore, the basis for the functional unit of muscles. The steps of myotube formation are extensively regulated by transcription factors as well as intercellular communication with myoblasts and cells of surrounding tissues (Lehka & Rędowicz, 2020). To examine the impact of NELL ligands on myoblast fusion, an assay with C2C12 cells was carried out as described earlier.

For NELL1, no effect on the normalized fused area (107.6 ± 16.06%), compared to HS 2% (normalized at 100 ± 0%) can be seen (p=0.709)(Figure 3.12). NELL2 (82.19 ± 11.57%), on the other hand, shows a reduction in fusion (Figure 3.12). With a p-value of 0.216, this effect is again not significant (Figure 3.12).

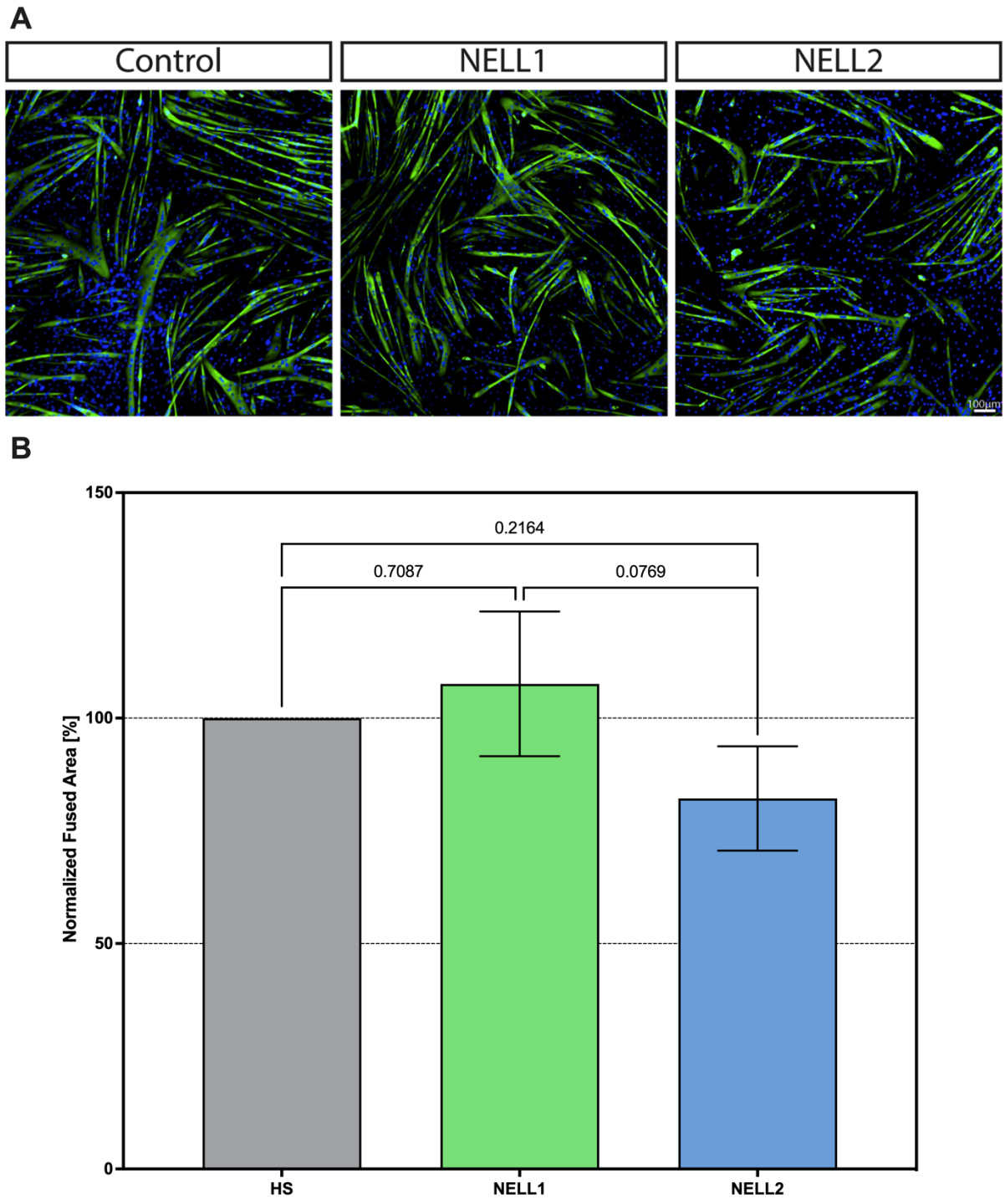

Figure 3.12: Fusion assay and quantification by the proportion of myosin heavy chain positive area

A Fused C2C12 cells were stained by antibody staining for myosin heavy chain (green). Nuclei were stained with DAPI (blue). Scale bar: 100µm **B** Normalized fused proportion of MF20 positive pixels to the total amount of pixels was used for quantification. A non-significant lower proportion of MF20 positive pixels to the total amount of pixels was seen in myoblasts treated with NELL2 ($p=0.216$). For NELL1, no effect could be seen ($p=0.709$).

4. Discussion

Dissecting the pathways involved in myogenesis is pivotal for muscle tissue engineering. Various arguments highlighted NELLs as a possible signaling molecule in myogenesis. Therefore, through this study, I aimed to uncover the role of NELLs in muscle development. To determine which cell type involved in myogenesis expresses *Nell1/2*, I performed an mRNA sequencing of nMMC. By analyzing the effect of NELLs on myoblasts in different differentiation stages, I uncovered a pro-migratory impact of NELL2 on myoblasts, concurring with the expression profile of *Nell2*.

4.1 Non-myogenic muscle cells weakly express *Nells*

Myogenesis does not just involve MPCs. The expression of *Nell2* during myogenesis was identified, but the exact cell type expressing *Nell2* is still unknown (Nelson et al., 2002). Fibroblasts have been proven to positively influence correct muscle development through transcription factors TCF4 and GATA4 (Merrell et al., 2015; T. Takahashi et al., 2016). Saller et al. hypothesized that motor neurons attracted myoblast by SLIT1 or SLIT2 expression, and they could show the attractive effect of SLIT1 and SLIT2 on a subpopulation of MPCs (Halperin-Barlev & Kalcheim, 2011; Saller, 2016; SG Kramer et al., 2001). Therefore, it is also likely that other cell types, like neurons or fibroblasts, influence myoblasts during myogenesis, possibly through NELLs. To address this hypothesis, I created a reporter line to separate MMCs from nMMCs by FACS. The qPCR results validated that GFP-positive cells expressed *Desmin*, a myogenic-specific protein, while no *Desmin* expression could be detected in mT-positive cells. Therefore mT-positive cells were correctly identified as non-myogenic. Disappointingly, mRNA sequencing was only possible for nMMCs since, even when pooling five diaphragms, not enough MMC mRNA was present in the probes. This problem likely arose due to a low cell count in E15.5 diaphragms and the apparent sensitivity of myofibers to digestion and shear stress in the FACS.

On the other hand, interestingly, the qPCR could detect *Desmin* in the GFP-positive probes. The high *Desmin* Ct-value (42) in the qPCR suggests a low amount of mRNA in the probe. I presume that the library preparation protocols then needed a higher input of mRNA. Even though I pooled multiple embryos and increased the number of pregnant mice, I was unsuccessful in reaching a sufficient number of embryos with

the correct genotype. Therefore, in this study, I could not assess the expression differences of NELLs and ROBOs between MMCs and nMMCs.

However, the gene expression pattern of nMMCs provides interesting information. *Nells* are expressed weakly in nMMCs from E15.5 diaphragms. This implies two possible reasonings: 1.) nMMCs only weakly express *Nells* during myogenesis. Therefore, *Nell2* would have to be expressed by MMCs, as strong *Nell2* expression during myogenesis was previously demonstrated by Nelson et al. (Nelson et al., 2002). 2.) *Nell2* might be already downregulated in E15.5 diaphragms. NELL2 expression during chicken migration was shown to be reduced after migration (Nelson et al., 2002). In addition, at developmental stage E15.5, myoblasts in the PPFs are already fused across the diaphragm (Merrell et al., 2015). Therefore, my results show an expression of *Nell*s in nMMCs even though a stronger expression in MMCs cannot be excluded.

Of all ROBO isoforms, only *Robo1* shows a slightly higher expression in nMMCs, compared to the other genes of interest. However, as a consequence of this weak expression, no conclusions can be drawn.

4.2 *Nell2* expression in myoblasts is intrinsically downregulated during differentiation

As nMMC is an unspecific term summing up various non-myogenic cell types in a muscle, I compared it to more specific cell sequencing data and whole muscle samples.

Nell1 was only weakly expressed in nMMCs. As no expression of Nell1 in myogenesis has been reported yet, these results align with the previously described specific osteogenic and neural expression profile of *Nell1* (S. Kuroda et al., 1999; Ting et al., 1999). Based on the sequencing data, I do not expect NELL1 to be involved in physiological myogenesis.

The comparison of *Nell* sequencing data revealed a *Nell2* expression in the cells of the whole muscles of a 3.5-month mouse and of an *Mstn* overexpressing mouse. Hence, *Nell2* is expressed in adult muscles and might have a role in skeletal muscle homeostasis. The intense expression and downregulation of *Nell2* in differentiating C2C12 cells aligns with the expression profile described by Nelson et al. (Nelson et al., 2002). *Nell2* downregulation starts on the third day of differentiation as myoblasts begin to fuse, and Nelson et al. described an expression profile mainly during myoblast migration (Nelson et al., 2002). Consequently, NELL2 seems to be involved in myoblast migration (Nelson et al., 2002). Furthermore, the expression profile I showed in C2C12 cells, in general, makes myoblasts the likeliest origin of the *Nell2* expression reported by Nelson et al. in myogenesis (Nelson et al., 2002). Therefore, if NELL2 affects myoblasts, it most likely acts as an autocrine or paracrine signal expressed by MPCs.

The tendon-mimicking cell line SCP1$^{GFP/SCX}$ does not show any *Nell* or *Robo* expression. While SLIT-ROBO signaling is required for correct muscle-tendon development in drosophila, the sequencing data does not suggest the same for NELL (SG Kramer et al., 2001). However, as SCP1$^{GFP/SCX}$ cells only mimic tendon cells while not precisely matching the physiological expression profile of tendon progenitor cells, the involvement of NELLs in muscle-tendon development cannot be excluded.

4.3 NELL2 acts as a migration stimulus for myoblasts

Due to the expression pattern of NELL2 and its influence on axon migration, I hypothesize that NELL2 acts as a migratory signal on myoblasts (Hayashi et al., 2015; Nelson et al., 2002). Saller et al. demonstrated the attractive effect of SLIT1 and SLIT2 on a subpopulation of MPCs (Saller, 2016). This utilization of shared ligand-receptor pathways between axon and MPC migration, facilitated by a receptor of NELLs, suggests a role for NELL signaling. I tested this hypothesis with RP and CM random migration assays. In line with our hypothesis, our results indicate that NELL2 positively influences the movement of cells.

Even though a slight increase in velocity was seen, the RP experiments did not show a significant effect of NELLs on C2C12 chemokinesis. This could be due to various reasons. NELL1 might not influence myoblast migration, which seems plausible considering it is not expressed in muscles during migration. However, for NELL2, however, the velocity increase, even though insignificant, suggests a different purpose. The slight increase in velocity could be due to an insufficient protein concentration or a deficient receptor expression in C2C12 cells. The CM results further supported this hypothesis as an increased velocity was shown in myoblasts treated with SCPI$^{RFP;NELL2::AP}$ medium.

For the CM assays, a significant velocity increase of cells treated with NELL2::AP CM, compared to FBS 5%, could be seen. However, no significant increase in the CM of SCPI^{RFP} was observed. As CM of SCP1^{RFP} and SCPI$^{RFP;NELL2::AP}$ contain numerous other proteins besides NELL2, the effect of NELL2 might be too delicate to be significantly detectable. Another reason may be that the effect of NELL2 is reduced by other proteins in the secretome. Regular media change with new proteins might also show more significant results in both the RP and CM experiments.

Interestingly a subpopulation of myoblasts exposed to RP NELL1, RP NELL2, and NELL2::AP showed an increase in velocity compared to the controls. Therefore, it is conceivable that NELLs can positively impact myoblast velocity in specific differentiation phases.

All in all, our findings suggest that NELL2 has a positive effect on myoblast migration by enhancing the migration velocity. NELL1, due to its absent expression during myogenesis and lacking effect on C2C12 cells, does not seem to influence myoblast

migration. Further studies should be conducted with different NELL2 concentrations and different experimental setups.

4.4 NELLs do not act as guidance cues for myoblasts

NELL2 acts as a directional guidance cue for axons through its receptor ROBO3 (Hayashi et al., 2015). As confirmed by our sequencing data, *Robo3* is, contrary to ROBO1/2, not expressed by MPCs in myogenesis. On the other hand, the attractive effect of SLIT1/2, expressed by axons, on *Robo2* expressing primary MPCs was previously described (Saller, 2016). As the binding of NELLs to ROBO2 was shown, I hypothesized NELLs could act as a directional guidance signal for MPCs expressing *Robo2* (Yamamoto et al., 2019a). C2C12 and whole muscles demonstrated a higher expression of *Robo1* compared to *Robo2*. But no binding site for NELLs was previously shown on ROBO1. As previously described, this is conceivably due to ROBO1 acting as the receptor for SLIT1/2 while NELLs and SLITs act through ROBO2 (Long et al., 2004).

Contrary to this hypothesis, my results did not show a significant attractive or repellent effect on C2C12 cells exposed to NELLs. A slight repulsion of C2C12 cells was observed when treated with NELL1, but this weak repulsion is most likely merely an artifact. A subtle, attractive effect of NELL2::AP CM on myoblasts could be observed, but this remains smaller compared to the control of SCP1^{RFP} CM. Therefore, other proteins of the secretome are probably responsible for this effect.

In conclusion, our results do not give any evidence that NELLs are involved in myoblast guidance. Of course, this could be due to insufficient protein concentration in the RP experiments or other proteins suppressing NELL binding to its receptors in the CM experiments.

4.5 NELLs do not influence myoblast fusion and alignment

As moving cells cannot fuse, myoblast migration needs to be reduced in order for myoblasts to align and fuse (Bondesen et al., 2007). Due to the expected migratory effect of NELLs, I hypothesized NELLs would enhance alignment but inhibit fusion, keeping MPCs mobile.

Our *in vitro* results did not show any significant influence of NELLs on alignment. NELL1 seems to inhibit alignment slightly, while NELL2 does not show any effect. For alignment, the spatial concentration of proteins is essential. Thus, our experimental setup, in which the protein concentration in the medium was balanced, is not ideal for assessing alignment. A more suitable experiment would be one in which the RP or the CM is delivered to the cells from one or two directions.

Even though again not significant, the fusion experiments presented results that potentially correspond to our hypothesis. While C2C12 cells treated with NELL1 showed a slight but most likely neglectable increase in fusion, myoblasts treated with NELL2 reduced the fusion area to 82% compared to 2% HS. In order to validate my hypothesis, further experiments using varying protein concentrations are crucial.

5. Conclusion & Outlook

In conclusion, this study gives valuable insights into the role of NELLs in myogenesis. Firstly, NELL1 does not seem to have any impact on myoblasts, which is unsurprising considering its absent expression in muscle-forming cells and their surrounding tissue. Secondly, in line with previous research, I provide evidence that NELL2 is involved in MPC migration as a chemokinesis signal. Corresponding to this effect, our sequencing data also provided the information that NELL2 is most likely expressed by myoblasts and downregulated during fusion. Hence our study identified a new pro-migratory signal for myogenesis. Further research should focus on NELL2's effect on migration and fusion through some of the following approaches:

1. Random migration and fusion assays should be conducted with different NELL2 concentrations. As NELL2 binds to a cryptic binding site on ROBO2, higher concentrations might be needed to significantly influence myoblasts. With higher concentrations, I predict a more consequential pro-migratory and fusion-inhibiting effect of NELL2.

2. For the assessment of migration, directed migration, alignment, and fusion, a co-culture of C2C12 cells with an SCP1$^{RFP;NELL2::AP}$ pellet could be a valuable addition to our experiments. A more distinct effect might be observed through the continuous and directional *Nell2* expression. I expect C2C12 cells close to the pellet to migrate faster. Moreover, cells close to the pellet will most likely not fuse, while myoblast with a more significant distance from the palette will fuse.

3. An AP-binding assay of NELL2::AP to C2C12 at different differentiation stages should be conducted to assess if NELL2 binds to MPCs *in vitro*. I expect binding, especially before C2C12 fusion, to occur during the migration phase.

4. A NELL2::AP binding assay could also be conducted with C2C12 cells overexpressing *Robo1* and *Robo2* to evaluate whether NELL2 binds to the cryptic

binding side of ROBO2 *in vitro*. This could also provide information on the concentration of NELL2::AP needed to achieve ROBO2 binding. These results should then be compared with the *Robo* sequences and expression patterns in C2C12 and MPCs to understand whether these are the NELL binding sites on myogenic cells.

5. Conditional ablation of *Nell2* in cells of the myogenic cell line (Acta1-Cre, Pax3-Cre) should be assessed in murine animal models. I expect flawed or absent MPC migration and abnormal limb muscle development. Also, the phenotype of the conditional ablation of *Robo1* and *Robo2* in myogenic cell lines should be evaluated and compared to the phenotype of *Nell2* ablation. Similar results would suggest that NELL2 acts through ROBO during myogenesis.

6. The comparison of mRNA expression in nMMCs and MMCs could identify a variety of new ligand-receptor pathways involved in myogenesis at different stages. Thus, optimizing the MMC isolation protocol and obtaining the sequencing data hereof would generate great insights into the myogenesis communication between myoblasts and other cell types.

6. Bibliography

Ackerman, K. G., Herron, B. J., Vargas, S. O., Huang, H., Tevosian, S. G., Kochilas, L., Rao, C., Pober, B. R., Babiuk, R. P., Epstein, J. A., Greer, J. J., & Beier, D. R. (2005). Fog2 Is Required for Normal Diaphragm and Lung Development in Mice and Humans. *PLoS Genetics*, *1*(1), 0058–0065. https://doi.org/10.1371/JOURNAL.PGEN.0010010

Aghaloo, T., Cowan, C. M., Chou, Y. F., Zhang, X., Lee, H., Miao, S., Hong, N., Kuroda, S., Wu, B., Ting, K., & Soo, C. (2006). Nell-1-induced bone regeneration in calvarial defects. *The American Journal of Pathology*, *169*(3), 903–915. https://doi.org/10.2353/AJPATH.2006.051210

Amano, O., Yamane, A., Shimada, M., Koshimizu, U., Nakamura, T., & Iseki, S. (2002). Hepatocyte growth factor is essential for migration of myogenic cells and promotes their proliferation during the early periods of tongue morphogenesis in mouse embryos. *Developmental Dynamics*, *223*(2), 169–179. https://doi.org/10.1002/DVDY.1228

Amthor, H., Christ, B., & Patel, K. (1999). A molecular mechanism enabling continuous embryonic muscle growth - a balance between proliferation and differentiation. *Development*, *126*(5), 1041–1053. https://doi.org/10.1242/DEV.126.5.1041

Anthwal, N., Chai, Y., & Tucker, A. S. (2008). The Role of Transforming Growth Factor-Signalling in the Patterning of the Proximal Processes of the Murine Dentary. *Developmental Dynamics*, *237*, 1604–1613. https://doi.org/10.1002/dvdy.21567

Aoyama, H. (1993). Developmental Plasticity of the Prospective Dermatome and the Prospective Sclerotome Region of an Avian Somite. *Development, Growth & Differentiation*, *35*(5), 507–519. https://doi.org/10.1111/J.1440-169X.1993.00507.X

Asahina, K., Zhou, B., Pu, W. T., & Tsukamoto, H. (2011). Septum Transversum-Derived Mesothelium Gives Rise to Hepatic Stellate Cells and Perivascular Mesenchymal Cells in Developing Mouse Liver. *Hepatology (Baltimore, Md.)*, *53*(3), 983. https://doi.org/10.1002/HEP.24119

Babiuk, R. P., Zhang, W., Clugston, R., Allan, D. W., & Greer, J. J. (2003). Embryological origins and development of the rat diaphragm. *The Journal of Comparative Neurology*, *455*(4), 477–487. https://doi.org/10.1002/CNE.10503

Beckett, K., & Baylies, M. K. (2007). 3D analysis of founder cell and fusion competent myoblast arrangements outlines a new model of myoblast fusion. *Developmental Biology*. https://doi.org/10.1016/j.ydbio.2007.06.024

Bendall, A. J., Ding, J., Hu, G., Shen, M. M., & Abate-Shen, C. (1999). Msx1 antagonizes the myogenic activity of Pax3 in migrating limb muscle precursors. *Development*, *126*(22), 4965–4976. https://doi.org/10.1242/DEV.126.22.4965

Bentzinger, C. F., Wang, Y. X., & Rudnicki, M. A. (2012). Building muscle: molecular regulation of myogenesis. In *Cold Spring Harbor perspectives in biology* (Vol. 4, Issue 2). https://doi.org/10.1101/cshperspect.a008342

Benwell, B. L., Singh, N. C., & Ramsay, D. A. (1994). Prolonged survival in neonatal nemaline rod myopathy. *Pediatric Neurology*, *10*(4), 335–337. https://doi.org/10.1016/0887-8994(94)90134-1

Ben-Yair, R., & Kalcheim, C. (2004). Lineage analysis of the avian dermomyotome sheet reveals theexistence of single cells with both dermal and muscle progenitorfates. *Development*. https://doi.org/10.1242/dev.01617

Blackshaw, S., Harpavat, S., Trimarchi, J., Cai, L., Huang, H., Kuo, W. P., Weber, G., Lee, K., Fraioli, R. E., Cho, S. H., Yung, R., Asch, E., Ohno-Machado, L., Wong, W. H., & Cepko, C. L. (2004). Genomic analysis of mouse retinal development. *PLoS Biology*, *2*(9). https://doi.org/10.1371/JOURNAL.PBIO.0020247

Blondin, D. P., & Haman, F. (2018). Shivering and nonshivering thermogenesis in skeletal muscles. In *Handbook of Clinical Neurology* (Vol. 156, pp. 153–173). Elsevier B.V. https://doi.org/10.1016/B978-0-444-63912-7.00010-2

Bober, E., Franz, T., Arnold, H. H., Gruss, P., & Tremblay, P. (1994). Pax-3 is required for the development of limb muscles: a possible role for the migration of dermomyotomal muscle progenitor cells. *Development*, *120*(3), 603–612. https://doi.org/10.1242/DEV.120.3.603

Bondesen, B. A., Jones, K. A., Glasgow, W. C., & Pavlath, G. K. (2007). Inhibition of myoblast migration by prostacyclin is associated with enhanced cell fusion; Inhibition of myoblast migration by prostacyclin is associated with enhanced cell fusion. *The FASEB Journal • Research Communication*. https://doi.org/10.1096/fj.06-7070com

Bonkowsky, J. L., Yoshikawa, S., O'Keefe, D. D., Scully, A. L., & Thomas, J. B. (1999). Axon routing across the midline controlled by the Drosophila Derailed receptor. *Nature*, *402*(6761), 540–544. https://doi.org/10.1038/990122

Bour, B. A., Chakravarti, M., West, J. M., & Abmayr, S. M. (2000). Drosophila SNS, a member of the immunoglobulin superfamily that is essential for myoblast fusion. *Genes & Development*, *14*(12), 1498–1511. https://doi.org/10.1101/GAD.14.12.1498

Brohmann, H., Jagla, K., & Birchmeier, C. (2000). The role of Lbx1 in migration of muscle precursor cells. *Development*, *127*(2), 437–445. https://doi.org/10.1242/DEV.127.2.437

Callahan, C. A., Bonkovsky, J. L., Scully, A. L., & Thomas, J. B. (1996). derailed is required for muscle attachment site selection in Drosophila. *Development*, *122*(9), 2761–2767. https://doi.org/10.1242/DEV.122.9.2761

Carmona, R., Cañete, A., Cano, E., Ariza, L., Rojas, A., & Muñoz-Chápuli, R. (2016). Conditional deletion of WT1 in the septum transversum mesenchyme causes congenital diaphragmatic hernia in mice. *ELife*, *5*(September). https://doi.org/10.7554/ELIFE.16009

Chargé, S., & Rudnicki, M. A. (2003). Fusion with the Fused: A New Role for Interleukin-4 in the Building of Muscle. *Cell*, *113*(4), 422–423. https://doi.org/10.1016/S0092-8674(03)00358-1

Choi, E. J., Kim, D. H., Kim, J. G., Kim, D. Y., Kim, J. D., Seol, O. J., Jeong, C. S., Park, J. W., Choi, M. Y., Kang, S. G., Costa, M. E., Ojeda, S. R., & Lee, B. J. (2010). Estrogen-dependent transcription of the NEL-like 2 (NELL2) gene and its role in protection from cell death. *Journal of Biological Chemistry*, *285*(32), 25074–25084. https://doi.org/10.1074/JBC.M110.100545

Choi, S., Ferrari, G., & Tedesco, F. S. (2020). Cellular dynamics of myogenic cell migration: molecular mechanisms and implications for skeletal muscle cell

therapies. *EMBO Molecular Medicine*, *12*(12). https://doi.org/10.15252/EMMM.202012357

Christ, B., Jacob, H. J., & Jacob, M. (1972). Experimentelle Untersuchungen zur Somitenentstehung beim Hühnerembryo. *Zeitschrift Für Anatomie Und Entwicklungsgeschichte 1972 138:1*, *138*(1), 82–97. https://doi.org/10.1007/BF00519926

Christ, B., & Ordahl, C. P. (1995). Early stages of chick somite development. *Anatomy and Embryology 1995 191:5*, *191*(5), 381–396. https://doi.org/10.1007/BF00304424

Christophers, B., Lopez, M. A., Gupta, V. A., Vogel, H., & Baylies, M. (2022a). Pediatric Nemaline Myopathy: A Systematic Review Using Individual Patient Data. *Journal of Child Neurology*, *37*(7), 652–663. https://doi.org/10.1177/08830738221096316

Christophers, B., Lopez, M. A., Gupta, V. A., Vogel, H., & Baylies, M. (2022b). Pediatric Nemaline Myopathy: A Systematic Review Using Individual Patient Data. *Journal of Child Neurology*, *37*(7), 652–663. https://doi.org/10.1177/08830738221096316

Clugston, R. D., Zhang, W., & Greer, J. J. (2008). Gene expression in the developing diaphragm: significance for congenital diaphragmatic hernia. *American Journal of Physiology. Lung Cellular and Molecular Physiology*, *294*(4). https://doi.org/10.1152/AJPLUNG.00027.2008

Cowan, C. M., Cheng, S., Ting, K., Soo, C., Walder, B., Wu, B., Kuroda, S., & Zhang, X. (2006). Nell-1 induced bone formation within the distracted intermaxillary suture. *Bone*, *38*(1), 48–58. https://doi.org/10.1016/J.BONE.2005.06.023

Cramer, A. A. W., Prasad, V., Eftestøl, E., Song, T., Hansson, K. A., Dugdale, H. F., Sadayappan, S., Ochala, J., Gundersen, K., & Millay, D. P. (2020). Nuclear numbers in syncytial muscle fibers promote size but limit the development of larger myonuclear domains. *Nature Communications 2020 11:1*, *11*(1), 1–14. https://doi.org/10.1038/s41467-020-20058-7

Daston, G., Lamar, E., Olivier, M., & Goulding, M. (1996). Pax-3 is necessary for migration but not differentiation of limb muscle precursors in the mouse. *Development*, *122*(3), 1017–1027. https://doi.org/10.1242/dev.122.3.1017

Desai, J., Shannon, M. E., Johnson, M. D., Ruff, D. W., Hughes, L. A., Kerley, M. K., Carpenter, D. A., Johnson, D. K., Rinchik, E. M., & Culiat, C. T. (n.d.). *Nell1-deficient mice have reduced expression of extracellular matrix proteins causing cranial and vertebral defects*. https://doi.org/10.1093/hmg/ddl053

Desai, J., Shannon, M. E., Johnson, M. D., Ruff, D. W., Hughes, L. A., Kerley, M. K., Carpenter, D. A., Johnson, D. K., Rinchik, E. M., & Culiat, C. T. (2006). *Nell1-deficient mice have reduced expression of extracellular matrix proteins causing cranial and vertebral defects*. https://doi.org/10.1093/hmg/ddl053

Dockter, J. L. (2000). Sclerotome induction and differentiation. *Current Topics in Developmental Biology*, *48*(C), 77–127. https://doi.org/10.1016/S0070-2153(08)60755-3

Duan, D., Goemans, N., Takeda, S., Mercuri, & Aartsma-Rus, A. (2021). Duchenne muscular dystrophy. *Nature*. https://doi.org/10.1038/s41572-021-00248-3

Dunwoodie, S. L., Rodriguez, T. A., & Beddington, R. S. P. (1998). Msg1 and Mrg1, founding members of a gene family, show distinct patterns of gene expression during mouse embryogenesis. *Mechanisms of Development*, *72*(1–2), 27–40. https://doi.org/10.1016/S0925-4773(98)00011-2

Eissa, S., Khalifa, A., Laban, M., Elian, A., & Bolton, W. E. (1998). Comparison of flow cytometric DNA content analysis in fresh and paraffin-embedded ovarian neoplasms: a prospective study. *British Journal of Cancer*, *77*(3), 421–425. https://doi.org/10.1038/BJC.1998.67

Engel, J. (1989). EGF-like domains in extracellular matrix proteins: localized signals for growth and differentiation? *FEBS*, *251*(1). https://doi.org/10.1016/0014-5793(89)81417-6

Erskine, L., Williams, S. E., Brose, K., Kidd, T., Rachel, R. A., Goodman, C. S., Tessier-Lavigne, M., & Mason, C. A. (2000). *Retinal Ganglion Cell Axon Guidance in the Mouse Optic Chiasm: Expression and Function of Robos and Slits*. https://doi.org/10.1523/JNEUROSCI.20-13-04975.2000

Fan, C. M., & Tessier-Lavigne, M. (1994). Patterning of mammalian somites by surface ectoderm and notochord: Evidence for sclerotome induction by a hedgehog homolog. *Cell*, *79*(7), 1175–1186. https://doi.org/10.1016/0092-8674(94)90009-4

Fortier, M., Comunale, F., Kucharczak, J., Blangy, A., Charrasse, S., & Gauthier-Rouviè, C. (2008). RhoE controls myoblast alignment prior fusion through RhoA and ROCK. *Cell Death and Differentiation*, *15*, 1221–1231. https://doi.org/10.1038/cdd.2008.34

Frasch, M. (1999). Controls in patterning and diversification of somatic muscles during Drosophila embryogenesis. *Current Opinion in Genetics & Development*, *9*(5), 522–529. https://doi.org/10.1016/S0959-437X(99)00014-3

Fukuhara, N., Howitt, J. A., Hussain, S. A., & Hohenester, E. (2008). Structural and functional analysis of slit and heparin binding to immunoglobulin-like domains 1 and 2 of Drosophila robo. *Journal of Biological Chemistry*, *283*(23), 16226–16234. https://doi.org/10.1074/JBC.M800688200

Galli, L. M., Willert, K., Nusse, R., Yablonka-Reuveni, Z., Nohno, T., Denetclaw, W., & Burrus, L. W. (2004). A proliferative role for Wnt-3a in chick somites. *Developmental Biology*, *269*(2), 489–504. https://doi.org/10.1016/J.YDBIO.2004.01.041

González-Alonso, J. (2012). Experimental Physiology Human thermoregulation and the cardiovascular system Heat production in skeletal muscle. *Exp Physiol*, *97*, 340–346. https://doi.org/10.1113/expphysiol.2011.058701

Griffin, C. A., Kafadar, K. A., & Pavlath, G. K. (2009). MOR23 Promotes Muscle Regeneration and Regulates Cell Adhesion and Migration. *Developmental Cell*, *17*(5), 649–661. https://doi.org/10.1016/J.DEVCEL.2009.09.004

Gros, J., Manceau, M., Thomé, V., & Marcelle, C. (2005). A common somitic origin for embryonic muscle progenitors and satellite cells. *Nature*. https://doi.org/10.1038/nature03572

Gross, M. K., Moran-Rivard, L., Velasquez, T., Nakatsu, M. N., Jagla, K., & Goulding, M. (2000). Lbx1 is required for muscle precursor migration along a lateral pathway into the limb. *Development*, *127*(2), 413–424. https://doi.org/10.1242/DEV.127.2.413

Ha, C. M., Choi, J., Choi, E. J., Costa, M. E., Lee, B. J., & Ojeda, S. R. (2008). NELL2, a neuron-specific EGF-like protein, is selectively expressed in glutamatergic

neurons and contributes to the glutamatergic control of GnRH neurons at puberty. *Neuroendocrinology*, *88*(3), 199–211. https://doi.org/10.1159/000139579

Halperin-Barlev, O., & Kalcheim, C. (2011). Sclerotome-derived Slit1 drives directional migration and differentiation of Robo2-expressing pioneer myoblasts. *Development*, *138*(14), 2935–2945. https://doi.org/10.1242/DEV.065714

Hasebe, A., Nakamura, Y., Tashima, H., Takahashi, K., Iijima, M., Yoshimoto, N., Ting, K., Kuroda, S., & Niimi, T. (2012). The C-terminal region of NELL1 mediates osteoblastic cell adhesion through integrin $\alpha 3\beta 1$. *FEBS Letters*, *586*(16), 2500–2506. https://doi.org/10.1016/J.FEBSLET.2012.06.014/FORMAT/PDF

Hayashi, Y., Kashiwagi, M., Yasuda, K., Ando, R., Kanuka, M., Sakai, K., & Itohara, S. (2015). Cells of a common developmental origin regulate REM/non-REM sleep and wakefulness in mice. *Science*, *350*(6263), 957–961. https://doi.org/10.1126/science.aad1023

He, T.-C., Zhang, J., Wang, J., Liao, J., Zhang, F., Song, D., Lu, M., Liu, J., Wei, Q., Tang, S., Liu, H., Fan, J., Zou, Y., Guo, D., Huang, J., Liu, F., Ma, C., Hu, X., Li, L., … He, T.-C. (2017). NEL-Like Molecule-1 (Nell1) Is Regulated by Bone Morphogenetic Protein 9 (BMP9) and Potentiates BMP9-Induced Osteogenic Differentiation at the Expense of Adipogenesis in Mesenchymal Stem Cells. *Cell Physiol Biochem*, *41*, 484–500. https://doi.org/10.1159/000456885

Hirsinger, E., Jouve, C., Dubrulle, J., & Pourquié, O. (2000). Somite formation and patterning. *International Review of Cytology*, *198*, 1–65. https://doi.org/10.1016/S0074-7696(00)98002-1

Holder, A. M., Klaassens, M., Tibboel, D., de Klein, A., Lee, B., & Scott, D. A. (2007). Genetic Factors in Congenital Diaphragmatic Hernia. *The American Journal of Human Genetics*, *80*(5), 825–845. https://doi.org/10.1086/513442

Hollway, G., & Currie, P. (2005). *Vertebrate Myotome Development*. https://doi.org/10.1002/bdrc.20046

Iritani, I. (1984). Experimental study on embryogenesis of congenital diaphragmatic hernia. *Anatomy and Embryology*, *169*(2), 133–139. https://doi.org/10.1007/BF00303142

Itoh, N., Mima, T., & Mikawa, T. (1996). Loss of fibroblast growth factor receptors is necessary for terminal differentiation of embryonic limb muscle. *Development*, *122*(1), 291–300. https://doi.org/10.1242/DEV.122.1.291

Jansen, K. M., & Pavlath, G. K. (2006). Mannose receptor regulates myoblast motility and muscle growth. *The Journal of Cell Biology*, *174*(3), 403–413. https://doi.org/10.1083/JCB.200601102

Jaworski, A., & Tessier-Lavigne, M. (2012). Autocrine/juxtaparacrine regulation of axon fasciculation by Slit-Robo signaling. *Nature Neuroscience 2012 15:3*, *15*(3), 367–369. https://doi.org/10.1038/nn.3037

Jaworski, A., Tom, I., Tong, R. K., Gildea, H. K., Koch, A. W., Gonzalez, L. C., & Tessier-Lavigne, M. (2015). Operational redundancy in axon guidance through the multifunctional receptor Robo3 and its ligand NELL2. *Science*, *350*(6263), 961–965. https://doi.org/10.1126/SCIENCE.AAD2615

Jen, J. C., Chan, W. M., Bosley, T. M., Wan, J., Carr, J. R., Rüb, U., Shattuck, D., Salamon, G., Kudo, L. C., Ou, J., Lin, D. D. M., Salih, M. A. M., Kansu, T., al Dhalaan, H., al Zayed, Z., MacDonald, D. B., Stigsby, B., Plaitakis, A., Dretakis, E. K., … Engle, E. C. (2004). Mutations in a Human ROBO Gene Disrupt Hindbrain Axon Pathway Crossing and Morphogenesis. *Science (New York, N.Y.)*, *304*(5676), 1509. https://doi.org/10.1126/SCIENCE.1096437

Jensen, J. H., Cakal, S. D., Li, J., Pless, C. J., Radeke, C., Leth Jepsen, M., Jensen, T. E., Dufva, M., & Lind, J. U. (2020). Large-scale spontaneous self-organization and maturation of skeletal muscle tissues on ultra-compliant gelatin hydrogel substrates. *Nature Scientific Reports*, *10*, 13305. https://doi.org/10.1038/s41598-020-69936-6

Jensen, J., Rustad, I., Kolnes, A. J., Lai, Y.-C., Huikuri, H. V., Giorgino, F., Degli Studi Di Bari, U., Moro, A., & Jessen, N. (2011). The role of skeletal muscle glycogen breakdown for regulation of insulin sensitivity by exercise. *Frontiers in Physiology*. https://doi.org/10.3389/fphys.2011.00112

Jeong, J. K., Ryu, B. J., Choi, J., Kim, D. H., Choi, E. J., Park, J. W., Park, J. J., & Lee, B. J. (2008). NELL2 participates in formation of the sexually dimorphic nucleus of

the pre-optic area in rats. *Journal of Neurochemistry*, *106*(4), 1604–1613. https://doi.org/10.1111/J.1471-4159.2008.05505.X

Jin, Z., Mori, Y., Yang, J., Sato, F., Ito, T., Cheng, Y., Paun, B., Hamilton, J. P., Kan, T., Olaru, A., David, S., Agarwal, R., Abraham, J. M., Beer, D., Montgomery, E., & Meltzer, S. J. (2007). Hypermethylation of the nel-like 1 gene is a common and early event and is associated with poor prognosis in early-stage esophageal adenocarcinoma. *Oncogene*, *26*, 6332–6340. https://doi.org/10.1038/sj.onc.1210461

Johnson, D. S., & Chen, Y. H. (2012). Ras Family of Small GTPases In Immunity And Inflammation. *Current Opinion in Pharmacology*, *12*(4), 458. https://doi.org/10.1016/J.COPH.2012.02.003

Kahane, N., Cinnamon, Y., Bachelet, I., & Kalcheim, C. (2001). The third wave of myotome colonization by mitotically competent progenitors: regulating the balance between differentiation and proliferation during muscle development. *Development*, *128*(12), 2187–2198. https://doi.org/10.1242/DEV.128.12.2187

Kardon, G., Harfe, B. D., & Tabin, C. J. (2003). A Tcf4-Positive Mesodermal Population Provides a Prepattern for Vertebrate Limb Muscle Patterning. In *Developmental Cell* (Vol. 5). https://doi.org/10.1016/s1534-5807(03)00360-5

Kassar-Duchossoy, L., Giacone, E., Gayraud-Morel, B., Jory, A., Gomès, D., & Tajbakhsh, S. (2005). Pax3/Pax7 mark a novel population of primitive myogenic cells during development. *Genes & Dev*. https://doi.org/10.1101/gad.345505

Kim, B. J., Lee, Y. S., Lee, S. Y., Baek, W. Y., Choi, Y. J., Moon, S. A., Lee, S. H., Kim, J. E., Chang, E. J., Kim, E. Y., Yoon, J., Kim, S. W., Ryu, S. H., Lee, S. K., Lorenzo, J. A., Ahn, S. H., Kim, H., Lee, K. U., Kim, G. S., & Koh, J. M. (2018). Osteoclast-secreted SLIT3 coordinates bone resorption and formation. *The Journal of Clinical Investigation*, *128*(4), 1429–1441. https://doi.org/10.1172/JCI91086

Kim, D. H., Kim, H. R., Choi, E. J., Kim, D. Y., & Kim, K. K. (2014). Neural Epidermal Growth Factor-Like ike Protein 2 (NELL2) Promotes Aggregation of Embryonic Carcinoma P19 Cells by Inducing N-Cadherin Expression. *PLoS ONE*, *9*(1), 85898. https://doi.org/10.1371/journal.pone.0085898

Kocherlakota, K. S., Wu, J. M., McDermott, J., & Abmayr, S. M. (2008). Analysis of the cell adhesion molecule sticks-and-stones reveals multiple redundant functional

domains, protein-interaction motifs and phosphorylated tyrosines that direct myoblast fusion in Drosophila melanogaster. *Genetics*, *178*(3), 1371–1383. https://doi.org/10.1534/GENETICS.107.083808

Kohler, J., Popov, C., Klotz, B., Alberton, P., Prall, W. C., Haasters, F., Müller-Deubert, S., Ebert, R., Klein-Hitpass, L., Jakob, F., Schieker, M., & Docheva, D. (2013). Uncovering the cellular and molecular changes in tendon stem/progenitor cells attributed to tendon aging and degeneration. *Aging Cell*, *12*(6), 988. https://doi.org/10.1111/ACEL.12124

Kowarz, E., Löscher, D., & Marschalek, R. (2015). Optimized Sleeping Beauty transposons rapidly generate stable transgenic cell lines. *Biotechnology Journal*, *10*(4), 647–653. https://doi.org/10.1002/BIOT.201400821

Kuroda, ichi, & Tanizawa, K. (1999). Involvement of Epidermal Growth Factor-like Domain of NELL Proteins in the Novel Protein-Protein Interaction with Protein Kinase C 1. *Biochemical and Biophysical Research Communications*. https://doi.org/10.1006/bbrc.1999.1753

Kuroda, S., Oyasu, M., Kawakami, M., Kanayama, N., Tanizawa, K., Saito, N., Abe, T., Matsuhashi, S., & Ting, K. (1999). Biochemical characterization and expression analysis of neural thrombospondin-1-like proteins NELL1 and NELL2. *Biochemical and Biophysical Research Communications*, *265*(1), 79–86. https://doi.org/10.1006/bbrc.1999.1638

Lanser, M. E., & Fallon, J. F. (1987). Development of the Brachial Lateral Motor Column in the Wingless Mutant Chick Embryo: Motoneuron Survival Under Varying Degrees of Peripheral Load. *The Journal of Comperative Neurology*. https://doi.org/10.1002/cne.902610307

Lehka, L., & Rędowicz, M. J. (2020). Mechanisms regulating myoblast fusion: A multilevel interplay. In *Seminars in Cell and Developmental Biology* (Vol. 104, pp. 81–92). Elsevier Ltd. https://doi.org/10.1016/j.semcdb.2020.02.004

Léjard, V., Brideau, G., Blais, F., Salingcarnboriboon, R., Wagner, G., Roehrl, M. H. A., Noda, M., Duprez, D., Houillier, P., & Rossert, J. (2007). Scleraxis and NFATc Regulate the Expression of the Pro-α1(I) Collagen Gene in Tendon Fibroblasts *.

Journal of Biological Chemistry, *282*(24), 17665–17675. https://doi.org/10.1074/JBC.M610113200

Li, Y., Zhang, X. tan, Wang, X. yu, Wang, G., Chuai, M., Münsterberg, A., & Yang, X. (2017). Robo signaling regulates the production of cranial neural crest cells. *Experimental Cell Research*, *361*(1), 73–84. https://doi.org/10.1016/J.YEXCR.2017.10.002

Liu, J., Liu, D., Zhang, X., Li, Y., Fu, X., He, W., Li, M., Chen, P., Zeng, G., DiSanto, M. E., Wang, X., & Zhang, X. (2021). NELL2 modulates cell proliferation and apoptosis via ERK pathway in the development of benign prostatic hyperplasia. *Clinical Science*, *135*(13), 1591–1608. https://doi.org/10.1042/CS20210476

Liu, J., Zhang, L., Wang, D., Shen, H., Jiang, M., Mei, P., Hayden, P. S., Sedor, J. R., & Hu, H. (2003). Congenital diaphragmatic hernia, kidney agenesis and cardiac defects associated with Slit3-deficiency in mice. *Mechanisms of Development*, *120*(9), 1059–1070. https://doi.org/10.1016/S0925-4773(03)00161-8

Logan, M., Martin, J. F., Nagy, A., Lobe, C., Olson, E. N., & Tabin, C. J. (2002). Expression of Cre Recombinase in the developing mouse limb bud driven by a Prxl enhancer. *Genesis*, *33*(2), 77–80. https://doi.org/10.1002/GENE.10092

Long, H., Sabatier, C., Ma, L., Plump, A., Yuan, W., Ornitz, D. M., Tamada, A., Murakami, F., Goodman, C. S., & Tessier-Lavigne, M. (2004). Conserved roles for Slit and Robo proteins in midline commissural axon guidance. *Neuron*, *42*(2), 213–223. https://doi.org/10.1016/S0896-6273(04)00179-5

Luce, M. J., & Burrows, P. D. (1999). The neuronal EGF-related genes NELL1 and NELL2 are expressed in hemopoietic cells and developmentally regulated in the B lineage. *Gene*, *231*, 121–126. https://doi.org/10.1016/s0378-1119(99)00093-1

Lynch CJ. (1969). The so-called Swiss mouse. *Subject Strain Bibliography*. https://mouseion.jax.org/ssbb1969/1067

Maeda, K., Maeda, K., Matsuhashi, S., Tabuchi, K., Watanabe, T., Katagiri, T., Oyasu, M., Saito, N., & Kuroda, S.-I. (2001). Brain Specific Human Genes, NELL1 and NELL2, Are Predominantly Expressed in Neuroblastoma and Other Embryonal Neuroepithelial Tumors. *Neurologia Medico-Chirurgica*, *41*. https://doi.org/10.2176/nmc.41.582

Mátés, L., Chuah, M. K. L., Belay, E., Jerchow, B., Manoj, N., Acosta-Sanchez, A., Grzela, D. P., Schmitt, A., Becker, K., Matrai, J., Ma, L., Samara-Kuko, E., Gysemans, C., Pryputniewicz, D., Miskey, C., Fletcher, B., Vandendriessche, T., Ivics, Z., & Izsvák, Z. (2009). Molecular evolution of a novel hyperactive Sleeping Beauty transposase enables robust stable gene transfer in vertebrates. *Nature Genetics*, *41*(6), 753–761. https://doi.org/10.1038/NG.343

Matsuhashi, S., Noji, S., Koyama, E., Myokai, F., Ohuchi, H., Taniguchi, S., & Hori, K. (1995). nel, Encoding a Mr 93 K Protein With EGF-Like Strongly Expressed in Neural Tissues of Early Stage Chick Embryos. *Developmental Dynamics*. https://doi.org/10.1002/aja.1002030209

Meijering, E., Dzyubachyk, O., & Smal, I. (2012). Methods for Cell and Particle Tracking. *Imaging and Spectroscopic Analysis of Living Cells*, *504*(9), 183–200. https://doi.org/10.1016/B978-0-12-391857-4.00009-4

Mennerich, D., Schäfer, K., & Braun, T. (1998). Pax-3 is necessary but not sufficient for lbx1 expression in myogenic precursor cells of the limb. *Mechanisms of Development*, *73*(2), 147–158. https://doi.org/10.1016/S0925-4773(98)00046-X

Menon, S. D., Osman, Z., Chenchill, K., & Chia, W. (2005). A positive feedback loop between Dumbfounded and Rolling pebbles leads to myotube enlargement in Drosophila. *Journal of Cell Biology*, *169*(6), 909–920. https://doi.org/10.1083/JCB.200501126

Merrell, A. J., Ellis, B. J., Fox, Z. D., Lawson, J. A., Weiss, J. A., & Kardon, G. (2015). Muscle connective tissue controls development of the diaphragm and is a source of congenital diaphragmatic hernias. *Nature Genetics*, *47*(5), 496–504. https://doi.org/10.1038/NG.3250

Merrell, A. J., & Kardon, G. (2013). Development of the diaphragm -- a skeletal muscle essential for mammalian respiration. *The FEBS Journal*, *280*(17), 4026–4035. https://doi.org/10.1111/FEBS.12274

Miosge, N., Klenczar, C., Herken, R., Willem, M., & Mayer, U. (1999). Organization of the myotendinous junction is dependent on the presence of alpha7beta1 integrin. *Laboratory Investigation; a Journal of Technical Methods and Pathology*, *79*(12), 1591–1599. https://pubmed.ncbi.nlm.nih.gov/10616209/

Mori, Y., Cai, K., Cheng, Y., Wang, S., Paun, B., Hamilton, J. P., Jin, Z., Sato, F., Berki, A. T., Kan, T., Ito, T., Mantzur, C., Abraham, J. M., & Meltzer, S. J. (2006). A Genome-Wide Search Identifies Epigenetic Silencing of Somatostatin,Tachykinin-1, and 5 Other Genes in Colon Cancer. *Gastroenterology*. https://doi.org/10.1053/j.gastro.2006.06.006

Morlot, C., Thielens, N. M., Ravelli, R. B. G., Hemrika, W., Romijn, R. A., Gros, P., Cusack, S., & McCarthy, A. A. (2007). Structural insights into the Slit-Robo complex. *Proceedings of the National Academy of Sciences of the United States of America*, *104*(38), 14923–14928. https://doi.org/10.1073/PNAS.0705310104

Murchison, N. D., Price, B. A., Conner, D. A., Keene, D. R., Olson, E. N., Tabin, C. J., & Schweitzer, R. (2007). Regulation of tendon differentiation by scleraxis distinguishes force-transmitting tendons from muscle-anchoring tendons. *Development*, *134*(14), 2697–2708. https://doi.org/10.1242/DEV.001933

Murphy, M., & Kardon, G. (2011). Origin of Vertebrate Limb Muscle: The Role of Progenitor and Myoblast Populations. *Current Topics in Developmental Biology*, *96*, 1. https://doi.org/10.1016/B978-0-12-385940-2.00001-2

Muzumdar, M. D., Tasic, B., Miyamichi, K., Li, N., & Luo, L. (2007). A global double-fluorescent Cre reporter mouse. *Genesis* , *45*(9), 593–605. https://doi.org/10.1002/DVG.20335

Naidu, P. S., Ludolph, D. C., To, R. Q., Hinterberger, T. J., & Konieczny, S. F. (1995). Myogenin and MEF2 function synergistically to activate the MRF4 promoter during myogenesis. *Molecular and Cellular Biology*, *15*(5), 2707–2718. https://doi.org/10.1128/MCB.15.5.2707

Nakamoto, C., Durward, E., Horie, M., & Nakamoto, M. (2019). Nell2 regulates the contralateral-versus-ipsilateral visual projection as a domain-specific positional cue. *The Company of Biologists*. https://doi.org/10.1242/dev.170704

Nakamoto, C., Kuan, S.-L., Findlay, A. S., Durward, E., Ouyang, Z., Zakrzewska, E. D., Endo, T., & Nakamoto, M. (2014). Nel positively regulates the genesis of retinal ganglion cells by promoting their differentiation and survival during development. *MBoC*. https://doi.org/10.1091/mbc.E13-08-0453

Nelson, B. R., Claes, K., Todd, V., Chaverra, M., & Lefcort, F. (2004). NELL2 promotes motor and sensory neuron differentiation and stimulates mitogenesis in DRG in vivo. *Developmental Biology*, *270*(2), 322–335. https://doi.org/10.1016/J.YDBIO.2004.03.004

Nelson, B. R., Matsuhashi, S., & Lefcort, F. (2002). Restricted neural epidermal growth factor-like like 2 (NELL2) expression during muscle and neuronal differentiation. *Mechanisms of Development* . https://doi.org/10.1016/S0925-4773(03)00084-4

Niimi, T. (2021). Roles of Slit Ligands and Their Roundabout (Robo) Family of Receptors in Bone Remodeling. *Advances in Experimental Medicine and Biology*, *21*, 143–154. https://doi.org/10.1007/5584_2020_586

Nimmagadda, S., Geetha-Loganathan, P., Scaal, M., Christ, B., & Huang, R. (2007). FGFs, Wnts and BMPs mediate induction of VEGFR-2 (Quek-1) expression during avian somite development. *Developmental Biology*, *305*(2), 421–429. https://doi.org/10.1016/J.YDBIO.2007.02.031

Ordan, E., & Volk, T. (2015). A non-signaling role of Robo2 in tendons is essential for Slit processing and muscle patterning. *The Company of Biologists*. https://doi.org/10.1242/dev.128157

Patel, T. J., & Lieber, R. L. (1997). Force transmission in skeletal muscle: from actomyosin to external tendons. *Exercise and Sport Sciences Reviews*, *25*(1), 321–364. https://doi.org/10.1249/00003677-199700250-00014

Pearce, J. M. S. (2009). Henry Gray's Anatomy. *Clinical Anatomy*, *22*(3), 291–295. https://doi.org/10.1002/CA.20775

Perry, S. F., Similowski, T., Klein, W., & Codd, J. R. (2010). The evolutionary origin of the mammalian diaphragm. *Respiratory Physiology & Neurobiology*, *171*(1), 1–16. https://doi.org/10.1016/J.RESP.2010.01.004

Pober, B. R. (2007). Overview of Epidemiology, Genetics, Birth Defects, and Chromosome Abnormalities Associated With CDH. *Am J Med Genet Part C Semin Med Genet*, *145C*(2), 158. https://doi.org/10.1002/AJMG.C.30126

Pryce, B. A., Watson, S. S., Murchison, N. D., Staverosky, J. A., Dünker, N., & Schweitzer, R. (2009). Recruitment and maintenance of tendon progenitors by

TGFβ signaling are essential for tendon formation. *Development*, *136*(8), 1351–1361. https://doi.org/10.1242/DEV.027342

Rajagopalan, S., Nicolas, E., Vivancos, V., Berger, J., & Dickson, B. J. (2000). Crossing the Midline: Roles and Regulation of Robo Receptors. *Neuron*, *28*(3), 767–777. https://doi.org/10.1016/S0896-6273(00)00152-5

Rochlin, K., Yu, S., Roy, S., & Baylies, M. K. (2010). Myoblast fusion: When it takes more to make one. *Developmental Biology*, *341*(1), 66–83. https://doi.org/10.1016/J.YDBIO.2009.10.024

Romero, N. B., Sandaradura, S. A., & Clarke, N. F. (2013). Recent advances in nemaline myopathy. *Current Opinion in Neurology*, *26*(5), 519–526. https://doi.org/10.1097/WCO.0B013E328364D681

Rothberg, J. M., Jacobs, J. R., Goodman, C. S., & Artavanis-Tsakonas, S. (1990). slit: an extracellular protein necessary for development of midline glia and commissural axon pathways contains both EGF and LRR domains. *Genes & Development*, *4*(12A), 2169–2187. https://doi.org/10.1101/GAD.4.12A.2169

Ruiz-Gómez, M., Coutts, N., Price, A., Taylor, M. v., & Bate, M. (2000). Drosophila Dumbfounded: A Myoblast Attractant Essential for Fusion. *Cell*, *102*(2), 189–198. https://doi.org/10.1016/S0092-8674(00)00024-6

Ryu, B. J., Kim, H. R., Jeong, J. K., & Lee, B. J. (2011). Regulation of the Female Rat Estrous Cycle by a Neural Cell-Specific Epidermal Growth Factor-like Repeat Domain Containing Protein, NELL2. *Mol. Cells*, *32*, 203–207. https://doi.org/10.1007/s10059-011-0086-7

Saller, M. M. (2016). *Molecular mechanisms of phrenic nerve outgrowth and innervation of the diaphragm*. https://doi.org/10.5282/edoc.20092

Saller, M. M., Alberton, P., Huber, A. B., & Huettl, R. E. (2017). How to Wire the Diaphragm: Wholemount Staining Methods to Analyze Mammalian Respiratory Innervation. *Methods in Molecular Biology (Clifton, N.J.)*, *1668*, 177–192. https://doi.org/10.1007/978-1-4939-7283-8_13

Sarnat, H. B. (1994). New insights into the pathogenesis of congenital myopathies. *Journal of Child Neurology*, *9*(2), 193–201. https://doi.org/10.1177/088307389400900218

Schäfer, K., & Braun, T. (1999). Early specification of limb muscle precursor cells by the homeobox gene Lbx1h. *Nature Genetics 1999 23:2*, *23*(2), 213–216. https://doi.org/10.1038/13843

Schejter, E. D., & Baylies, M. K. (2010). Born to run: creating the muscle fiber. *Current Opinion in Cell Biology*. https://doi.org/10.1016/j.ceb.2010.08.009

Schindelin, J., Arganda-Carreras, I., Frise, E., Kaynig, V., Longair, M., Pietzsch, T., Preibisch, S., Rueden, C., Saalfeld, S., Schmid, B., Tinevez, J. Y., White, D. J., Hartenstein, V., Eliceiri, K., Tomancak, P., & Cardona, A. (2012). Fiji: an open-source platform for biological-image analysis. *Nature Methods 2012 9:7*, *9*(7), 676–682. https://doi.org/10.1038/nmeth.2019

Schmidt, C., Bladt, F., Goedecke, S., Brinkmann, V., Zschiesche, W., Sharpe, M., Gherardi, E., & Goedecke, S. (1995). Scatter factor/hepatocyte growth factor is essential for liver development. *Nature 1995 373:6516*, *373*(6516), 699–702. https://doi.org/10.1038/373699a0

Schnorrer, F., Kalchhauser, I., & Dickson, B. J. (2007). The transmembrane protein Kon-tiki couples to Dgrip to mediate myotube targeting in Drosophila. *Developmental Cell*, *12*(5), 751–766. https://doi.org/10.1016/J.DEVCEL.2007.02.017

Schwander, M., Leu, M., Stumm, M., Dorchies, O. M., Ruegg, U. T., Schittny, J., & Müller, U. (2003). β1 Integrins Regulate Myoblast Fusion and Sarcomere Assembly. *Developmental Cell*, *4*(5), 673–685. https://doi.org/10.1016/S1534-5807(03)00118-7

Schweitzer, R., Chyung, J. H., Murtaugh, L. C., Brent, A. E., Rosen, V., Olson, E. N., Lassar, A., & Tabin, C. J. (2001). Analysis of the tendon cell fate using Scleraxis, a specific marker for tendons and ligaments. *Development*, *128*(19), 3855–3866. https://doi.org/10.1242/DEV.128.19.3855

SG Kramer, T Kidd, JH Simpson, & CS Goodman. (2001). Switching repulsion to attraction: changing responses to slit during transition in mesoderm migration. *Science*. https://doi.org/10.1126/science.1058766

Shirakabe, K., Terasawa, K., Miyama, K., Shibuya, H., & Nishida, E. (2001). Regulation of the activity of the transcription factor Runx2 by two homeobox proteins, Msx2 and Dlx5. *Genes to Cells*, *6*(10), 851–856. https://doi.org/10.1046/J.1365-2443.2001.00466.X

Shukunami, C., Takimoto, A., Nishizaki, Y., Yoshimoto, Y., Tanaka, S., Miura, S., Watanabe, H., Sakuma, T., Yamamoto, T., Kondoh, G., & Hiraki, Y. (2018). Scleraxis is a transcriptional activator that regulates the expression of Tenomodulin, a marker of mature tenocytes and ligamentocytes. *Scientific Reports 2018 8:1*, *8*(1), 1–17. https://doi.org/10.1038/s41598-018-21194-3

Sohn, R. L., Huang, P., Kawahara, G., Mitchell, M., Guyon, J., Kalluri, R., Kunkel, L. M., & Gussoni, E. (2009). A role for nephrin, a renal protein, in vertebrate skeletal muscle cell fusion. *Proceedings of the National Academy of Sciences of the United States of America*, *106*(23), 9274–9279. https://doi.org/10.1073/PNAS.0904398106

Strünkelnberg, M., Bonengel, B., Moda, L. M., Hertenstein, A., Gert de Couet, H., Ramos, R. G. P., & Fischbach, K. F. (2001). Rst and its paralogue kirre act redundantly during embryonic muscle development in Drosophila. *Development*, *128*(21), 4229–4239. https://doi.org/10.1242/DEV.128.21.4229

Subramanian, A., Wayburn, B., Bunch, T., & Volk, T. (2007). Thrombospondin-mediated adhesion is essential for the formation of the myotendinous junction in Drosophila. *Development*, *134*(7), 1269–1278. https://doi.org/10.1242/DEV.000406

Tajbakhsh, S., Rocancourt, D., Cossu, G., & Buckingham, M. (1997). Redefining the Genetic Hierarchies Controlling Skeletal Myogenesis: Pax-3 and Myf-5 Act Upstream of MyoD. *Cell*, *89*(1), 127–138. https://doi.org/10.1016/S0092-8674(00)80189-0

Takahashi, K., Imai, A., Iijima, M., Yoshimoto, N., Maturana, A. D., Kuroda, S., & Niimi, T. (2015). Mapping the heparin-binding site of the osteoinductive protein NELL1 by site-directed mutagenesis. *FEBS Letters*, *589*(24), 4026–4032. https://doi.org/10.1016/J.FEBSLET.2015.11.032/FORMAT/PDF

Takahashi, T., Zimmer, J., Friedmacher, F., & Puri, P. (2016). Expression of Prx1 and Tcf4 is decreased in the diaphragmatic muscle connective tissue of nitrofen-

induced congenital diaphragmatic hernia. *Journal of Pediatric Surgery*, *51*(12), 1931–1935. https://doi.org/10.1016/J.JPEDSURG.2016.09.007

Tatsumi, R., Anderson, J. E., Nevoret, C. J., Halevy, O., & Allen, R. E. (1998). HGF/SF Is Present in Normal Adult Skeletal Muscle and Is Capable of Activating Satellite Cells. *Developmental Biology*, *194*(1), 114–128. https://doi.org/10.1006/DBIO.1997.8803

Tidball, J. G. (1991). Myotendinous junction injury in relation to junction structure and molecular composition. *Exercise and Sport Sciences Reviews*, *19*(1), 419–445. https://doi.org/10.1249/00003677-199101000-00012

Tidball, J. G. (1994). Assembly of Myotendinous Junctions in the Chick Embryo: Deposition of P68 Is an Early Event in Myotendinous Junction Formation. *Developmental Biology*, *163*(2), 447–456. https://doi.org/10.1006/DBIO.1994.1161

Ting, K., Vastardis, H., Mulliken, J. B., Soo, C., Tieu, A., Kwong, E., Bertolami, C. N., Kawamoto, H., Kuroda, I., & Longaker, M. T. (1999). Human NELL-1 Expressed in Unilateral Coronal Synostosis. *Journal of Bone and Mineral Research*. https://doi.org/10.1359/jbmr.1999.14.1.80

Trotter, J. A. (1993). Functional morphology of force transmission in skeletal muscle. A brief review. *Acta Anatomica*, *146*(4), 205–222. https://doi.org/10.1159/000147459

Trotter, J. A. (2002). Structure–function considerations of muscle–tendon junctions. *Comparative Biochemistry and Physiology Part A: Molecular & Integrative Physiology*, *133*(4), 1127–1133. https://doi.org/10.1016/S1095-6433(02)00213-1

Truong, T., Zhang, X., Pathmanathan, D., Soo, C., & Ting, K. (2007). Craniosynostosis-Associated Gene Nell-1 Is Regulated by Runx2. *J Bone Miner Res*, *22*, 7–18. https://doi.org/10.1359/JBMR.061012

Turner, N. J., Londono, R., Dearth, C. L., Culiat, C. T., & Badylak, S. F. (2014). Human NELL1 protein augments constructive tissue remodeling with biologic scaffolds. *Cells Tissues Organs*, *198*(4), 249–265. https://doi.org/10.1159/000356491

Vasyutina, E., Martarelli, B., Wende, H., & Birchmeier, C. (2009). The small G-proteins Rac1 and Cdc42 are essential for myoblast fusion in the mouse. *PNAS*. https://doi.org/10.1073/pnas.0902501106

Venuti, J. M., Morris, J. H., Vivian, J. L., Olson, E. N., & Klein, W. H. (1995). Myogenin is required for late but not early aspects of myogenesis during mouse development. *Journal of Cell Biology*, *128*(4), 563–576. https://doi.org/10.1083/JCB.128.4.563

Watanabe, T. K., Katagiri, T., Suzuki, M., Shimizu, F., Fujiwara, T., Kanemoto, N., Nakamura, Y., Hirai, Y., Maekawa, H., & Takahashi, E. I. (1996). Cloning and Characterization of Two Novel Human cDNAs (NELL1 and NELL2) Encoding Proteins with Six EGF-like Repeats. *Genomics*, *38*(3), 273–276. https://doi.org/10.1006/GENO.1996.0628

Webb, S. E., Lee, K. K. H., Tang, M. K., & Ede, D. A. (1997). Fibroblast Growth Factors 2 and 4 Stimulate Migration of Mouse Embryonic Limb Myogenic Cells. *Developmental Dynamics*, *209*, 206–216. https://doi.org/10.1002/(SICI)1097-0177(199706)209:2

Wharton, K. A., Johansen, K. M., Xu, T., & Artavanis-Tsakonas, S. (1985). Nucleotide sequence from the neurogenic locus Notch implies a gene product that shares homology with proteins containing EGF-like repeats. *Cell*, *43*(3), 567–581. https://doi.org/10.1016/0092-8674(85)90229-6

Xinli Zhang, Kang Ting, & Saito. (2002). Craniosynostosis in transgenic mice overexpressing Nell-1. *JCI*. https://doi.org/10.1172/JCI200215375

Yamamoto, N., Kashiwagi, M., Ishihara, M., Kojima, T., Maturana, A. D., Kuroda, ichi, & Niimi, T. (2019a). This article contains Figs. S1-S12. *J. Biol. Chem*, *294*(12), 4693. https://doi.org/10.1074/jbc.RA118.005819

Yamamoto, N., Kashiwagi, M., Ishihara, M., Kojima, T., Maturana, A. D., Kuroda, S., & Niimi, T. (2019b). Robo2 contains a cryptic binding site for neural EGFL-like (NELL) protein 1/2. *Journal of Biological Chemistry*, *294*(12), 4693–4703. https://doi.org/10.1074/jbc.RA118.005819

Yee, S.-P., & Rigby, P. W. J. (1993). The regulation of myogenin gene expression during the embryonic development of tile mouse. *Genes & Development*. https://doi.org/10.1101/gad.7.7a.1277

Yin, H., Price, F., & Rudnicki, M. A. (2013). Satellite cells and the muscle stem cell niche. *Physiological Reviews*, *93*(1), 23–67.

https://doi.org/10.1152/PHYSREV.00043.2011/ASSET/IMAGES/LARGE/Z9J00113 26380003.JPEG

Yu, L., Wynn, J., Cheung, Y. H., Shen, Y., Mychaliska, G. B., Crombleholme, T. M., Azarow, K. S., Lim, F. Y., Chung, D. H., Potoka, D., Warner, B. W., Bucher, B., Stolar, C., Aspelund, G., Arkovitz, M. S., & Chung, W. K. (2013). Variants in GATA4 are a rare cause of familial and sporadic congenital diaphragmatic hernia. *Human Genetics*, *132*(3), 285–292. https://doi.org/10.1007/S00439-012-1249-0

Yuan, W., Rao, Y., Babiuk, R. P., Greer, J., Wu, J. Y., & Ornitz, D. M. (2003). A genetic model for a central (septum transversum) congenital diaphragmatic hernia in mice lacking Slit3. *Proceedings of the National Academy of Sciences of the United States of America*, *100*(9), 5217–5222. https://doi.org/10.1073/PNAS.0730709100

Zhai, Y., Wei, R., Sha, S., Lin, C., Wang, H., Jiang, X., & Liu, G. (2019). Effect of NELL1 on lung cancer stem-like cell differentiation. *Oncology Reports*, *41*(3), 1817–1826. https://doi.org/10.3892/or.2019.6954

Zhang, X., Carpenter, D., Bokui, N., Soo, C., Miao, S., Truong, T., Wu, B., Chen, I., Vastardis, H., Tanizawa, K., Kuroda, S., & Ting, K. (2003). Overexpression of Nell-1, a Craniosynostosis-Associated Gene, Induces Apoptosis in Osteoblasts During Craniofacial Development. In *J Bone Miner Res* (Vol. 18). https://doi.org/10.1359/jbmr.2003.18.12.2126

Zhao, J., & Mommersteeg, M. T. M. (2018). Slit-Robo signalling in heart development. *Cardiovascular Research*, *114*(6), 794–804. https://doi.org/10.1093/cvr/cvy061

Zierz, S., Deschauer, M., Eger, K., Jordan, B., Kornhuber, M., Kraya, T., & Müller, T. J. (2014). Muskelerkrankungen. In *Muskelerkrankungen*. Thieme Verlag. https://doi.org/10.1055/B-002-96293

7. Supplementary Data

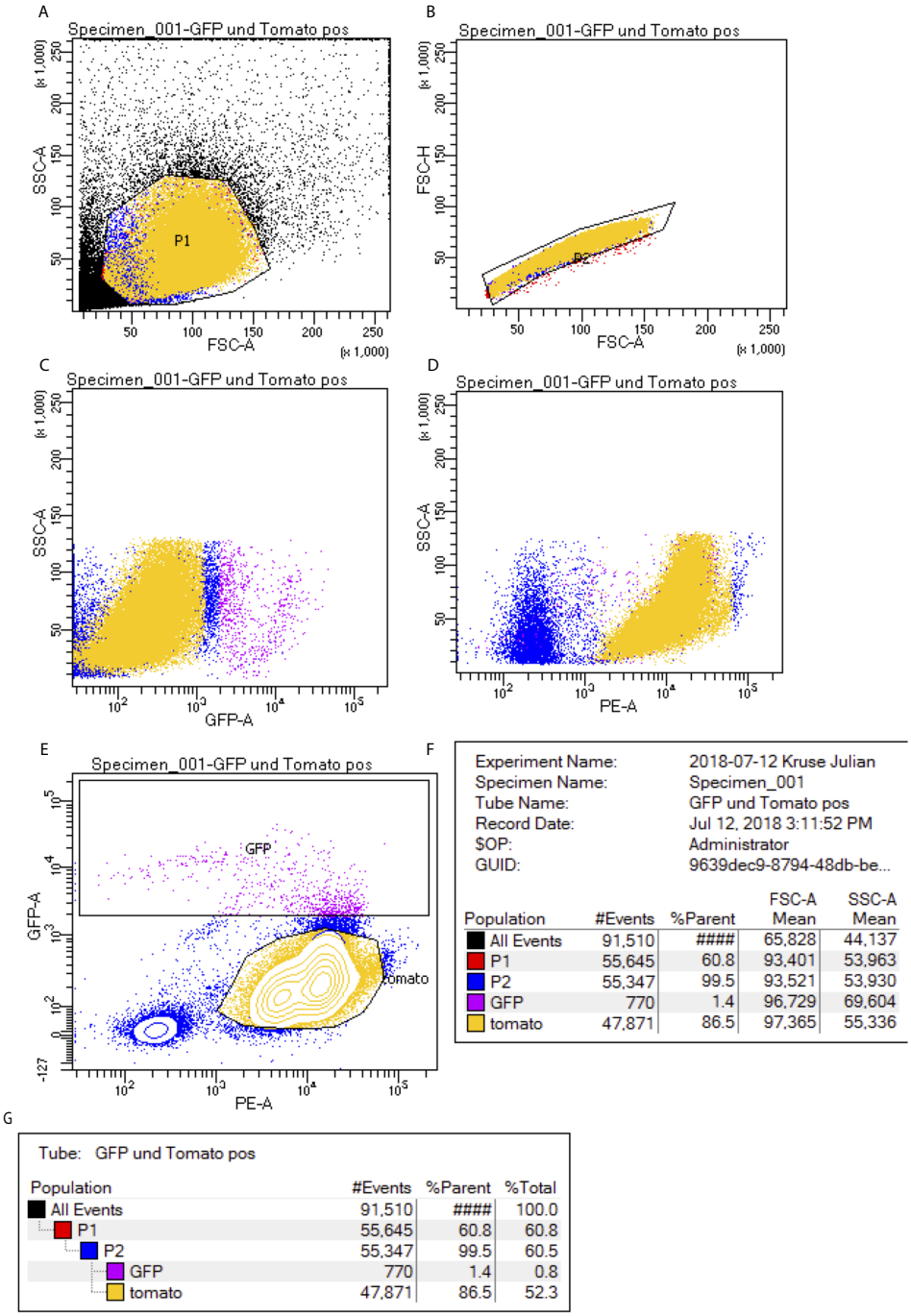

Figure 7.1: FACS of the digested E15.5 diaphragm - Batch2

Cells were sorted using forward scatter (FSC), side scatter (SSC), red fluorescence (RFP, PE), and green fluorescence (GFP). In **E,** the separation of GFP-positive and mT-positive cells is presented. Notably, in **G,** the number of GFP-positive cells is with 770 GFP-positive events in 91,510 events very low.

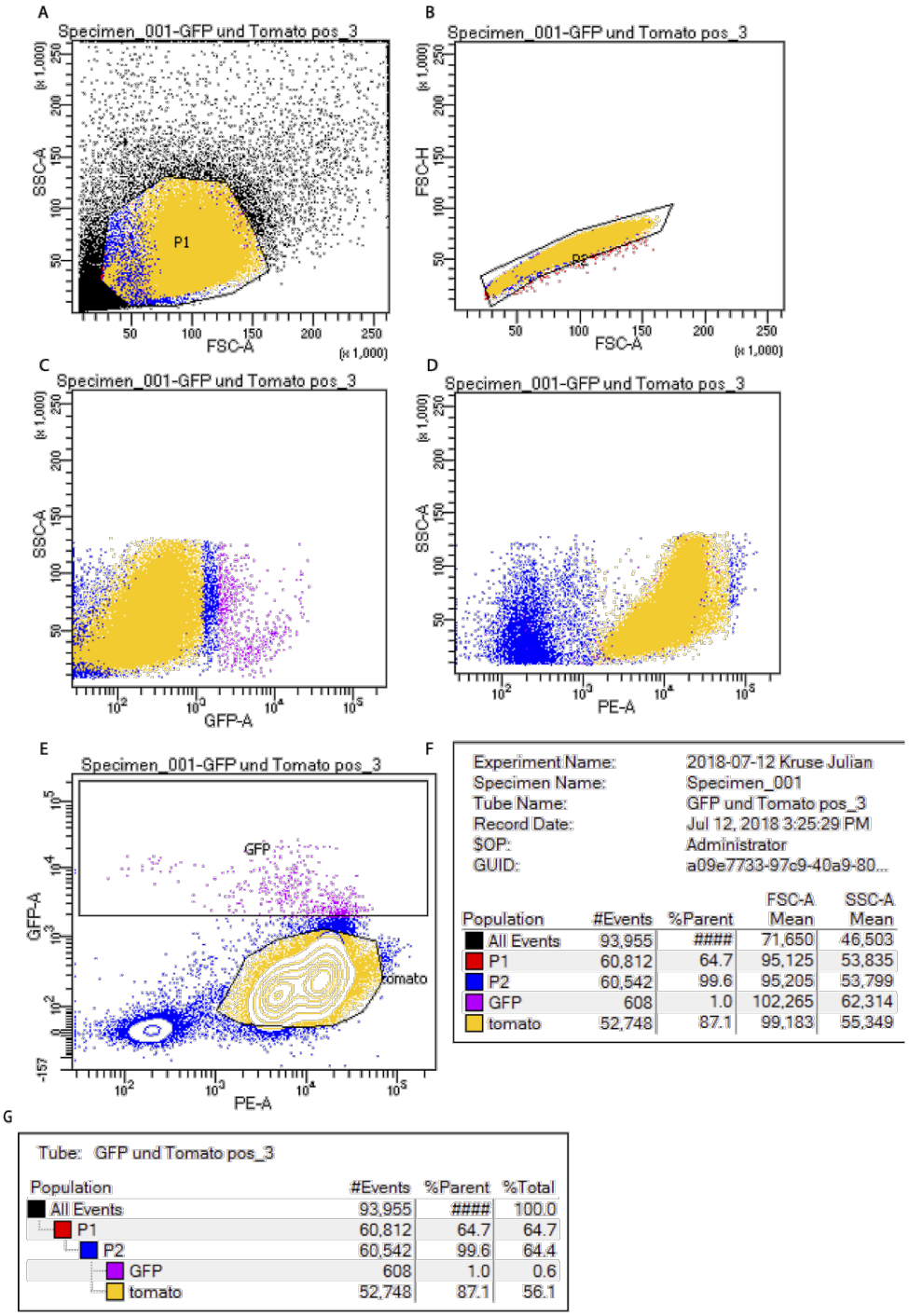

Figure 7.2: FACS of the digested E15.5 diaphragm – Batch 3

Cells were sorted using forward scatter (FSC), side scatter (SSC), red fluorescence (RFP, PE) and green fluorescence (GFP). In **E,** the separation of GFP-positive and mT-positive cells is presented. Notably, in **G,** the number of GFP-positive cells is with 608 GFP-positive events in 93,955 events very low.

Acknowledgments

Finally, I would like to express my gratitude to the following individuals that contributed to the realization my thesis in various ways:

Prof. Dr. med. Wolfgang Böcker, for welcoming me into your research group and providing me with a challenging and intriguing thesis topic.

Dr. Maximilian Saller, thank you for your excellent supervision and mentorship. Your optimism, energy, and curiosity are contagious and have kept me focused throughout the years. I could not have undertaken this journey without your scientific and emotional support.

Prof. Dr. Attila Aszódi, for challenging me with your questions and providing a well-organized laboratory that has become a part of my life for the last few years.

Maximilian Strenzke and Philipp Zeimet, for your friendship and for making our time in the laboratory a lot of fun and the nights even more.

Martina Burggraf, for all your support on experiments and everything else in betweeen. Without you, I would still be stuck on genotyping the mice.

Zsuzsanna Farkas and Heidrun Grondinger for enabling the ideal laboratory conditions, free from any technical limitations, to be able to complete my thesis.

Dr. Paolo Alberton and Sebastian Reiprich, for bringing your positive and humorous attitudes to the laboratory throughout the years.

Dr. Lisa Richter and Pardis Khosravani, for your support on multiple difficult FACS, with tight deadlines.

Dr. Alexander Jaworski, for providing us with the NELL2::AP backbone and for sharing your knowledge and expertise on NELLs.

Dr. Helmut Blum, Dr. Stefan Krebs and Marlis Fischaleck, for your advice and for performing the next-generation sequencing.

Elif Akova, for your work and help on the bioinformatics of the sequencing data.

My parents and stepparents, for their ongoing encouragement during my years of study, as well as during the process of conducting the research and finally writing the thesis. Thank you for your love and unwavering support.

My siblings and friends, for everything joyful in the best and worst days and for your love in the last years.

Camille, for your love during the last efforts to finish this thesis.

Finally, I would like to thank all my other colleagues at the Musculoskeletal University Center Munich.

Affidavit

Eidesstattliche Versicherung

_____

_____

Kruse, Julian

Ich erkläre hiermit an Eides statt, dass ich die vorliegende Dissertation mit dem Titel:

Dissecting the role of NELL-ligands and their possible receptors in myogenesis

selbständig verfasst, mich außer der angegebenen keiner weiteren Hilfsmittel bedient und alle Erkenntnisse, die aus dem Schrifttum ganz oder annähernd übernommen sind, als solche kenntlich gemacht und nach ihrer Herkunft unter Bezeichnung der Fundstelle einzeln nachgewiesen habe.

Ich erkläre des Weiteren, dass die hier vorgelegte Dissertation nicht in gleicher oder in ähnlicher Form bei einer anderen Stelle zur Erlangung eines akademischen Grades eingereicht wurde.

Amsterdam, 04.08.2023 Julian Kruse

Ort, Datum Unterschrift

Doktorandin bzw. Doktorand